doi.org/10.26434/chemrxiv.12844301.v1

N-Alkylation of 2-Methoxy-10H-Phenothiazine Revisited. A Facile Entry to Diversely N-substituted Phenothiazine-Coumarin Hybrid Dyes

Valentin Quesneau, Kevin Renault, Myriam Laly, Sébastien Jenni, Flavien Ponsot, Anthony ROMIEU

Submitted date: 21/08/2020 • Posted date: 24/08/2020

Citation information: Quesneau, Valentin; Renault, Kevin; Laly, Myriam; Jenni, Sébastien; Ponsot, Flavien; ROMIEU, Anthony (2020): N-Alkylation of 2-Methoxy-10H-Phenothiazine Revisited. A Facile Entry to Diversely N-substituted Phenothiazine-Coumarin Hybrid Dyes. ChemRxiv. Preprint. https://doi.org/10.26434/chemrxiv.12844301.v1

N-Alkylation of 2-methoxy-10H-phenothiazine, a valuable building block for the synthesis of bioactive compounds and reaction-based fluorescent probes, has been revisited aimed at introducing a substituent easily convertible into cationic or zwitterionic side chains. We focused our attention on the 3-dimethylaminopropyl group since its derivatization through reactions with various alkyl halides or sultones is a well-established and effective way to enhance polarity of diverse hydrophobic molecular scaffolds. This two-step functionalization approach was applied to the synthesis of novel phenothiazine-coumarin hybrid dyes whose spectral features, especially their NIR-I emission, have been determined in aqueous media with the ultimate goal of identifying novel fluorescent markers for bioanalytical applications, including fluorogenic detection of reactive oxygen species (ROS) through selective S-oxidation reaction of phenothiazine scaffold.

N-Alkylation of 2-methoxy-10*H*-phenothiazine revisited. A facile entry to diversely N-substituted phenothiazine-coumarin hybrid dyes

Valentin Quesneau[a,‡,*], Kévin Renault[a,‡], Myriam Laly[a], Sébastien Jenni[a], Flavien Ponsot[a], Anthony Romieu[a,*]

[a]*ICMUB, UMR 6302, CNRS, Univ. Bourgogne Franche-Comté, 9, Avenue Alain Savary, 21078 Dijon cedex, France*

N-Alkylation of 2-methoxy-10H-phenothiazine, a valuable building block for the synthesis of bioactive compounds and reaction-based fluorescent probes, has been revisited aimed at introducing a substituent easily convertible into cationic or zwitterionic side chains. We focused our attention on the 3-dimethylaminopropyl group since its derivatization through reactions with various alkyl halides or sultones is a well-established and effective way to enhance polarity of diverse hydrophobic molecular scaffolds. This two-step functionalization approach was applied to the synthesis of novel phenothiazine-coumarin hybrid dyes whose spectral features, especially their NIR-I emission, have been determined in aqueous media with the ultimate goal of identifying novel fluorescent markers for bioanalytical applications, including fluorogenic detection of reactive oxygen species (ROS) through selective S-oxidation reaction of phenothiazine scaffold.

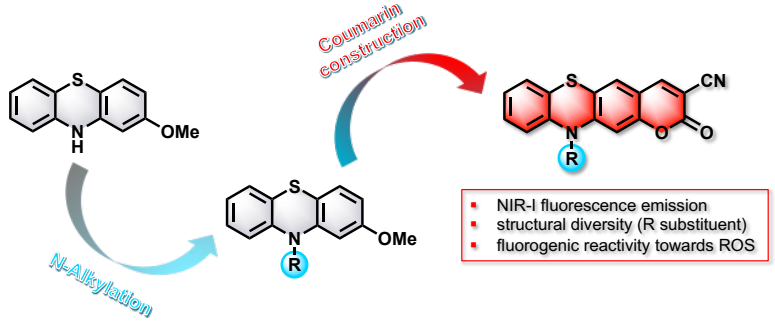

Introduction

Since the discovery and first syntheses of methylene blue (**MB**) [1] and 10*H*-dibenzo-1,4-thiazine (**PTZ**) [2] in the late 19th century (Fig. 1), the interest shown by the scientific community (especially chemists and biologists) for phenothiazine derivatives has exploded [3]. This is notably reflected in the fact that there are many thousands of different molecules belonging to this class of N,S-heterocycles, and finding diverse applications in industry (*e.g.*, as dyestuffs, antioxidants in lubricants and fuels, polymerization inhibitors, ...) and medicine (*e.g.*, as antipsychotic medications, (photo)therapeutic agents, biological staining/labeling agents, ...) [4]. Aside from these traditional usages, PTZ-based molecular systems endowed with remarkable electronic properties, have recently found further applications in optoelectronics (*e.g.*, bulk hetero-junction solar cells, dye sensitized solar cells, organic light emitting diodes, ...) [5] and fluorescent sensing and bioimaging [6]. Among the myriad PTZ derivatives with different substitution patterns, some of them are constructed from the structurally simple building block 2-methoxy-10*H*-phenothiazine **1** (Fig. 1). They have been recently popularized either as long-wavelength fluorescent dyes [7] or as fluorogenic probes in the field of activity-based sensing. In this latter context, they are effective tools for detecting reactive analytes (*e.g.*, phosgene, SO_2, thiophenol) in different matrices or tracking relevant species in biological systems (*e.g.*, ROS/RNS, H_2S_n), for analytical and diagnostics purposes respectively (see Fig. 1 for selected examples) [8]. Curiously, the vast majority of these reaction-based fluorescent probes and related fluorophores display minor structural changes in their PTZ ring, which severely limits opportunities for fine-tuning their spectral and physicochemical properties (*e.g.*, solubility in water) and/or installation of a suitable handle for bioconjugation to perform fluorescent biolabeling or to dramatically enhance their performances as imaging agents (*e.g.*, targeting properties). A good illustration of this fact is *N*-substituent (*i.e.*, the 10-position of **PTZ**) found in the core structure of its photoactive PTZ-based compounds. This is always a simple alkyl chain (*i.e.*, ethyl or butyl substituent) whereas this position may be better exploited to introduce a post-synthetically derivatizable reactive group such as amino, carboxylic acid, or hydroxyl. To the best of our knowledge, few examples of such *N*-substituted derivatives of 2-methoxy-10*H*-phenothiazine have been described in the literature even if several modulations of its N-10 substituent were regarded in effort to identify new drugs [9].

In order both to fill this gap and to devise a novel approach towards PTZ molecular diversity, we thought it would be interesting to revisit N-alkylation of 2-methoxy-10*H*-phenothiazine to introduce a substituent easily convertible into another group. Inspired by the structure of levomepromazine (maleate salt, Fig. 1), a neuroleptic drug used in palliative care and developed in the 1960s by a Japanese company namely Yoshitomi Pharmaceutical Industries [10], we have rapidly identified 3-dimethylaminopropyl moiety as the appropriate substituent to achieve this goal. It is worth mentioning that the use of this tertiary-amine-terminated alkyl chain or related analogs was popularized for the water-solubilization of various organic-based fluorophores, through their site-specific introduction and post-synthetic quaternarization with

* Corresponding authors. Tel.: +33-3-80-39-61-26 or +33-3-80-39-36-24; e-mail: valentin.quesneau@u-bourgogne.fr or anthony.romieu@u-bourgogne.fr.

‡ These authors contributed equally to this work.

alkyl halides or sultones, thereby yielding positively-charged or zwitterionic dyes [11],[12]. Similarly to PTZ uses, diketopyrrolopyrroles (DPPs), a class of industrial pigments known since the early 1970s, were recently applied as promising fluorescent organic dyes owing to their valuable spectral properties [13] but curiously, this N-functionalization strategy was never applied to these bis-lactam-based molecules. Indeed, N-alkylation of these cyclic amide moieties is often the preferred way to convert DPP pigments into soluble dyes, and the practical implementation of this reaction with versatile 3-dimethylaminopropyl substituent, would deserve to be explored to meet demands in molecular diversity for such photoactive compounds. Indeed, the current available methods are based on formal exchange and/or post-functionalization of 3,6-(hetero)aryl substituents, and are sometimes tricky and/or require *de novo* synthesis [13c, 14].

In this Letter, we report our findings related to optimization of the *N*-alkylation of **1** with butyl bromide and 3-dimethylaminopropyl chloride. A comparison with the reactivity of selected DPP pigments was also established. The availability of *N*-substituted 2-methoxyphenothiazine derivative **3** led us to consider the synthesis and photophysical characterization of novel PTZ-coumarin hybrid dyes. Their ability to act as ratiometric fluorescent chemodosimeters for hypochlorous acid/hypochlorite ($HClO/ClO^-$) detection, through oxidation of their sulfur atom was finally assessed.

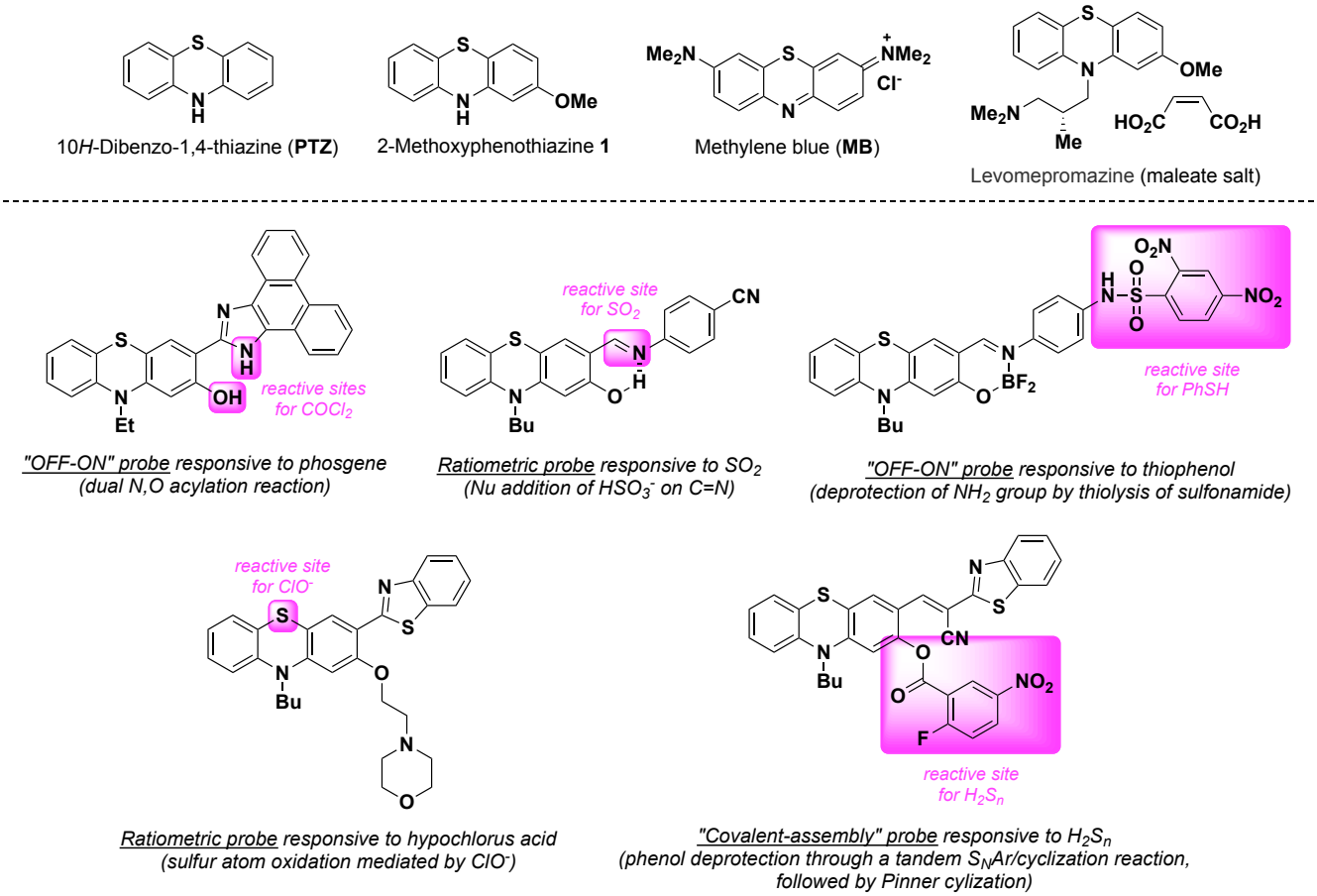

Fig. 1. (Top) Structures of 10*H*-dibenzo-1,4-thiazine, 2-methoxy-10*H*-phenothiazine and methylene blue; (bottom) selected examples of reaction-based fluorescent probes (intensiometric "OFF-ON" or ratiometric response) bearing a PTZ photoactive scaffold (Bu = *n*-butyl, $COCl_2$ = phosgene, Et = ethyl, H_2S_n = hydrogen polysulfides, PhSH = thiophenol and SO_2 = sulfur dioxide) [8m],[8i],[8b],[8h],[8e].

Results and discussion

*Optimization of N-alkylation of 2-methoxyphenothiazine **1***

As illustrated by the examples displayed in Fig. 1, N-alkyl 2-hydroxyphenothiazine moiety is the structural unit common to a wide range of analyte-responsive PTZ-based fluorescent probes. The first stages of their multi-step preparation are aimed to achieve the conversion of commercial 2-methoxyphenothiazine **1** into the corresponding N-alkyl salicylaldehyde derivative (Scheme 1). Thus, N-substitution of PTZ scaffold with *n*-butyl bromide or ethyl iodide, was achieved by treatment of **1** with a large excess of this alkylating reagent (10 equiv.), in the presence of NaOH and cat. amount of KI in the case of 1-bromobutane, in dry DMSO heated above 100 °C [8a], but experimental details for such reactions are often omitted and only reference to former publications was given. In our hands, these conditions led to disappointing results and especially, the degradation of phenothiazine ring system was observed. A literature survey on the preparation of levomepromazine and related N-alkyl PTZ derivatives revealed the use of other strong bases such as $NaNH_2$ or NaH to perform such N-alkylation reaction, often conducted in an aromatic hydrocarbon solvent (toluene or xylene) possibly in mixture with DMSO or DMF [6i, 10, 15]. By drawing on these previous works, we have devised a new protocol based on the treatment of **1** with 2 equiv. of *n*-butyl bromide, in the presence of 2 equiv. of NaH in

dry DMF at room temperature, that provided the desired N-butyl derivative **2** with a good isolated 85% yield within 90 min (and deployable to gram scale synthesis, Scheme 1). At this stage, it seemed relevant for us to expand the scope of this optimized protocol to more sophisticated alkyl pendant arms bearing a further reactive group for post-synthetic functionalization of PTZ heterocycle. Thus, N-alkylation of **1** with commercial 3-dimethylaminopropyl chloride (HCl salt) conducted under the same conditions, was next considered and the desired product **3** was obtained with a modest 23% yield. No substantial improvement was obtained with the mesylate derivative freshly prepared from 3-dimethylamino-1-propanol. These results are consistent with those previously obtained by us with unsymmetrical DPP pigments **4-6** (Scheme 1) for which the N-alkylation of lactam moieties is essential to impart to them both solubility and functionality. Indeed, reaction of **4** with 3-dimethylaminopropyl chloride (HCl salt, 10 equiv., previously neutralized with 10 equiv. of NaH), in the presence of NaH (5.5 equiv) and tetrabutylammonium iodide (TBAI, 0.05 equiv) in dry DMF at 80 °C provided bis-N,N'-substituted DPP dye **7** with an isolated 29% yield. Conversely, no trace of bis-N,N'-alkylated derivative was detected when unsymmetrical DPP pigments **5** and **6** were subjected to the same alkylation conditions. This perfectly illustrates how difficult it is to generalize this functionalization strategy that may sound simple on paper. Furthermore, it is important to specify that the major difficulty associated with this alkylation reaction is closely related to the high propensity of 3-dimethylaminopropyl halide (or mesylate) to react with itself leading to its self-polymerization or premature quaternarization of dimethylamino group pre-introduced onto the fluorophore scaffold. Thus, the above-mentioned reaction has led to a mixture of **7** and **8** in the ratio 78:22 and our further attempts to minimize the quaternarized-related side-product formation failed.

Both optimized N-alkylation methods of 2-methoxyphenothiazine heterocycle can readily provide hundreds of milligrams of **2** and **3**. We wished to valorize these building blocks in the synthesis of phenothiazine-coumarin hybrid dyes [7], with the dual aim of accurately determining the spectral properties of these NIR-I emitters under simulated physiological conditions, and confirming the chemical inertness of N-alkyl pendant arm during multi-step synthetic processes.

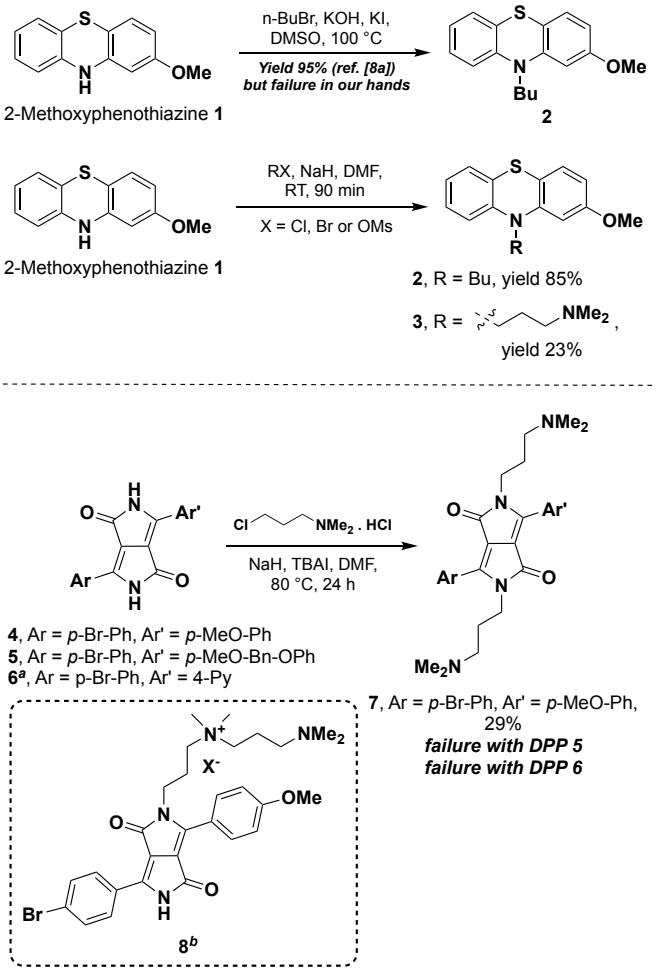

Scheme 1. (Top) Background information and revisited N-alkylation of 2-methoxyphenothiazine with *n*-butyl bromide and 3-dimethylaminopropyl chloride (HCl salt); (bottom) N-Alkylation of DPP pigments with 3-dimethylaminopropyl chloride (HCl salt) (*p*-Br-Ph = *para*-bromophenyl, p-MeO-Ph = *para*-methoxyphenyl, p-MeO-Bn-OPh = *para*-methoxybenzyloxyphenyl, 4-Py = 4-pyridyl, RT = room temperature, TBAI = tetrabutylammonium iodide, X^- = Cl^- or I^-). *[a]Please note: for this DPP, only 3 equiv. of alkylating agent was used and a mixture of N-alkyl pyridinium and mono N-substituted lactam derivative was obtained. [b]Please note: an alternative structure for this side-product may be the N,O-dialkyl DPP derivative.*

*Synthesis of PTZ-coumarin hybrid dyes **10**, **15** and **16***

Coumarins fused with other (hetero)aromatic units have been recently identified as attractive fluorescent markers for performing biosensing/bioimaging operations within the far-red or NIR-I spectral region [16]. Among the myriad of π-expanded coumarins currently available and already studied in this context, 4*H*-benzo[1,4]thiazine-fused compounds (also known as phenothiazine coumarin hybrids) have been used to produce a fluorescence output upon the selective activation of "covalent-assembly" type probes by targeted (bio)analytes (see Fig. 1 for example of H_2S_n-responsive probe) [8a, 8e, 8k, 8l]. A multi-step synthesis based on the preparation of the key intermediate N-alkyl 2-hydroxy-10*H*-phenothiazine-3-carboxaldehyde (through Vilsmeier-Haack formylation followed by deprotection of the methoxy group) and its subsequent Knoevenagel condensation with a latent *C*-nucleophile (*e.g.*, malononitrile, heteroaryl-acetonitriles) complemented by an acid hydrolysis of iminolactone to lactone, was devised to access to a set of PTZ-coumarin hybrid dyes diversely substituted at the C-3 position. Both N-alkyl PTZ derivatives **2** and **3** have been subjected to this reaction sequence (Scheme 2). Formylation with $POCl_3$/DMF yielded the

corresponding PTZ-based *ortho*-anisaldehydes **9** and **11** both in good yields, which supports the fact that the presence of tertiary amino group on N-alkyl pendant arm did not interfere with *in situ* generated chloroiminium ion. Deprotection of aryl methyl ether was achieved with AlI_3, generated *in situ* from aluminum powder and iodine in dry MeCN. From a practical point of view, we found that the use of a carousel-type parallel reaction station is particularly needed for effective gram scale synthesis of PTZ-based salicylaldehyde **12** because of the low yield obtained when the reaction was performed at hundreds of mg scale, in a single batch. This method was found to prevent partly the undesired deactivation of AlI_3 by the dimethylpropylamino group and through strong Lewis acid-base complexation, and a satisfying yield of 63% was obtained for **12** (to compare to 92% for N-butyl derivative **9**). Next, chemoselective *N*-alkylation of **12** was performed either with methyl iodide to obtain cationic derivative **13** or 1,3-propanesultone to install a zwitterionic side-chain onto PTZ scaffold (compound **14**). Both reactions were conducted without base to avoid undesired O-alkylation reaction (10-20 equiv. of alkylating reagent, in dry DCM at 40 °C for 17-24 h). Finally, the three PTZ-coumarin hybrid dyes **10**, **15** and **16** were synthesized through Knoevenagel condensation reaction with malononitrile under conventional conditions previously optimized by us. All purifications were achieved by semi-preparative RP-HPLC under acidic conditions (*i.e.*, linear gradient of MeCN in aq. TFA 0.1%, pH 1.9) that enable both conversion of 2-iminocoumarins into coumarins **10**, **15** and **16**, and their isolation in a pure form (>95%) required for photophysical studies (*vide infra*). After recovery by freeze-drying, we noted that the solid form of zwitterionic PTZ-coumarin hybrid dye **16**, is poorly soluble in water and polar organic solvent such as DMF, DMSO, MeCN and MeOH. To overcome this solubility problem, a further counter-ion exchange operation was performed by semi-preparative RP-HPLC using aq. triethylammonium bicarbonate buffer (TEAB, 50 mM, pH 7.5) and MeCN as eluents. Unfortunately, the benefit was found to be negligible. All spectroscopic data (see Supplementary data for the corresponding spectra, Figs. S8-S10, S13, S33-S36, S39, S43-S44 and S47), especially NMR and mass spectrometry, were in agreement with the structures assigned. The purity of each coumarin sample was confirmed by RP-HPLC analysis with UV-vis detection at different wavelengths, and mass percentage of TFA was determined by ionic chromatography (see Supplementary data, Figs. S11-S12, S37-S38 and S45-S46).

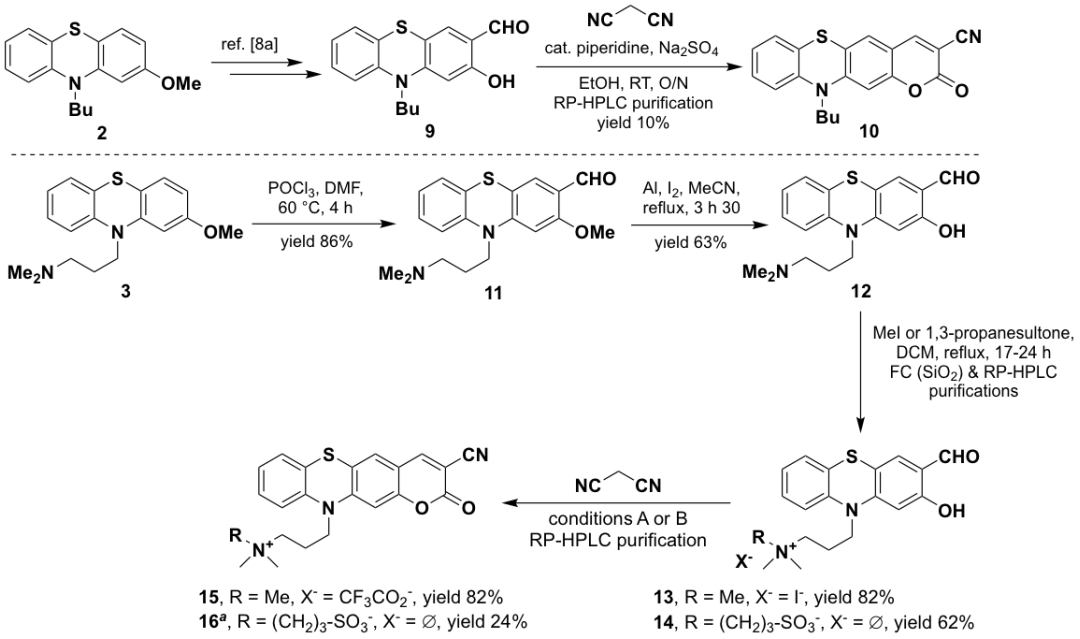

Scheme 2. (Top) Synthesis of PTZ-coumarin hybrid dye **10** from N-butyl 2-methoxyphenothiazine **1**; (bottom) synthesis of cationic and zwitterionic PTZ-coumarin hybrid dyes **15** and **16** from N-(3-dimethylaminopropyl) 2-methoxyphenothiazine **3**: conditions A for **15** = piperidine, EtOH-MeCN (1:1, v/v), RT, 16 h; conditions B for **16** = piperidine, anhydrous Na_2SO_4, EtOH-DMF (8:1, v/v), RT, 16 h. (O/N = overnight, FC (SiO_2) = flash-column chromatography over silica gel, RT = room temperature). [a]*Please note: compound **16** was isolated as triethylammonium salt.*

Photophysical characterization of PTZ-coumarin hybrid dyes

Although several PTZ-coumarin hybrid dyes, especially the derivative **17** bearing a 2-benzothiazolyl (BZT) moiety as C-3 substituent, have already been implemented in different biosensing operations [8a, 8e], their spectral features have never been determined in pure aq. buffers that mimic physiological conditions. To fill this gap, we assessed the optical photophysical properties of **10**, **15** and **16** in phosphate buffered saline (PBS, pH 7.3) alone but also in the presence of a non-ionic surfactant (Tween® 80) to disrupt potential formation of aggregates. Further spectral measurements in MeOH were also achieved. All results are summarized in Table 1 (see Fig. 2 for the absorption/fluorescence spectra of **10** and Supplementary data for the absorption/fluorescence spectra of compounds **15** and **16**, Figs. S40-S42 and S48-S50).

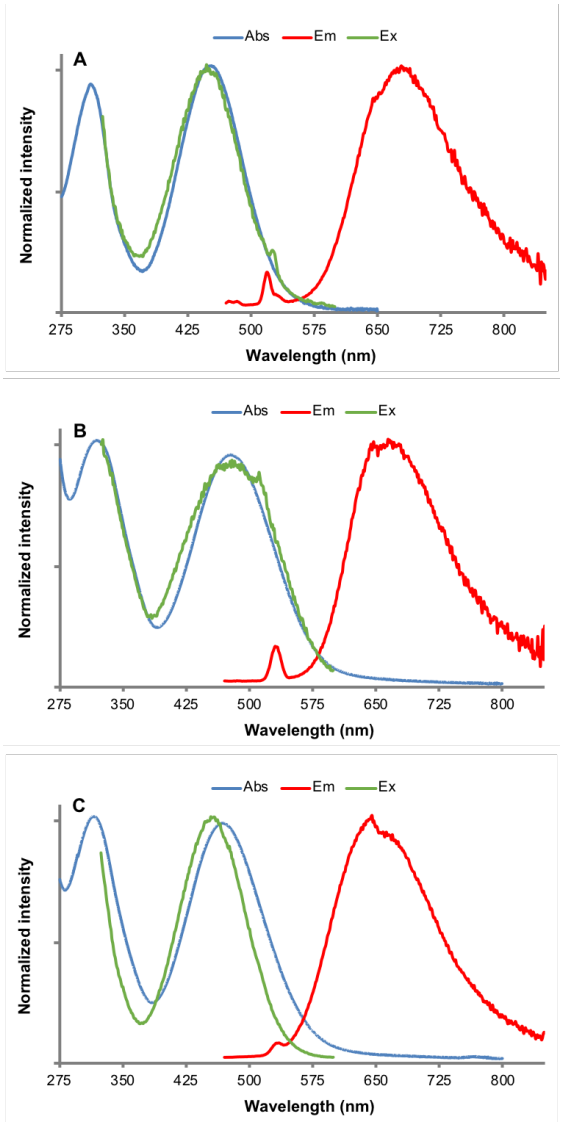

Fig. 2. Normalized absorption (blue), excitation (Em. 625 nm, slit 5 nm, green) and emission (Ex. 450 nm, slit 5 nm, red) spectra of PTZ-coumarin hybrid dye 10 in MeOH (A), PBS (B) and PBS + Tween® 80 (C) at 25 °C. *Please note: peak at 519 nm/530 nm is assigned to Raman scattering.*

As already reported by Chen *et al.* for BZT derivatives **17** [8a], all spectral features of PTZ-coumarin hybrids **10**, **15** and **16** are characteristic of photoactive molecules where strong internal charge transfer (ICT) process operates: (1) broad structureless absorption and emission bands with full-width at half maximum (FWHM) $\Delta\lambda_{1/2max}$ in the range 80-110 nm and 130-165 nm respectively, (2) huge Stokes' shift values, and (3) NIR-I emission with a very low fluorescence quantum yield in polar solvents. Concerning this latter point, it is important to specify that the standard used by Chen *et al.* (*i.e.*, fluorescein in EtOH) for the determination of relative fluorescence quantum yield of **17** was not really the most suited because its absorption/emission curves do not really display similarities with those of this class of ICT-based compounds. We found that tris(2,2'-bipyridyl)ruthenium dichloride ($Ru(bpy_3)Cl_2$) in air-saturated water is more suitable for such determinations. Somewhat unexpectedly, the replacement of *n*-butyl substituent by a polar pendant arm is not having a positive effect on emissive effectiveness in aq. media. Indeed, in the concentration range used for fluorescence measurements (10^{-7} M), no formation of non-emissive H-type aggregates as evidenced by the good matching between the absorption and excitation spectra recorded in PBS, was observed whatever the N-substituent introduced onto the PTZ scaffold (Fig. 2 and Figs S40-S42 and S48-S50). Further molecular motions of trimethylpropylammonium and sulfobetain moieties could promote non-radiative deactivation and may explain the decrease of quantum yields compared to those determined with N-butyl derivative **10**[11a]. Likewise, addition of Tween® 80 (300 µM) in aq. buffer does not have a positive impact on fluorescence efficiency of these ICT-based fluorophores. Furthermore, in the present case, we were not able to use a more biorelevant disaggregating agent such as bovine serum albumin (BSA, typically added to PBS at a content of 5% (w/v) to simulate body fluid) because emission spectrum of PBS + 5% BSA solution displays an intense broad band centered at 530 nm that partly overlap emission band of **10**, **15** and **16**. Despite their poor fluorescence in aq. media, we finally examined the ability of these phenothiazine derivatives to act as effective fluorogenic chemodosimeters for detection of reactive oxygen species (ROS).

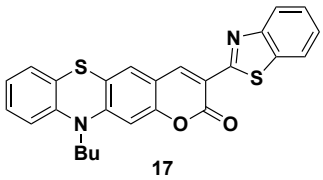

17

Sensing response of PTZ-coumarin hybrid dyes to HClO/ClO⁻ analyte

The need for a comprehensive understanding of biological functions of ROS linked to their positive effects and adverse impacts on human health and the environment, has promoted the development of luminescent probe-based strategies for detecting such oxidative bioanalytes *in vitro* and *in vivo* [17]. This is true, in particular for hypochlorous acid (HClO) that is produced by neutrophils and monocytes *in vivo* upon the reaction between H_2O_2 and Cl^- ions catalyzed by myeloperoxidase [18]. This reaction also takes place in mitochondria and due to its pKa = 7.46, HClO is in equilibrium with ClO^- under physiological conditions. Among the myriad of reaction-based fluorescent probes responsive to HClO/ClO^-, described in the literature [19], one of the preferred strategies involves functionalizing a fluorescent scaffold with a phenothiazine moiety that readily quenches its emission through the photoinduced electron transfer (PeT) mechanism. Hypochlorite-mediated oxidation of sulfur to sulfoxide prevents this PeT process and thus triggered fluorescence unveiling [6b-d, 6f-i, 8f, 20]. Depending the chromophoric structure of the probe, an intensiometric or a ratiometric response can be obtained. In this context, we wished to examine the fluorogenic reactivity of PTZ-coumarin hybrid dyes **10**, **15** and **16** towards this ROS. Preliminary

experiments have revealed that reaction of these phenothiazine derivatives with NaOCl (bleach) leads to a large hypsochromic shift (-110 nm, -161 nm and -168 nm for **10**, **15** and **16** respectively) of their emission maximum (data not shown). By analogy with the recent work of the Hou group [8f] and to avoid signal saturation, we selected the Ex/Em 400/520 nm pair for time-dependent fluorescence analyses and to highlight the ratiometric behavior of **10**, **15** and **16**. On treatment of the three probes with 1 equiv. of ClO^- in PBS (pH 7.3) at 25 °C, an immediate and dramatic fluorescence enhancement at 520 nm was observed in each case. The most substantial increase in green fluorescence emission intensity was obtained with cationic PTZ-based probe **15**. Conversely, *in vitro* assays conducted with zwitterionic PTZ-based probe **16** has led to the least spectacular fluorogenic response. Furthermore, no significant fluorescence signal changes were observed in the absence of ROS, confirming the stability of the three ratiometric probes **10**, **15** and **16** in PBS.

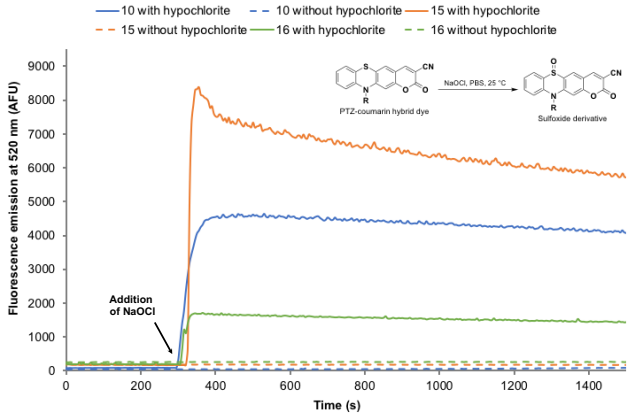

Fig. 3. Fluorescence emission time course (Ex/Em 400/520 nm, slit 2 nm) of PTZ-coumarin hybrid dyes **10**, **15** and **16** (concentration: 2.0 µM) in the presence of hypochlorite ions (1 equiv.) in PBS (pH 7.3) at 25 °C.

In order both to have an accurate idea of the conversion rate of such fluorogenic S-oxidation processes and to gain insights into the sensing mechanism through addressing issues related to the formation of a single or several oxidized species and the possible existence of further reactions triggered by this oxidation event, each reaction mixture was first subjected to RP-HPLC-fluorescence analyses (see Supplementary data, Fig. S63-S75). Under acidic conditions (*i.e.*, linear gradient of MeCN in aq. formic acid 0.1%, pH 2.5, as eluent) used for these analyses, the starting ICT-based probe **10** was detected on both Ex/Em channels (400/520 nm and 450/700 nm, t_R = 5.7 min). After treatment with 1 equiv. of ClO^-, a new major peak at t_R = 4.6 min was detected, characterized by an intense emission at 520 nm and a negligible emission at 700 nm, that was assigned to sulfoxide derivative. When the S-oxidation reaction was conducted with 10 equiv. or 100 equiv. of ClO^-, a slight decrease of peak intensity or its complete disappearance was observed (see Supplementary data, Figs. S66-S67). That would suggest that sulfoxide derivative may undergone over-oxidation (formation of sulfone derivative?) and subsequent degradation of PTZ heterocycle. RP-HPLC-fluorescence results obtained with cationic PTZ derivative **15** are quite similar (see Supplementary data, Figs. S68-S70, t_R = 3.3 min and 3.9 min for sulfoxide and starting PTZ derivatives respectively). Conversely, a less substantial result was revealed with zwitterionic PTZ derivative **16** even a new peak (t_R = 3.4 min) assigned to sulfoxide product was detected. The large remaining amount of **16** observed on the elution profile (see Supplementary data, Figs. S71-S73, t_R = 3.9 min) highlighted the poor conversion rate for this S-oxidation reaction. To confirm that the reaction between the probes **10**, **15** and **16** and ClO^- led to the formation of a sulfoxide derivative, the same mixtures were next analyzed by RP-HPLC-MS (see Supplementary data, Figs. S76-S91). The partial disappearance of the probe **10** peak (t_R = 5.6 min) and the formation of sulfoxide derivative (t_R = 4.6 min) was clearly observed and the structure of this latter green-emissive fluorophore was supported by MS-ESI+ data (both in "full scan" and single ion monitoring (SIM) modes). Interestingly, we also noted the formation of other minor products, one of which at t_R = 3.4 min was possibly identified as the sulfinic acid derivative or more probably the carboxamide derivative (MS(ESI+): *m/z* = 383.2 $[M + H]^+$, calcd for $C_{20}H_{19}N_2O_4S^+$ 383.1, see Fig. S90). Indeed, the nitrile moiety introduced onto the C-3 position of coumarins, is prone to facile hydrolysis [21]. The same valuable information has been gathered with the cationic PTZ derivatives (see Supplementary data, Figs. S83-S85 and S91, t_R = 3.0 min, *m/z* = 426.2 $[M]^+$, and t_R = 3.2 min, *m/z* = 408.2 $[M]^+$ for the sulfoxide derivatives bearing -$CONH_2$ and -CN as C-3 substituent). We have also confirmed the presence of a small amount of sulfoxide derivative in blank experiment (*i.e.*, incubation of probe in PBS alone) whose formation may arise from a photooxidation process (*i.e.*, sulfide oxidation mediated by singlet oxygen, formed by triplet energy transfer to molecular oxygen since PTZ scaffold is known to be an effective photosensitizer) [6a]. Regarding the PTZ-coumarin hybrid **16** bearing a sulfobetain pendant arm, its poor reactivity towards ClO^- was further confirmed by these RP-HPLC-MS analyses (see Supplementary data, Figs. S87-S89). Therefore, thanks to these complementary analytical tools, we have shown for the first time that fluorogenic reactions between PTZ-based probes and stoichiometric amount of ClO^- is not a quantitative and unequivocal process. Furthermore, depending on the nature of N-substituent (length and net electrostatic charge) of PTZ scaffold, the ability of sulfide moiety to be readily oxidized and thus both quality and intensity of the fluorogenic ratiometric response are dramatically impacted.

Table 1 Photophysical properties of PTZ-coumarin hybrid dyes studied in this work, determined at 25 °C.

Cmpd[a]	Solvent	λ_{max} Abs (nm)	λ_{max} Em (nm)	Stokes' shift (nm / cm^{-1})	ε (M^{-1} cm^{-1})	Φ_F (%)[b]
10	MeOH	309, 451	678	369 / 17 613 227 / 7 423	10 800, 11 950	1.6
10	PBS	310, 478	664	354 / 17 198 186 / 5 860	10 300, 9 850	2.8
10	PBS + Tween® 80	314, 462	645	331 / 16 343 183 / 6 141	11 550, 11 250	4.8

15	MeOH	309, 433	678	369 / 17 972 245 / 8 345	21 550, 20 700	1.6
15	PBS	310, 443	700	390 / 17 972 257 / 8 287	19 650, 21 810	0.2[c]
15	PBS + Tween® 80	309, 443	700	391 / 18 076 257 / 8 287	19 425, 22 050	0.4[c]
16[e]	MeOH	307, 432	672	365 / 17 692 240 / 8 267	9 400, 8 850	1.6
16[e]	PBS	307, 440	706	399 / 18 409 266 / 8 563	8 150, 9 275	0.3[c]
16[d]	PBS + Tween® 80	308, 440	702	394 / 18 222 262 / 8 482	8 750, 9 125	0.3[c]
17[e]	PB-MeCN (7:3, v/v)	467	662	195 / 6 307	-	7

[a] Stock solutions (1.0 mg/mL) of fluorophores were prepared in peptide synthesis grade DMF. *Please note*: do not use DMSO to achieve this because this solvent accelerates the photooxidative degradation of these PTZ-based fluorophores.
[b] Determined using $Ru(bpy)_3Cl_2$ as a standard (Φ_F = 2.8% in water, Ex. at 450 nm) [22].
[c] Fluorescence efficiency was too low to establish a linear relationship between Abs at 450 nm and Em 470-880 nm with four distinct points. Only one measurement was possible (and additional zero) to calculate these values below 1%.
[d] Difficulties were encountered to completely solubilize this compound in DMF (1.0 mg/mL) despite prolonged sonication. That explains lower values of molar extinction coefficients obtained for this dye.
[e] Values determined and reported by Chen *et al.* [8a] Relative fluorescence quantum yield was determined using fluorescein as a standard (Φ_F = 79% in EtOH).

Conclusion

In summary, we have revisited and examplified N-alkylation reaction of 2-methoxyphenothiazine **1** with the convertible 3-dimethylaminopropyl substituent. Selective quaternarization of its tertiary amine moiety has been achieved and this N-functionalization approach has opened the way for preparing novel hydrophilic PTZ-based pharmacophores and fluorophores. As an example, three PTZ-coumarin hybrid dyes with a marked ICT character, have been synthesized and photophysically characterized. Despite their modest fluorescence quantum yields in neutral aq. buffer, N-butyl and cationic PTZ derivatives **10** and **15** have been identified as practical fluorogenic probes for ratiometric detection of highly oxidative ROS, namely hypochlorite ions, through selective S-oxidation of their phenothiazine heterocycle. For the first time, the accurate analysis of such reaction by means of RP-HPLC coupled to fluorescence and mass detections, has enabled to show that this activity-based sensing strategy did not necessarily result in the quantitative formation of a single oxidized species (*i.e.*, sulfoxide derivative). We are convinced that the implementation of such analytical methodology by (bio)chemists working in the field of reaction-based fluorescent probes would be helpful for deciphering precisely their activation mechanism and thus improving their performances.

Declaration of Competing Interest

The authors declare that they have no known competing financial interests or personal relationships that could have appeared to influence the work reported in this paper

Acknowledgments

This work is part of the project "Pharmacoimagerie et Agents Theranostiques", supported by the Université de Bourgogne and Conseil Régional de Bourgogne through the Plan d'Actions Régional pour l'Innovation (PARI) and the European Union through the PO FEDER-FSE Bourgogne 2014/2020 programs. Financial support from Agence Nationale de la Recherche (ANR, AAPG 2018, DetectOP_BChE, ANR-18-CE39-0014 and LuminoManufac-Oligo, ANR-18-CE07-0045), especially for the post-doc fellowships of Drs. Valentin Quesneau and Kévin Renault is also greatly acknowledged. Part of this work devoted to chemistry of DPP dyes was supported by the French "Investissements d'Avenir" program, project ISITE BFC (contract ANR-15-IDEX-0003), especially for the post-doc fellowship of Dr. Sébastien Jenni. Flavien Ponsot gratefully acknowledges the French Ministry of National Education, Higher Education and Research for his Ph. D. grant (2107-2020). The authors thank the "Plateforme d'Analyse Chimique et de Synthèse Moléculaire de l'Université de Bourgogne" (PACSMUB, http://www.wpcm.fr) for access to analytical instrumentation, especially Dr. Quentin Bonnin (CNRS, PACSMUB) for his help during variable temperature NMR experiments, COBRA lab (UMR CNRS 6014) and Iris Biotech company for the generous gift of some chemical reagents used in this work.

Supplementary data

Supplementary data (all synthetic procedures, spectroscopic and photophysical characterizations of PTZ-coumarin hybrid dyes described in this work) associated with this article can be found, in the online version:

References and note

A preprint was previously posted on ChemRxiv, see

[1] H. Caro US Pat. 204796, 1878.
[2] A. Bernthsen, Ber. Dtsch. Chem. Ges. 16 (1883) 2896-2904.
[3] E. A. Onoabedje, S. A. Egu, M. A. Ezeokonkwo, U. C. Okoro, J. Mol. Struct. 1175 (2019) 956-962.
[4] a) K. Pluta, B. Morak-Mlodawska, M. Jelen, Eur. J. Med. Chem. 46 (2011) 3179-3189; b) M. Wainwright, J. Braz. Chem. Soc. 26 (2015) 2390-2404; c) C. Gopi, M. D. Dhanaraju, Rev. J. Chem. 9 (2019) 95-126.
[5] a) Z.-S. Huang, H. Meier, D. Cao, J. Mater. Chem. C 4 (2016) 2404-2426; b) I. J. Al-Busaidi, A. Haque, N. K. Al Rasbi, M. S. Khan, Synth. Met. 257 (2019) 116189; c) S. Thokala, S. P. Singh, ACS Omega 5 (2020) 5608-5619.
[6] a) M. Barra, G. S. Calabrese, M. T. Allen, R. W. Redmond, R. Sinta, A. A. Lamola, R. D. Small, Jr., J. C. Scaiano, Chem. Mater. 3 (1991) 610-616; b) F. Liu, T. Wu, J. Cao, H.

Zhang, M. Hu, S. Sun, F. Song, J. Fan, J. Wang, X. Peng, Analyst 138 (2013) 775-778; c) H. Xiao, K. Xin, H. Dou, G. Yin, Y. Quan, R. Wang, Chem. Commun. 51 (2015) 1442-5; d) L. Liang, C. Liu, X. Jiao, L. Zhao, X. Zeng, Chem. Commun. 52 (2016) 7982-7985; e) S. S. Deshpande, H. S. Kumbhar, G. S. Shankarling, Spectrochim. Acta, Part A 174 (2017) 154-163; f) D. Soni, S. Gangada, N. Duvva, T. K. Roy, S. Nimesh, G. Arya, L. Giribabu, R. Chitta, New J. Chem. 41 (2017) 5322-5333; g) M. Vedamalai, D. Kedaria, R. Vasita, I. Gupta, Sens. Actuators, B 263 (2018) 137-142; h) L. Wang, X. Chen, Q. Xia, R. Liu, J. Qu, Ind. Eng. Chem. Res. 57 (2018) 7735-7741; i) W. Wang, J.-Y. Ning, J.-T. Liu, J.-Y. Miao, B.-X. Zhao, Dyes Pigm. 171 (2019) 107708.

[7] J. Sheng, W. Shen, X. Yue, C. Huang CN Pat. 108250220A, 2018.

[8] a) W. Chen, X. Yue, W. Li, Y. Hao, L. Zhang, L. Zhu, J. Sheng, X. Song, Sens. Actuators, B 245 (2017) 702-710; b) W. Chen, L. Zhu, Y. Hao, X. Yue, J. Gai, Q. Xiao, S. Huang, J. Sheng, X. Song, Tetrahedron 73 (2017) 4529-4537; c) P. Hou, J. Wang, S. Fu, L. Liu, S. Chen, Spectrochim. Acta, Part A 213 (2019) 342-346; d) P. Hou, J. Wang, S. Fu, L. Liu, S. Chen, Anal. Bioanal. Chem. 411 (2019) 935-942; e) W. Li, S. Zhou, L. Zhang, Z. Yang, H. Chen, W. Chen, J. Qin, X. Shen, S. Zhao, Sens. Actuators, B 284 (2019) 30-35; f) J.-T. Hou, B. Wang, P. Fan, R. Duan, X. Cao, L. Zhu, S. Wang, Dyes Pigm. 182 (2020) 108675; g) J.-T. Hou, B. Wang, S. Wang, Y. Wu, Y.-X. Liao, W. X. Ren, Dyes Pigm. 178 (2020) 108366; h) P. Hou, S. Chen, G. Liang, H. Li, H. Zhang, Spectrochim. Acta, Part A 229 (2020) 117866; i) S. Wang, B. Zhu, B. Wang, P. Fan, Y. Jiu, M. Zhang, L. Jiang, J.-T. Hou, Dyes Pigm. 173 (2020) 107933; j) W. Wang, N. Li, J.-T. Liu, J.-Y. Miao, B.-X. Zhao, Z.-M. Lin, Dyes Pigm. 181 (2020) 108639; k) X. Yue, J. Wang, J. Han, B. Wang, X. Song, Chem. Commun. 56 (2020) 2849-2852; l) J. Han, X. Liu, H. Xiong, J. Wang, B. Wang, X. Song, W. Wang, Anal. Chem. 92 (2020) 5134-5142; m) T. Zhang, L. Zhu, Y. Ma, W. Lin, Analyst 145 (2020) 1910-1914.

[9] a) M. Schmidt, M. Teitge, M. E. Castillo, T. Brandt, B. Dobner, A. Langner, Arch. Pharm. 341 (2008) 624-638; b) K. Kubota, H. Kurebayashi, H. Miyachi, M. Tobe, M. Onishi, Y. Isobe, Bioorg. Med. Chem. Lett. 19 (2009) 2766-2771; c) H. Prinz, B. Chamasmani, K. Vogel, K. J. Boehm, B. Aicher, M. Gerlach, E. G. Guenther, P. Amon, I. Ivanov, K. Mueller, J. Med. Chem. 54 (2011) 4247-4263; d) Y. Zhao, B. Huang, C. Yang, W. Xia, Org. Lett. 18 (2016) 3326-3329; e) R. Jin, C. L. Bub, F. W. Patureau, Org. Lett. 20 (2018) 2884-2887; f) K. Voegerl, N. Ong, J. Senger, D. Herp, K. Schmidtkunz, M. Marek, M. Mueller, K. Bartel, T. B. Shaik, N. J. Porter, D. Robaa, D. W. Christianson, C. Romier, W. Sippl, M. Jung, F. Bracher, J. Med. Chem. 62 (2019) 1138-1166.

[10] M. Nakanishi, G. Hasegawa JP Pat. 40009030, 1965.

[11] For selected examples, see: a) H. Itoi, T. Kambe, N. Kano, T. Kawashima, Inorg. Chim. Acta 381 (2012) 117-123; b) A. Romieu, C. Massif, S. Rihn, G. Ulrich, R. Ziessel, P.-Y. Renard, New J. Chem. 37 (2013) 1016-1027; c) N. Bisballe, B. W. Laursen, Chem. - Eur. J. (2020) in press, DOI: 10.1002/chem.202002457.

[12] S. Wang, A. Natrajan, RSC Adv. 5 (2015) 19989-20002.

[13] a) D. G. Farnum, G. Mehta, G. G. I. Moore, F. P. Siegal, Tetrahedron Lett. 15 (1974) 2549-2552; b) M. Grzybowski, D. T. Gryko, Adv. Optical Mater. 3 (2015) 280-320; c) M. Kaur, D. H. Choi, Chem. Soc. Rev. 44 (2015) 58-77.

[14] W. Li, L. Wang, H. Tang, D. Cao, Dyes Pigm. 162 (2019) 934-950.

[15] a) S. Dollinger, S. Löber, R. Klingenstein, C. Korth, P. Gmeiner, J. Med. Chem. 49 (2006) 6591-6595; b) N. L. Agarwal, P. P. Mistri, N. M. Patel EP Pat. 2743263, 2014.

[16] M. Tasior, D. Kim, S. Singha, M. Krzeszewski, K. H. Ahn, D. T. Gryko, J. Mater. Chem. C 3 (2015) 1421-1446.

[17] For selected reviews, see: a) X. Chen, F. Wang, J. Y. Hyun, T. Wei, J. Qiang, X. Ren, I. Shin, J. Yoon, Chem. Soc. Rev. 45 (2016) 2976-3016; b) D. Andina, J.-C. Leroux, P. Luciani, Chem. - Eur. J. 23 (2017) 13549-13573; c) X. Jiao, Y. Li, J. Niu, X. Xie, X. Wang, B. Tang, Anal. Chem. 90 (2018) 533-555; d) L. Wu, A. C. Sedgwick, X. Sun, S. D. Bull, X.-P. He, T. D. James, Acc. Chem. Res. 52 (2019) 2582-2597.

[18] J. Zielonka, J. Joseph, A. Sikora, M. Hardy, O. Ouari, J. Vasquez-Vivar, G. Cheng, M. Lopez, B. Kalyanaraman, Chem. Rev. 117 (2017) 10043-10120.

[19] For selected reviews, see: a) S. Dong, L. Zhang, Y. Lin, C. Ding, C. Lu, Analyst 145 (2020) 5068-5089; b) T. Yudhistira, S. V. Mulay, Y. Kim, M. B. Halle, D. G. Churchill, Chem. - Asian J. 14 (2019) 3048-3084.

[20] a) C. Liu, Q. Wang, X. Jiao, H. Yao, S. He, L. Zhao, X. Zeng, Dyes Pigm. 160 (2019) 989-994; b) H. Li, Y. Miao, Z. Liu, X. Wu, C. Piao, X. Zhou, Dyes Pigm. 176 (2020) 108192; c) Y. Zhao, Y. Xue, J. Sun, H. Xuan, Y. Xu, Y. Cui, J. Dong, New J. Chem. 44 (2020) 12674-12679.

[21] a) F. Fringuelli, O. Piermatti, F. Pizzo, Synthesis (2003) 2331-2334; b) S. Debieu, A. Romieu, Org. Biomol. Chem. 13 (2015) 10348-10361.

[22] A. M. Brouwer, Pure Appl. Chem. 83 (2011) 2213-2228.

N-Alkylation of 2-methoxy-10*H*-phenothiazine revisited. A facile entry to diversely N-substituted phenothiazine-coumarin hybrid dyes

Valentin Quesneau[a,‡,*], Kévin Renault[a,‡], Myriam Laly[a], Sébastien Jenni[a], Flavien Ponsot[a], Anthony Romieu[a,*]

[a]*Institut de Chimie Moléculaire de l'Université de Bourgogne, UMR 6302, CNRS, Univ. Bourgogne Franche-Comté, 9 Avenue Alain Savary, 21078 Dijon cedex, France*

E-mail: *valentin.quesneau@u-bourgogne.fr* *or* *anthony.romieu@u-bourgogne.fr*

‡ These authors contributed equally to this work

Supporting Information

Table of Contents

Abbreviations

The following abbreviations/acronyms are used throughout the text of the SI file: Abs, absorption; AcOH, acetic acid; aq., aqueous; Ar, argon; ATR, attenuated total reflectance; BBOF, double resonance broadband observe; MeCN, acetonitrile; MeOH, methanol; d, doublet; dd, doublet of doublet; ddd, doublet of doublet of doublet; DAD, diode array detector/detection; DCM, dichloromethane; DME, 1,2-dimethoxyethane; DMF, *N*,*N*-dimethylformamide; DMSO, dimethylsulfoxide; equiv., equivalent(s); Em., emission; ESI, electrospray ionization; Et_2O, diethyl ether; EtOAc, ethyl acetate; EtOH, ethanol; Ex., excitation; FA, formic acid; FLD, fluorescence detector; h, heptuplet; HPLC, high-pressure liquid chromatography; iPrOH, isopropanol; IR, infrared; K, degree Kelvin; K_2CO_3, potassium carbonate; KI, potassium iodide; LRMS, low-resolution mass spectrum; m, multiplet; min, minutes; $MgSO_4$, magnesium sulfate; MS, mass spectrometry; MsCl, mesyl chloride; NaCl, sodium chloride; NaH, sodium hydride; $NaHCO_3$, sodium bicarbonate; Na_2SO_4, sodium sulfate; NH_4Cl, ammonium chloride; NH_4OAc, ammonium acetate; NMR, nuclear magnetic resonance; O/N, overnight; PACSMUB, plateforme d'analyse chimique et de synthèse moléculaire de l'université de bourgogne; PBS, phosphate buffered saline; PTZ, phenothiazine; q, quartet; qd, quartet of doublet; RP, reversed-phase; rpm, rounds per minute; RT, room temperature; $Ru(bpy)_3$, tris(2,2'-bipyridyl)dichlororuthenium(II) hexahydrate; s, singlet; t, triplet; TBO, triple resonance broadband; TEA, triethylamine or triethylammonium cation; TEAB, triethylammonium bicarbonate; TFA, trifluoroacetic acid or trifluoroacetate anion; TLC, thin-layer chromatography; t_R, retention time; Tween® 80, polysorbate 80; UV, ultraviolet; vis, visible.

General

Unless otherwise noted below, all commercially available reagents and solvents were used without further purification. Methanesulfonyl chloride (MsCl, [124-63-0]) was distilled prior to use[1]. TLC were carried out on Merck DC Kieselgel 60 F-254 aluminum sheets. The spots were directly visualized and through illumination with dual wavelength UV lamp (λ = 254 and 365 nm). Column chromatography purifications were performed with different types of silica gel for which specifications are given throughout the description of synthetic protocols. DCM, MeCN and THF were dried over alumina cartridges immediately prior to use, using a solvent purification system PureSolv PS-MD-5 model from Innovative Technology. EtOH was dried prior to use by stirring over anhydrous Na_2SO_4 prior and under Ar. DMF was purchased from Carlo Erba (RPE grade) and dried by storage over activated 3 Å molecular sieves. Peptide synthesis-grade piperidine (#SOL-010) and DMF (RS, #P0343521) were provided by Iris Biotech GmbH and Carlo Erba respectively. $Ru(bpy)_3$ (99.95% trace metal basis, #544981), DMSO (for molecular biology, #D8418) and formic acid (puriss p.a., ACS reagent, reag. Ph. Eur., ≥98%, #33015) were purchased from Sigma-Aldrich. The HPLC-gradient grade MeCN was obtained from Carlo Erba, Fisher Scientific or VWR. PBS (10 mM phosphate + 137 mM NaCl + 2.7 mM KCl, prepared from PBS tablets, Fisher BioReagents, #BP2944-100) and aq. mobile-phases for HPLC were prepared using ultrapure water produced by an ELGA PURELAB Ultra system (purified to 18.2 MΩ.cm). TEAB buffer (1.0 M, pH 7.5) was prepared from distilled TEA and CO_2 gas.

Instruments and methods

Centrifugation operations were performed with a Thermo Scientific Espresso Personal Microcentrifuge instrument. Centrifugation steps required for isolation of DPP pigments were performed with an Hettich Universal 320 instrument (with the following parameters: 15 min, 3000 rpm). ^{1}H-, ^{13}C- and ^{19}F-NMR spectra were recorded on Bruker spectrometers: Avance Neo 400 MHz equipped with a 5 mm TBO probe, Avance Neo 500 MHz equipped with a 5 mm BBOF iProbe and Avance III HD 600 MHz equipped with a 5 mm BBOF N_2 cryoprobe. NMR spectroscopy chemical shifts are quoted in parts per million (ppm) relative to TMS (for ^{1}H, and ^{13}C) and $CFCl_3$ (for ^{19}F). For ^{1}H and ^{13}C spectra, calibration was made by using residual signals of partially deuterated solvent summarized by Fulmer *et al.*[2] *J* values are expressed in Hz. IR spectra were recorded with a Bruker Alpha FT-IR spectrometer equipped with an universal ATR sampling accessory. The bond vibration frequencies are expressed in reciprocal centimeters (cm^{-1}). HPLC-MS analyses were performed on a Thermo-Dionex Ultimate 3000 instrument (pump + autosampler at 20 °C + column oven at 25 °C) equipped with a DAD (Thermo-Dionex DAD 3000-RS) and a MSQ Plus single quadrupole mass spectrometer. HPLC-fluorescence analyses were performed with the same instrument but connected to Thermo Scientific Dionex UltiMate 3000 fluorescence detector FLD-3400 RS dual-PMT. Purifications by semi-preparative HPLC were performed on a Thermo-Dionex Ultimate 3000 instrument (semi-preparative pump HPG-3200BX) equipped with a RS Variable

[1] W. L. F. Armarego, D. D. Perrin *Purification of Laboratory Chemicals, Fourth Edition*; Pergamon, 1997. pp 260.

[2] G. R. Fulmer, A. J. M. Miller, N. H. Sherden, H. E. Gottlieb, A. Nudelman, B. M. Stoltz, J. E. Bercaw, K. I. Goldberg, Organometallics 29 (2010) 2176-2179.

Detector (VWD-3400RS, four distinct wavelengths within the range 190-800 nm). Lyophilization operations were performed with a Christ Alpha 2-4 LD plus. TFA mass content of samples purified by semi-preparative was determined by ion chromatography according to a method developed by the PACMSUB staff. Such analyses were performed with an ion chromatograph Thermo Scientific Dionex ICS 5000 equipped with a conductivity detector CD (Thermo Scientific Dionex) and a conductivity suppressor ASRS-ultra II 4 mm (Thermo Scientific Dionex). Low-resolution mass spectra (LRMS) were recorded either on a Thermo Scientific MSQ Plus single quadrupole equipped with an electrospray (ESI) source (LC-MS coupling mode), or on a Bruker Amazon SL instrument equipped with an ESI source (direct introduction mode). UV-visible spectra were obtained on a Varian Cary 50 Scan (single-beam) spectrophotometer (software Cary WinUV) or on an Agilent Cary 60 UV-Vis (single-beam) spectrophotometer (software Cary WinUV) by using rectangular quartz cells (Hellma, 100-QS, 45 × 12.5 × 12.5 mm, pathlength: 10 mm, chamber volume: 3.5 mL), at 25 °C (using a temperature control system combined with water circulation, LAUDA). Fluorescence spectroscopic stuides were performed with an HORIBA Jobin Yvon Fluorolog spectrofluorometer (software FluorEssence) at 25 °C (using a temperature control system combined with water circulation, LAUDA), with standard fluorometer cells (Labbox, LB Q, light path: 10 mm, width:10 mm, chamber volume: 3.5 mL) Excitation/emission spectra were recorded after emission/excitation at the suitable wavelength (set of parameters for Fluorolog: shutter: Auto Open, excitation/emission slit = 5 nm, integration time = 0.1 s, 1 nm step, HV(S1) = 950 V). All fluorescence spectra were corrected until 850 nm. Fluorescence emission spectrum of solvent/buffer was also recorded under the same conditions to substract contribution of Raman scattering. Relative fluorescence quantum yields were measured in the corresponding buffer at 25 °C by a relative method using the suitable standard (see table S1, dilution by a factor ×10 between absorption and fluorescence measurements). The following equation was used to determine the relative fluorescence quantum yields:

$$\Phi_F(x) = (A_S/A_X)(F_X/F_S)(n_X/n_S)^2\Phi_F(s)$$

where A is the absorbance (in the range of 0.01-0.1 A.U.), F is the area under the emission curve reduced by the value of area under the emission curve of buffer solution, n is the refractive index of the solvents (at 25 °C) used in measurements, and the subscripts s and x represent standard and unknown, respectively. The following refractive index values have been used: 1.337 for PBS and PBS + Tween® 80, 1.333 for water and 1.328 for MeOH.

High-performance liquid chromatography systems

Five chromatographic systems were used for the analytical experiments: *System A-QC*: RP-HPLC (Phenomenex Kinetex C_{18} column, 2.6 µm, 2.1 × 50 mm) with MeCN (+ 0.1% FA) and 0.1% aq. formic acid (aq. FA, pH 2.5) as eluents [5% MeCN (0.1 min) followed by linear gradient from 5% to 100% (5 min) MeCN, then 100% MeCN (5 min)] at a flow rate of 0.5 mL/min. UV-visible detection was achieved at four distinct wavelengths in the range 220-450 nm (variables according to the compound to be analyzed + DAD in the range 220-600 nm). Low resolution ESI-MS detection in the positive/negative mode (full scan, 100-2000 a.m.u., peaking format: centroid, needle

voltage: 3.0 kV, probe temperature: 350 °C, cone voltage: 75 V and scan time: 1 s). *System B-QC*: system A-QC with the following parameters, UV-visible detection was achieved at 214, 260, 460 and 520 nm (+diode array detection in the range of 200-800 nm). *System C-QC*: system A-QC with the following parameters, UV-visible detection was achieved at 220, 260, 450 and 500 nm (+ DAD in the range 220-700 nm). Low resolution ESI-MS detection in the positive/negative mode (full scan, 100-1000 a.m.u., data type: centroid, needle voltage: 3.0 kV, probe temperature: 350 °C, cone voltage: 75 V and scan time: 1 s). *System D-Fluo*: RP-HPLC (Phenomenex Kinetex C_{18} column, 2.6 µm, 2.1 × 50 mm) with MeCN (+ 0.1% FA) and 0.1% aq. FA as eluents [5% MeCN (0.1 min) followed by linear gradient from 5% to 100% (5 min) MeCN, then 100% MeCN (3 min)] at a flow rate of 0.5 mL/min. Fluorescence detection was achieved at 45 °C at the following Ex./Em. channels: 450/700 nm and 400/520 nm (sensitivity: 1, PMT Auto, filter wheel: auto). *System E-MS*: system D-Fluo with the following detection parameters, UV-visible detection at 220, 250, 310 and 455 nm for **10**, 220, 250, 300 and 425 nm for **15** and 220, 250, 310 and 440 nm for **16** (+DAD in the range 220-800 nm). Low resolution ESI-MS detection in the positive/negative mode (full scan, 100-1000 a.m.u. and SIM mode (ESI+ at the corresponding *m/z* value, specific to each PTZ-coumarin hybrid dye and its sulfoxide derivative).

Six chromatographic systems were used for purification of several PTZ derivatives: *System A*: semi-preparative RP-HPLC (SiliCycle SiliaChrom C_{18} column, 10 µm, 20 × 250 mm) with MeCN and ultrapure H_2O as eluents [10% MeCN (5 min), followed by a linear gradient from 10% to 25% MeCN (7.5 min), then 25% to 100% MeCN (87.5 min)] at a flow rate of 20.0 mL/min. Quadruple UV-vis detection was achieved at 220, 260, 316 and 503 nm. *System B*: semi-preparative RP-HPLC (SiliCycle SiliaChrom C_{18} column, 10 µm, 20 × 250 mm) with MeCN and 0.1% TFA (pH 2.0) as eluents [25% MeCN (5 min), followed by a linear gradient from 25% to 50% MeCN (12.5 min), then 50% to 100% MeCN (60 min)] at a flow rate of 20.0 mL/min. Quadruple UV-vis detection was achieved at 220, 260, 450 and 500 nm. *System C*: system B with the followiong gradient [0% MeCN (5 min), followed by a linear gradient from 0% to 20% MeCN (10 min), then 20% to 100% MeCN (80 min)] at a flow rate of 20.0 mL/min. Quadruple UV-vis detection was achieved at 220, 240, 270 and 385 nm. *System D*: system B with the following gradient [0% MeCN (5 min), followed by a linear gradient from 0% to 10% MeCN (5 min), then 10% to 100% MeCN (100 min)] at a flow rate of 20.0 mL/min. Quadruple UV-vis detection was achieved at 220, 250, 310 and 440 nm. *System E*: semi-preparative RP-HPLC (SiliCycle SiliaChrom C_{18} column, 10 µm, 20 × 250 mm) with MeCN and ultrapure H_2O as eluents [0% MeCN (5 min), followed by a linear gradient from 0% to 10% MeCN (5 min), then 10% to 100% MeCN (100 min)] at a flow rate of 20.0 mL/min. Quadruple UV-vis detection was achieved at 220, 250, 310 and 440 nm. *System F*: semi-preparative RP-HPLC (SiliCycle SiliaChrom C_{18} column, 10 µm, 20 × 250 mm) with MeCN and aq. TEAB (50 mM, pH 7.5) [0% MeCN (5 min), followed by a linear gradient from 0% to 20% MeCN (10 min), then 20% to 100% MeCN (80 min)] at a flow rate of 20.0 mL/min. Quadruple UV-vis detection was achieved at 220, 250, 310 and 440 nm.

Synthesized compounds

Please note: All PTZ derivatives described in this section, must be kept at -20 °C, under Ar, protected from light, to avoid degradation over prolonged storage.

N-Butyl-2-methoxy-10*H*-phenothiazine [2131803-55-7] (2). 2-Methoxy-10*H*-phenothiazine [1771-18-2] **1** (1.0 g, 4.36 mmol, 1 equiv.) was solubilized in dry DMF (12 mL) at RT. Then, NaH (60% w/w dispersion in mineral oil, 209 mg, 8.72 mmol, 2 equiv.) was added portionwise to the previous solution at 0 °C. After 5 min, 1-bromobutane (936 μL, 8.72 mmol, 2 equiv.) was added and the resulting reaction mixture was stirred at 0 °C for 90 min. The reaction was checked for completion by TLC (eluent: DCM 100%). Thereafter, the reaction mixture was diluted with DCM and washed once with dionized water. The aqueous phase was washed twice with DCM and the combined organic phase was dried over anhydrous $MgSO_4$, filtered and concentrated under reduced pressure. The resulting residue was purified by flash-column chromatography over silica gel (VWR, technical grade 40-63 μm, #84814.360, eluent: DCM) to give N-butyl-2-methoxyphenothiazine **2** as colorless oil (1.18 g, 3.70 mmol, yield 85%). ^{1}H NMR (500 MHz, $CDCl_3$): δ = 7.14 (ddd, $^3J_{H\text{-}H}$ = 7.2 Hz, $^4J_{H\text{-}H}$ = 4.3 Hz, $^4J_{H\text{-}H}$ = 2.6 Hz, 2H), 7.02 (d, $^3J_{H\text{-}H}$ = 8.2 Hz, 1H), 6.94-6.88 (m, 1H), 6.88-6.85 (m, 1H), 6.53-6.44 (m, 2H), 3.83 (t, $^3J_{H\text{-}H}$ = 7.2 Hz, 2H), 3.78 (s, 3H), 1.80 (qd, $^3J_{H\text{-}H}$ = 7.5 Hz, $^3J_{H\text{-}H}$ = 5.8 Hz, 2H), 1.46 (h, $^3J_{H\text{-}H}$ = 7.4 Hz, 2H), 0.95 (t, $^3J_{H\text{-}H}$ = 7.4 Hz, 3H). All other spectroscopic data are identical to those reported in the literature[3].

3-Dimethylaminopropyl methanesulfonate (hydrochloride salt) [52413-48-6]. This procedure was adapted from a published protocol.[4] Under Ar, 3-dimethylamino-1-propanol (5.16 g, 5.92 mL, 50.0 mmol, 1 equiv.) was dissolved in dry THF (100 mL) an d cooled to 0 °C. Then, MsCl (5.73 g, 3.87 mL, 50.0 mmol, 1 equiv.) was added. The resulting reaction mixture become cloudy then a white precipitate appeared. The reaction mixture was stirred with the cool bath for 90 min. Therafter, the mixture was filtered to recover the white solid which was washed with Et_2O and finally dried. The filtrate was again filtered to obtain a second crop of solid. The desired compound was recovered as a white solid (10.2 g, yield 94%). *Please note: since this solid is very hygroscopic, it is recommended to use it immediately after its preparation*. ^{1}H NMR (500 MHz, DMSO-d_6): δ = 10.92 (s, 1H, N<u>*H*</u>), 4.30 (t, $^3J_{H\text{-}H}$ = 6.0 Hz, 2H, MsO-C<u>*H*</u>$_2$), 3.22 (s, 3H, C<u>*H*</u>$_3$-Ms), 3.15-3.08 (m, 2H, CH_2), 2.73 (s, 6H, N(C<u>*H*</u>$_3$)$_2$), 2.12 (m, 2H, CH_2); ^{13}C NMR (151 MHz, DMSO-d_6): δ = 67.6, 53.1, 42.0, 36.7, 23.7.

N-[3-(Dimethylamino)propyl]-2-methoxy-10*H*-phenothiazine [61-01-8] (3). 2-Methoxy-10*H*-phenothiazine [1771-18-2] **1** (5.04 g, 22.0 mmol, 1.0 equiv.) was dissolved in dry DMF (40 mL) and the solution was cooled to 0 °C with an ice bath. NaH (60% w/w dispersion in mineral oil, 2.90 g, 72.6 mmol, 3.3 equiv.) was added portionwise over 1 h. 3-Dimethylaminopropyl methanesulfonate (hydrochloride salt) (9.55 g, 44.0 mmol, 2.0 equiv.) was suspended in dry DMF (20 mL) and added dropwise over 1 h at 0 °C. The resulting reaction mixture was stirred at RT for 18 h. Thereafter, the mixture was

[3] (a) W. Chen, X. Yue, W. Li, Y. Hao, L. Zhang, L. Zhu, J. Sheng, X. Song, Sens. Actuators, B 245 (2017) 702-710; (b) W. Li, S. Zhou, L. Zhang, Z. Yang, H. Chen, W. Chen, J. Qin, X. Shen, S. Zhao, Sens. Actuators, B 284 (2019) 30-35.

[4] N. H. Krämer, H. F. G. Linde, Arch. Pharm. 324 (1991) 527-528.

concentrated under reduced pressure. The resulting residue was dissolved in a DCM-Et_2O mixture (1:1, v/v) and this organic phase was washed four times with deionized water, dried over anhydrous Na_2SO_4 and finally evaporated under reduced pressure. The resulting residue was purified by column chromatography over silica gel (VWR, technical grade 40-63 μm, #84814.360, 200 mL of dry silica, eluent: a step gradient of acetone in toluene from 0% to 100%). The first fraction (unreacted 2-methoxyphenothiazine **1**, 1.55 g) and the second one were collected. The desired N-alkyl phenothiazine derivative **3** was recovered as a dark brown viscous oil (1.58 g, 5.0 mmol, yield 23% or 33% based on the recovered unreacted starting PTZ). R_f (DCM-iPrOH, 4:1, v/v) = 0.22; IR (ATR): ν_{max} = 3400, 2954, 2925, 2869, 2855, 2330, 1584, 1491, 1461, 1444, 1378, 1289, 1264, 1207, 1174, 1129, 1107, 1033, 966, 800, 751, 454; ^{1}H NMR (500 MHz, $CDCl_3$): δ = 7.17-7.12 (m, 2H), 7.05-7.01 (m, 1H), 6.93-6.88 (m, 2H), 6.49 (d, $^3J_{H-H}$ = 7.2 Hz, 2H), 3.93-3.87 (m, 2H), 3.79 (s, 3H), 2.41 (t, $^3J_{H-H}$ = 7.1 Hz, 2H), 2.22 (s, 6H), 2.01-1.92 (m, 2H); ^{13}C NMR (151 MHz, $CDCl_3$): δ = 159.8, 146.7, 145.1, 127.6, 127.4, 127.1, 125.7, 122.4, 116.2, 115.6, 106.8, 103.4, 57.2, 55.5, 45.6, 45.5, 25.3; HPLC (system A-QC): t_R = 3.7 min (purity >98% at 280 nm and 350 nm); UV-vis (recorded during the HPLC analysis): λ_{max} = 221 and 251 nm; LRMS (ESI+, recorded during RP-HPLC analysis): *m/z* 315.3 $[M + H]^+$, calcd for $C_{18}H_{23}N_2OS^+$ 315.1

5-Oxo-2-(4-bromophenyl)-4,5-dihydropyrrole-3-carboxylic acid ethyl ester [1255381-83-9][5] (S1).
A solution of ethyl 3-(4-bromophenyl)-3-oxopropanoate [26510-95-2][6] (20.4 g, 75.4 mmol, 1.0 equiv.), ethyl chloroacetate (8.10 mL, 75.4 mmol, 1.0 equiv.), anhydrous K_2CO_3 (10.94 g, 79.1 mmol, 1.05 equiv.) and KI (1.88 g, 11.3 mmol, 0.15 equiv.) in acetone (80 mL) and DME (50 mL) was refluxed under Ar for 24 h. The mixture was then cooled to RT and filtered to remove remaining insoluble K_2CO_3. The solid was washed with acetone and the filtrate was evaporated to give a pale brown oil. The crude product was solubilized in glacial AcOH (130 mL) and NH_4OAc (56.34 g, 731.0 mmol, 9.7 equiv.) was added. The resulting reaction mixture was refluxed for 3 h. Thereafter, the mixture was then cooled to RT and poured in ice-water (400 mL) to form a precipitate that was filtered and washed with deionized water. The crude product was recrystallized in a EtOH-water (4:1, v/v, 400 mL) mixture, filtered and washed with cold EtOH-water mixture and finally with deionized water. **S1** was obtained as a dark-grey solid (14.7 g, 47.3 mmol, yield 63%). ^{1}H NMR (500 MHz, $CDCl_3$): δ = 8.29 (brs, 1H), 7.59 (d, $^3J_{H-H}$ = 8.6 Hz, 2H), 7.50 (d, $^3J_{H-H}$ = 8.6 Hz, 2H), 4.14 (q, $^3J_{H-H}$ = 7.1 Hz, 2H), 3.49 (s, 2H), 1.20 (t, $^3J_{H-H}$ = 7.1 Hz, 3H); ^{13}C NMR (126 MHz, $CDCl_3$): δ = 177.1, 163.1, 150.1, 131.8 (2C), 130.4 (2C), 128.3, 125.3, 105.2, 60.4, 38.8, 14.4; LRMS (ESI+, direct introduction): *m/z* = 309.9 $[M + H]^+$, calcd for $C_{13}H_{13}BrNO_3^+$ 310.0.

4-Methoxybenzonitrile [874-90-8][7] (S2). A mixture of 4-hydroxybenzonitrile (1.19 g, 10.0 mmol, 1.0 equiv.) and anhydrous K_2CO_3 (1.70g, 12.0 mmol, 1.2 equiv.) in acetone (30 mL) was refluxed. Methyl iodide (0.75 mL, 12.0 mmol, 1.2 equiv) was added and the resulting reaction mixture was refluxed O/N. The mixture was cooled down to RT,

[5] Y. Xu, Y. Jin, W. Lin, J. Peng, H. Jiang, D. Cao, Synth. Met. 160 (2010) 2135-2142.
[6] L. Li, E. Babaoglu, K. Harms, G. Hilt, Eur. J. Org. Chem. 2017 (2017) 4543-4547.
[7] M. Hatsuda, M. Seki, Tetrahedron 61 (2005) 9908-9917.

filtered and water was added. The product was extracted with DCM three times. The combined organic layers were dried over anhydrous Na_2SO_4, filtered and the solvent was evaporated under reduced pressure. The product was purified by column chromatography over silica gel (Aldrich, technical grade 40-63 μm, #717185, eluent: DCM). **S2** was obtained as a white solid (1.15 g, 8.63 mmol, yield 87%). ^{1}H NMR (500 MHz, $CDCl_3$): δ = 7.58 (d, $^3J_{H\text{-}H}$ = 8.9 Hz, 2H), 6.95 (d, $^3J_{H\text{-}H}$ = 8.9 Hz, 2H), 3.86 (s, 3H); ^{13}C NMR (126 MHz, $CDCl_3$): δ = 163.0, 134.1 (2C), 119.4, 114.9 (2C), 104.1, 55.7; LRMS (ESI+, direct introduction): *m/z* = 156.1 $[M + Na]^+$, calcd for $C_8H_7NNaO^+$ 156.0.

3-(4-Bromophenyl)-2,5-dihydro-6-(4-methoxyphenyl)-diketopyrrolopyrrole (4). Na° (415 mg, 18.1 mmol, 2.2 equiv.) was dissolved in 2-methybutan-2-ol (35 mL) at 100 °C under N_2. The solution was cooled down to 50 °C and **S1** (2.60 g, 8.4 mmol, 1.0 equiv.) was added followed by **S2** (1.00 g, 8.4 mmol, 1.0 equiv.). The resulting reaction mixture was stirred at 120 °C under N_2 for 24 h. The mixture was cooled down to RT and glacial AcOH (7 mL) was added. The mixture was centrifuged and the solid was washed with EtOH-water (1:1, v/v) until the recovered supernatant was clear. DPP pigment **4** was obtained as a dark-red solid (1.75 g, 4.4 mmol, yield 58%). *Please note: the very poor solubility of this unsymmetrical DPP pigment in most of organic solvents has prevented its spectroscopic characterization, especially by NMR measurements.*

Methoxybenzyl-protected unsymmetrical phenol-diketopyrrolopyrrole (5). This DPP pigment was prepared from **S1** (4.0 g, 12.9 mmol, 1.0 equiv.) and 4-[(4-methoxyphenyl)methoxy]-benzonitrile [31574-12-6][8] (3.09 g, 12.9 mmol, 1.0 equiv.), using the procedure described for **4**. Dark-red solid (3.51 g, 6.97 mmol, yield 54%). *Please note: the very poor solubility of this unsymmetrical DPP pigment in most of organic solvents has prevented its spectroscopic characterization, especially by NMR measurements.*

6-(4-Bromophenyl)-2,5-dihydro-3-(4-pyridyl)-diketopyrrolopyrrole (6). This DPP pigment was prepared from **S1** (2.0 g, 6.4 mmol, 1.0 equiv.) and 4-cyanopyridine (670 mg, 6.4 mmol, 1.0 equiv.), using the procedure described for **4**. Dark-red solid (1.72 g, 4.6 mmol, yield 73%). *Please note: the very poor solubility of this unsymmetrical DPP pigment in most of organic solvents has prevented its spectroscopic characterization, especially by NMR measurements.*

Methyl-protected unsymmetrical phenol-diketopyrrolopyrrole *N,N′*-dimethylaminopropyl (7). A suspension of DPP pigment **4** (100 mg, 0.25 mmol, 1.0 equiv.), NaH (60% w/w dispersion in mineral oil, 55.0 mg, 1.38 mmol, 5.5 equiv.) and TBAI (5.0 mg, 13.5 μmol, 0.05 equiv.) in dry DMF (8 mL) was stirred at 80 °C under N_2 for 30 min. A solution of 3-dimethyaminopropyl chloride hydrochloride (398 mg, 2.52 mmol, 10.0 equiv.) and NaH (60% w/w dispersion in mineral oil, 60 mg, 2.52 mmol, 10.0 equiv.) in dry DMF (2 mL) was added. The resulting reaction mixture was stirred at 80 °C under N_2 for 24 h. Thereafter, the mixture was cooled down to RT and the solvent was

[8] S. K. Yeon, J. W. Choi, J.-H. Park, Y. R. Lee, H. J. Kim, S. J. Shin, B. K. Jang, S. Kim, Y.-S. Bahn, G. Han, Y. S. Lee, A. N. Pae, K. D. Park, Bioorg. Med. Chem. 26 (2018) 232-244.

evaporated under reduced pressure. Deionized water was added and the product was extracted with DCM three times. The combined organic layers were dried over anhydrous Na_2SO_4, filtered and the solvent was evaporated under reduced pressure. The product was purified by column chromatography over silica gel (Aldrich, technical grade 40-63 μm, #717185, eluent: DCM-MeOH-TEA (98:1:1, v/v/v). Compound **7** was obtained as an orange solid (41.0 mg, 72.2 μmol, yield 29%). *Please note: due to the small amount recovered and the failure of the synthetic strategy involving the use of this N,N' dimethyl-aminopropyl-functionalized DPP dye, a second synthesis (at a larger scale) was not regarded and the compound was only characterized by HPLC-MS.* HPLC (system B-QC): t_R = 3.3 min (purity 97% at 460 nm); UV (recorded during RP-HPLC analysis): λ_{max} = 267, 324 and 466 nm; LRMS (ESI+, recorded during RP-HPLC analysis): *m/z* 567.3 $[M + H]^+$, calcd $C_{29}H_{36}BrN_4O_3^+$ for 567.2.

N-Butyl-3-carboxaldehyde-2-hydroxy-10*H*-phenothiazine (9) [2131803-57-9]. This compound was prepared from N-butyl-2-methoxy-10*H*-phenothiazine **2**, using a two-step procedure published in the literature[9].

N-Butyl-3-cyano-PTZ-coumarin hybrid dye [2241337-19-7] (10). Salicylaldehyde **9** (38 mg, 0.13 mmol, 1 equiv.) and malononitrile (9 mg, 0.13 mmol, 1.05 equiv.) were solubilized in absolute EtOH (5 mL) at RT. Then, anhydrous Na_2SO_4 (10 mg) and piperidine (1 drop) were sequentially added. The resulting reaction mixture was stirred O/N. The reaction was checked for completion by HPLC-MS (System C-QC). Thereafter, the reaction mixture was concentrated under reduced pressure. The resulting residue was purified by semi-preparative RP-HPLC (system A, t_R = 61.0-64.0 min). The product-containing fractions were freeze-dried to recover the corresponding 2-iminocoumarin as red amorphous powder (8.5 mg, 0.24 mmol, yield 19%). Imine hydrolysis was performed through incubation in a 1% aq. TFA-MeCN (2:3, v/v, 5 mL) mixture for 10 min and a change in color from orange-red to purple was observed. Thereafter, the crude solution was directly purified by semi-preparative RP-HPLC (system B, t_R = 43.0-46.0 min). The product-containing fractions were freeze-dried to give PTZ-coumarin hybrid dye **10** as red amorphous powder (2.6 mg, 80 μmol, yield 6%); IR (ATR): ν_{max} = 3433, 3039, 2957, 2917, 2850, 2224, 1983, 1786, 1734, 1719, 1598, 1571, 1542, 1492, 1465, 1439, 1412, 1383, 1365, 1349, 1333, 1289, 1263, 1250, 1230, 1209, 1171, 1143, 1112, 1100, 1051, 957, 899, 863, 840, 799, 780, 759, 732, 694, 672, 657, 620, 590, 548, 536, 465, 432; ^{1}H NMR (600 MHz, $CDCl_3$): δ = 7.99 (s, 1H), 7.23-7.18 (m, 1H), 7.16 (s, 1H), 7.10 (dd, $^3J_{H-H}$ = 7.6 Hz, $^4J_{H-H}$ =1.5 Hz, 1H), 7.05-7.00 (m, 1H), 6.93 (dd, $^3J_{H-H}$ = 8.3 Hz, $^4J_{H-H}$ = 1.1 Hz, 1H), 6.71 (s, 1H), 3.93-3.86 (m, 2H), 1.88-1.78 (m, 2H), 1.48 (h, $^3J_{H-H}$ = 7.4 Hz, 2H), 0.98 (t, $^3J_{H-H}$ = 7.4 Hz, 3H); ^{13}C NMR (151 MHz, $CDCl_3$) δ = 157.4, 156.3, 152.0, 150.0, 141.9, 128.1, 127.7, 125.7, 124.6, 122.8, 122.3, 116.5, 114.5, 112.2, 102.5, 97.9, 48.6, 28.6, 20.2, 13.8; HPLC (system C-QC): t_R = 5.6 min (purity >99% at 260 nm and 450 nm); UV-vis (recorded during the RP-HPLC analysis): λ_{max} = 253, 311 and 453 nm; LRMS (ESI+, recorded during RP-HPLC analysis): *m/z* 349.2 $[M + H]^+$ (100), 697.2 $[2M + H]^+$ (57), calcd for $C_{20}H_{17}N_2O_2S^+$ 349.1; UV-vis (MeOH, 25 °C):

[9] W. Chen, L. Zhu, Y. Hao, X. Yue, J. Gai, Q. Xiao, S. Huang, J. Sheng, X. Song, Tetrahedron 73 (2017) 4529-4537.

λ_{max} = 309 nm (ε 10 800 M^{-1} cm^{-1}) and 451 nm (ε 11 900 M^{-1} cm^{-1}); UV-vis (PBS, pH 7.3, 25 °C): λ_{max} = 320 nm (ε 10 300 M^{-1} cm^{-1}) and 483 nm (ε 9 800 M^{-1} cm^{-1}); UV-vis (PBS + 300 µM Tween® 80, pH 7.3, 25 °C): 314 nm (ε 11 600 M^{-1} cm^{-1}) and 462 nm (ε 11 200 M^{-1} cm^{-1}); Fluorescence (MeOH, 25 °C): λ_{max} = 678 nm (Φ_F 1.6%); Fluorescence (PBS, pH 7.3, 25 °C): λ_{max} = 664 nm (Φ_F 2.8%); Fluorescence (PBS + 300 µM Tween® 80, pH 7.3, 25 °C): λ_{max} = 645 nm (Φ_F 4.8%).

N-[3-(Dimethylamino)propyl]-3-carboxaldehyde-2-methoxy-10*H*-phenothiazine (11). Using Schlenk tube technique, $POCl_3$ (883 mg, 539 µL, 5.76 mmol, 1.2 equiv.) and dry DMF (750 µL) were mixed and stirred at 50 °C for 40 min. Then, compound **3** (1.51 g, 4.80 mmol, 1.0 equiv.) was dissolved in dry DMF (1.5 mL) and the resulting solution was added dropwise during 5 min. The resulting reaction mixture was stirred at 60 °C for 4 h. Thereafter, the reaction mixture was diluted with DCM, and sequentially washed with sat. aq. $NaHCO_3$, aq. K_2CO_3 (pH 12) and brine. The emulsion was extracted thrice with a DCM-iPrOH mixture (1:1, v/v, 3 × 200 mL). The combined organic phases were dried over anhydrous Na_2SO_4 and evaporated under reduced pressure. The resulting residue was purified by column chromatography over silica gel (VWR, technical grade 40-63 µm, #84814.360, 125 mL of dry bed, eluent: a step gradient of MeOH in DCM from 0% to 20%). The product-containing fractions (yellow color) were collected, combined and evaporated under reduced pressure to give aldehyde **11** as a yellow oil (1.41 g, 4.12 mmol, yield 86%). R_f (DCM-iPrOH 4:1, v/v) = 0.08; IR (ATR): ν_{max} = 2941, 2857, 2817, 2765, 1661, 1596, 1569, 1459, 1445, 1412, 1394, 1335, 1302, 1283, 1255, 1209, 1157, 1099, 1040, 995, 905, 823, 800, 645, 597, 558, 532, 491, 452; ^{1}H NMR (400 MHz, $CDCl_3$): δ = 10.12 (s, 1H, C*H*O), 7.46 (s, 1H), 7.10-7.01 (m, 2H,), 6.91-6.81 (m, 2H), 6.35 (s, 1H), 3.90 (dd, $^3J_{HH}$ = 7.8 Hz, $^3J_{HH}$ = 6.3 Hz, 2H), 3.83 (s, 3H), 2.33 (t, $^3J_{HH}$ = 6.9 Hz, 2H), 2.14 (s, 6H), 1.89 (p, $^3J_{HH}$ = 7.0 Hz, 2H); ^{13}C NMR (101 MHz, $CDCl_3$): δ = 187.2, 162.7, 152.5, 143.0, 127.6, 127.3, 126.9, 124.9, 123.6, 119.7, 116.2, 116.1, 98.9, 56.9, 55.8, 46.1, 45.6, 25.3; HPLC (system A-QC): t_R = 3.6 min (purity >98% at 280 and 350 nm); UV-vis (recorded during the RP-HPLC analysis): λ_{max} = 241, 267 and 386 nm; LRMS (ESI+, recorded during RP-HPLC analysis): *m/z* 343.4 $[M + H]^+$, calcd for $C_{19}H_{23}N_2O_2S^+$ 343.1.

N-[3-(Dimethylamino)propyl]-3-carboxaldehyde-2-hydroxy-10*H*-phenothiazine (12). *Please note: in order to increase the yield of this reaction, this latter was performed using a carousel 12 reaction tubes station (Radleys, #BN3818, picture below). Herein, is described the experimental procedure for one reaction tube.*

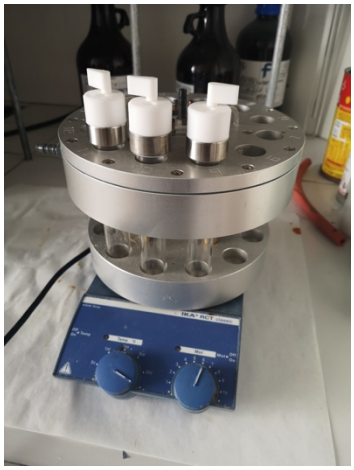

Under Ar, aluminum powder (Aldrich, #21,475-2, 74 µm, 23 mg, 0.85 mmol, 2.50 equiv.) was added in 1 mL of dry MeCN then, I_2 (134 mg, 0.53 mmol, 1.55 equiv.) was added. The color of solution turned from yellow-brown to colorless. To this solution, aryl methyl ether **11** (for one reaction, 117 mg, 0.34 mmol, 1.0 equiv.) in solution in dry MeCN (2 mL) was added dropwise. The color of solution turned to red then the reaction mixture was stirred at reflux for 3 h 30. Thereafter, all tubes were cooled to RT, diluted

with MeCN and DCM. The organic phase was washed with sat. aq. $NaHCO_3$ and brine, dried over anhydrous Na_2SO_4 and evaporated under reduced pressure. The resulting residue was purified by column chromatography over silica gel (VWR, technical grade 40-63 µm, #84814.360, 125 mL of dry bed, eluent: a step gradient of MeOH in DCM from 0% to 10%). Salicylaldehyde **12** was recovered as a yellow oil (for 12 reactions, 852 mg, 2.60 mmol, yield 63%). R_f (DCM-iPrOH 4:1, v/v) = 0.22; IR (ATR): ν_{max} = 2943, 2818, 2766, 1989, 1633, 1574, 1457, 1417, 1384, 1307, 1287, 1249, 1223, 1201, 1162, 1102, 1041, 883, 838, 797, 749, 481, 415; ^{1}H NMR (400 MHz, $CDCl_3$): δ = 11.36 (s, 1H, O*H*), 9.63 (s, 1H, C*H*O), 7.22-7.11 (m, 3H), 7.03-6.93 (m, 2H), 6.46 (s, 1H), 3.96 (dd, $^3J_{H\text{-}H}$ = 7.9 Hz, $^3J_{H\text{-}H}$ = 6.3 Hz, 2H), 2.42 (t, $^3J_{H\text{-}H}$ = 6.9 Hz, 2H), 2.24 (s, 6H), 1.98 (p, $^3J_{H\text{-}H}$ = 7.0 Hz, 2H); ^{13}C NMR (101 MHz, $CDCl_3$): δ = 193.4, 163.2, 153.3, 142.5, 131.0, 127.5, 124.2, 123.8, 116.4, 116.1, 114.7, 103.2, 56.8, 46.6, 45.5, 24.9; HPLC (system A-QC): t_R = 3.7 min (purity >98% at 280 nm and 350 nm); UV-vis (recorded during the RP-HPLC analysis): λ_{max} = 241, 269 and 388 nm; LRMS (ESI+, recorded during RP-HPLC analysis): *m/z* 329.3 $[M + H]^+$, calcd for $C_{18}H_{21}N_2O_2S^+$ 329.1.

N-[3-(Trimethylammonium)propyl]-3-carboxaldehyde-2-hydroxy-10*H*-phenothiazine, iodide salt (13). Tertiary amine **12** (197 mg, 0.6 mmol, 1.0 equiv.) was dissolved in dry DCM (4 mL), kept under Ar, and methyl iodide (1.7 g, 747 µL, 12.0 mmol, 20 equiv.) was added. The resulting reaction mixture was stirred at 45 °C for 17 h. The newly formed precipitate was isolated by centrifugation and rinsed thrice with DCM. Quaternary ammonium salt **13** was recovered as a yellow powder (220 mg, yield 82% based on 0.81 I^- as counter-ion, determined by ionic chromatogtaphy). IR (ATR): ν_{max} = 3468, 3013, 2861, 1631, 1577, 1455, 1418, 1391, 1332, 1310, 1286, 1262, 1242, 1229, 1199, 1133, 1106, 1056, 1041, 965, 935, 888, 833, 797, 759, 747, 735, 722, 702, 671, 575, 491, 450, 418; ^{1}H NMR (400 MHz, DMSO-d_6): δ = 11.00 (s, 1H, O*H*), 9.96 (s, 1H, C*H*O), 7.43 (s, 1H), 7.28-7.20 (m, 2H), 7.16 (d, $^3J_{H\text{-}H}$ = 8.2 Hz, 1H), 7.05 (t, $^3J_{H\text{-}H}$ = 7.4 Hz, 1H), 6.61 (s, 1H), 3.98 (t, $^3J_{H\text{-}H}$ = 7.0 Hz, 2H), 3.45-3.38 (m, 2H), 3.03 (s, 9H), 2.17-2.11 (m, 2H); ^{13}C NMR (101 MHz, DMSO-d_6): δ = 190.8, 162.3, 152.2, 142.5, 128.6, 128.3, 127.8, 124.4, 124.0, 117.8, 117.2, 114.2, 104.1, 63.5, 52.92, 52.88, 52.84, 44.6, 20.6; HPLC (system A-QC): t_R = 3.6 min (purity >98% at 280 nm and 350 nm); UV-vis (recorded during the RP-HPLC analysis): λ_{max} = 241, 269 and 387 nm; LRMS (ESI+, recorded during RP-HPLC analysis): *m/z* 343.3 $[M]^+$, calcd for $C_{19}H_{23}N_2O_2S^+$ 343.1.

N-[3-(3-Sulfonatopropyl)dimethylammonium)propyl]-3-carboxaldehyde-2-hydroxy-10*H*-phenothiazine, inner salt (14). Tertiary amine **12** (262 mg, 0.8 mmol, 1.0 equiv.) was dissolved in dry DCM (5 mL), kept under Ar, and 1,3 propanesultone (977 mg, 702 µL, 8.0 mmol, 10 equiv.) was added. The resulting reaction mixture was stirred at 45 °C for 24 h. Thereafter, the solution was directly purified by column chromatography over silica gel (VWR, technical grade 40-63 µm, #84814.360, 100 mL of dry bed, eluent: a step gradient of MeOH in DCM from 10% to 50%) to furnish sulfobetain **12** as a yellow amorphous solid (225 mg, yield 62%). To obtain a high purity product, a further purification by semi-preparative RP-HPLC (system C, t_R = 31.0 min) was performed on 55 mg to give 51 mg of TFA salt of **12**. IR (ATR): ν_{max} = 3439, 2191, 2013, 1979, 1654, 1631, 1603, 1571, 1485, 1461, 1442, 1387, 1307, 1289, 1181, 1164, 1106, 1035, 895, 843, 796, 752, 734, 675, 603, 522, 455; ^{1}H NMR (400 MHz, CD_3CN-CD_3OD 5:1, 0.6

mL): δ = 9.72 (s, 1H, C*H*O), 7.40 (s, 1H), 7.31-7.15 (m, 2H), 7.08-7.02 (m, 2H), 6.56 (s, 1H), 4.03 (t, $^3J_{H-H}$ = 6.6 Hz, 2H), 3.39-3.29 (m, 4H), 2.90 (s, 6H), 2.66 (t, $^3J_{H-H}$ = 6.8 Hz, 2H), 2.18 (p, $^3J_{H-H}$ = 6.7 Hz, 2H), 2.05 (p, $^3J_{H-H}$ = 6.9 Hz, 2H); ^{13}C NMR (101 MHz, CD_3CN-CD_3OD 5:1, v/v, 0.6 mL): δ = 194.9, 163.5, 153.8, 143.3, 132.0, 128.8, 128.4, 125.9, 125.1, 118.0, 117.7, 116.3, 104.6, 62.2, 51.51, 51.47, 51.43, 48.0, 45.0, 20.9, 19.6; HPLC (system A-QC): t_R = 3.6 min (purity >98% at 280 nm and 350 nm); UV-vis (recorded during the HPLC analysis): λ_{max} = 269 and 386 nm; LRMS (ESI+, recorded during RP-HPLC analysis): *m/z* 451.3 $[M + H]^+$ and 901.5 $[2M + H]^+$, calcd for $C_{21}H_{27}N_2O_5S_2^+$ 451.1.

N-[3-(Trimethylammonium)propyl]-3-cyano-PTZ-coumarin hybrid dye, TFA salt (15). Salicylaldehyde **13** (52.0 mg, 0.11 mmol, 1 equiv.) was dissolved in a mixture of dry EtOH-MeCN (1:1, v/v, 8 mL). Then, malononitrile (7.0 mg, 0.11 mmol, 1 equiv.) and piperidine (4.7 mg, 5.4 µL, 0.055 mmol, 0.5 equiv.) were sequentially added and the resulting reaction mixture was stirred at RT for 16 h. Thereafter, the reaction mixture was evaporated under reduced pressure and the resulting residue was directly purified by semi-preparative RP-HPLC (system D, t_R = 38.0-43.0 min) to give after freeze-drying TFA salt of PTZ-coumarin hybrid dye **15** (51 mg, 0.09 mmol, yield 82% based on 1.54 TFA as counter-ion, determined by ionic chromatogtaphy). IR (ATR): ν_{max} = 3400, 3038, 2969, 2227, 1722, 1684, 1596, 1573, 1547, 1466, 1445, 1415, 1377, 1339, 1312, 1289, 1247, 1232, 1197, 1169, 1127, 1048, 961, 913, 878, 826, 798, 757, 717, 706, 671, 623, 592, 550, 519, 444, 424; ^{1}H NMR (400 MHz, CD_3OD): δ = 8.49 (s, 1H), 7.54 (s, 1H), 7.34 (ddd, $^3J_{H-H}$ = 8.4 Hz, $^3J_{H-H}$ = 7.3 Hz, $^4J_{H-H}$ = 1.5 Hz, 1H), 7.26 (dd, $^3J_{H-H}$ = 7.7 Hz, $^4J_{H-H}$ = 1.5 Hz, 1H), 7.20 (dd, $^3J_{H-H}$ = 8.2 Hz, $^4J_{H-H}$ =1.1 Hz, 1H), 7.13 (dd, $^3J_{H-H}$ = 7.5 Hz, $^4J_{H-H}$ = 1.1 Hz, 1H), 7.11 (s, 1H), 4.21 (t, $^3J_{H-H}$ = 6.6 Hz, 2H), 3.52-3.45 (m, 2H), 3.09 (s, 9H), 2.33 (m, 2H); ^{13}C NMR (101 MHz, CD_3OD): δ = 157.6, 156.0, 151.8, 151.4, 142.0, 128.0, 127.5, 126.6, 124.5, 124.2, 123.1, 116.9, 114.0, 113.2, 103.1, 98.2, 63.9, 52.27, 52.23, 52.19, 44.2, 20.4; ^{19}F NMR (470 MHz, CD_3OD): δ = -77.08 (3F, C*F*$_3$-trifluoroacetate), -76.9 (0.2F, C*F*$_3$-free TFA); HPLC (system A-QC): t_R = 3.7 min (purity >99% at 350 nm and 450 nm); UV-vis (recorded during the RP-HPLC analysis): λ_{max} = 251, 309 and 442 nm; LRMS (ESI+, recorded during RP-HPLC analysis): *m/z* 392.2 $[M]^+$, calcd for $C_{22}H_{22}N_3O_2S^+$ 392.1; UV-vis (MeOH, 25 °C): λ_{max} = 309 nm (ε 21 500 M^{-1} cm^{-1}) and 433 nm (ε 20.700 M^{-1} cm^{-1}); UV-vis (PBS, pH 7.3, 25 °C): λ_{max} = 310 nm (ε 19 700 M^{-1} cm^{-1}) and 443 nm (ε 21 800 M^{-1} cm^{-1}); UV-vis (PBS + 300 µM Tween®, pH 7.3, 25 °C): 309 nm (ε 19 400 M^{-1} cm^{-1}) and 443 nm (ε 22 000 M^{-1} cm^{-1}); Fluorescence (MeOH, 25 °C): λ_{max} = 678 nm (Φ_F 1.6%); Fluorescence (PBS, pH 7.3, 25 °C): λ_{max} = 700 nm (Φ_F 0.2%); Fluorescence (PBS + 300 µM Tween® 80, pH 7.3, 25 °C): λ_{max} = 700 nm (Φ_F 0.4%).

N-[3-(3-Sulfonatopropyl)dimethylammonium)propyl]-3-cyano-PTZ-coumarin hybrid dye, TEA salt (16). Salicylaldehyde **14** (50.0 mg, 0.11 mmol, 1 equiv.) was dissolved in a mixture of dry EtOH-DMF (8:1, v/v, 9 mL). Then, malononitrile (7.0 mg, 0.11 mmol, 1 equiv.), anhydrous Na_2SO_4 (4.0 mg, 0.055 mmol, 0.5 equiv.) and piperidine (4.7 mg, 5.4 µL, 0.055 mmol, 0.5 equiv.) were sequentially added. and the resulting reaction mixture was stirred at RT for 16 h. Thereafter, the reaction mixture was

evaporated under reduced pressure and the resulting residue was directly purified by semi-preparative RP-HPLC (system E, t_R = 39.0-40.0 min) to give after freeze-drying TFA salt of PTZ-coumarin hybrid dye **16** (13 mg, 0.026 mmol, yield 24%). *Please note: in order to increase the solubility of this product in organic solvents, a counter-ion exchange operation (TFA replaced by TEA) was achieved through semi-preparative RP-HPLC (system F, t_R = 33.0 min). Unfortunately, the benefit was found to be negligible.* IR (ATR): ν_{max} = 3417, 2225, 2161, 2041, 1989, 1718, 1594, 1572, 1547, 148, 1441, 1413, 1374, 1333, 1309, 1270, 1236, 1168, 1036, 949, 913, 755, 672, 594, 541, 524, 449, 421; ^{1}H NMR (600 MHz, DMF-d_7-D_2O 5:3, 0.8 mL, 325 K): δ = 8.62 (s, 1H), 7.62 (s, 1H), 7.36 (t, $^3J_{H-H}$ = 7.6 Hz, 1H), 7.29-7.21 (m, 2H), 7.17-7.10 (m, 2H), 3.59-3.46 (m, 4H), 3.11 (s, 6H), 2.75 (d, $^3J_{H-H}$ = 7.2 Hz, 2H), 2.41-2.32 (m, 3H), 2.14 (m, 2H), 1.28 (t, $^3J_{H-H}$ = 7.7 Hz, 2H), 0.84 (t, $^3J_{H-H}$ = 7.2 Hz, 1H, 0.11 C$\underline{H}_3$-TEA); ^{13}C NMR (151 MHz, DMF-d_7-D_2O 5:3, 0.8 mL, 325 K): *it was not possible to obtain a good quality C13 spectrum despite of extended acquisition time on a 600 MHz spectrometer. This is due to the poor solubility of* ***16*** *even under its TEA salt form.* HPLC (system A-QC): t_R = 3.8 min (purity >99% at 350 nm and 450 nm); UV-vis (recorded during the HPLC analysis): λ_{max} = 251, 309 and 441 nm; LRMS (ESI+, recorded during RP-HPLC analysis): *m/z* 500.2 $[M + H]^+$ and 999.4 $[2M + H]^+$, calcd for $C_{24}H_{26}N_3O_5S_2^+$ 500.1; UV-vis (MeOH, 25 °C): λ_{max} = 307 nm (ε 9 400 M^{-1} cm^{-1}) and 432 nm (ε 8 800 M^{-1} cm^{-1}); UV-vis (PBS, pH 7.3, 25 °C): λ_{max} = 307 nm (ε 8 200 M^{-1} cm^{-1}) and 440 nm (ε 9 200 M^{-1} cm^{-1}); UV-vis (PBS + 300 µM Tween® 80, pH 7.3, 25 °C): λ_{max} = 308 nm (ε 8 700 M^{-1} cm^{-1}) and 440 nm (ε 9 100 M^{-1} cm^{-1}); Fluorescence (MeOH, 25 °C): λ_{max} = 672 nm (Φ_F 1.6%); Fluorescence (PBS, pH 7.3, 25 °C): λ_{max} = 706 nm (Φ_F 0.3%); Fluorescence (PBS + 300 µM Tween® 80, pH 7.3, 25 °C): λ_{max} = 702 nm (Φ_F 0.3%).

In vitro activation of PTZ-coumarin hybrid dyes 10, 15 and 16 by NaOCl - experimental details

Stock solutions of probes and NaOCl

- Solution A: commercial solution of bleach BEC (titrated at 2.72% w/w).
- Solution B: for kinetics with 1 equiv. of NaOCl, the commercial BEC solution was diluted 100-fold with ultrapure water.
- Solution Cx (x =1-3): stock solutions (accurate concentration close to 1.0 mg/mL) of probes prepared in peptide synthesi-grade DMF.

Fluorescence assays

All assays were performed at 25 °C (using a temperature control system combined with water circulation and conducted with magnetic stirring). For all probes **10**, **15** and **16** (final concentration in 3.5 mL fluorescence quartz cell: 2.0 µM, volume: 3.0 mL of PBS, pH 7.3), the fluorescence emission of the newly formed sulfoxide derivative was monitored at λ(Ex./Em.) = 400/520 nm, slit = 2 nm, over time with measurements recorded every 5 s. NaOCl (1.66 µL solution A (100 equiv.) or 16.64 µL of solution B (10 equiv.) or 1.66 µL of solution B (1 equiv.)) was added after 5 min of incubation of the probe in PBS. Blank experiments to assess the stability of the probes in PBS, were achieved in the same way but without adding the analyte.

RP-HPLC-fluorescence and RP-HPLC-MS (full scan and SIM modes) analyses

Oxidation reaction mixtures from fluorescence-based *in vitro* assays were analyzed by RP-HPLC-fluorescence (injected volume: 20 µL, system D-Fluo). Thereafter, each oxidation reaction mixture (ca. 3 mL) was freeze-dried; the resulting white amorphous powder was dissolved in a 1:1 (v/v) mixture of ultrapure H_2O and MeCN (total volume = 1.0 mL). The solution was vortexed followed by centrifugation (9 000 rpm, 1 min). 20 µL of supernatant was injected into the HPLC-MS apparatus (system E-MS).

Please note: injection of PBS was also achieved immediately prior to this latter analysis, especially to confirm the lack of residual contaminants within the C_{18} column or ESI probe at the corresponding m/z value selected for the SIM detection mode and then avoid misinterpretations

For RP-HPLC (fluorescence or MS detection) analyses of starting PTZ-coumarin hybrid dyes, 2.0 µM solution in PBS was prepared and 20 µL was injected into the HPLC-fluorescence/MS apparatus (systems D-Fluo and E-MS).

Analytical data

Fig. S1. ^{1}H NMR spectrum of compound 2 in $CDCl_3$ (500 MHz)

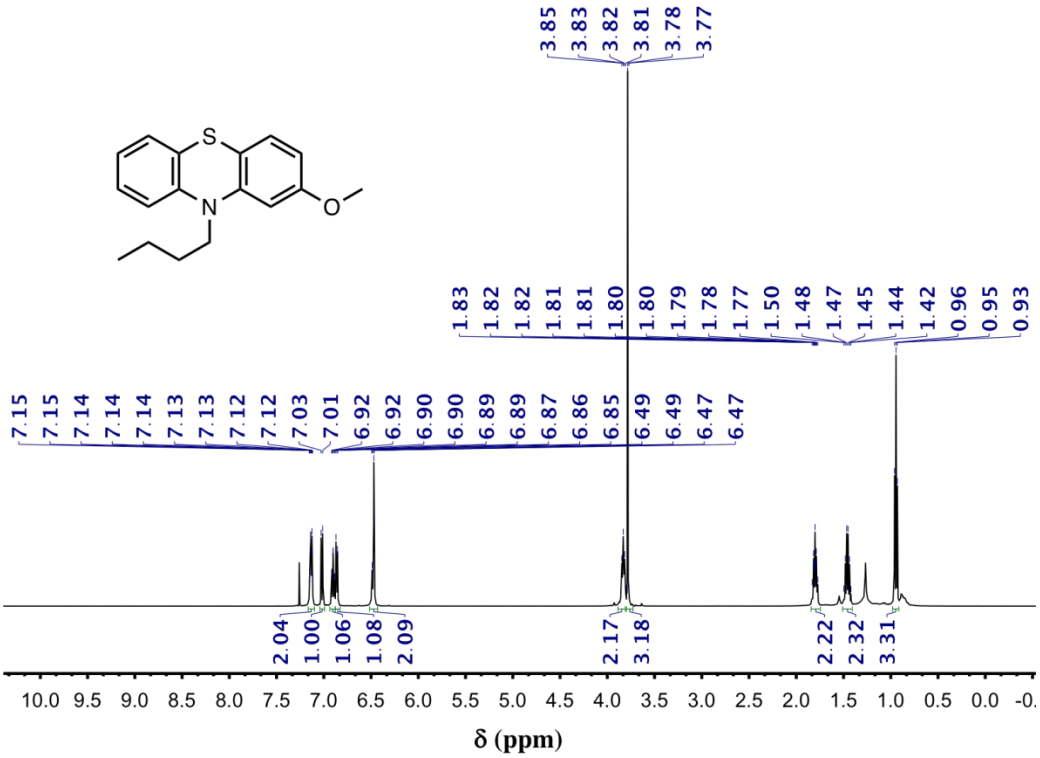

Fig. S2. ^{1}H NMR spectrum of 3-dimethylaminopropyl methanesulfonate (HCl salt) in DMSO-*d*$_6$ (500 MHz)

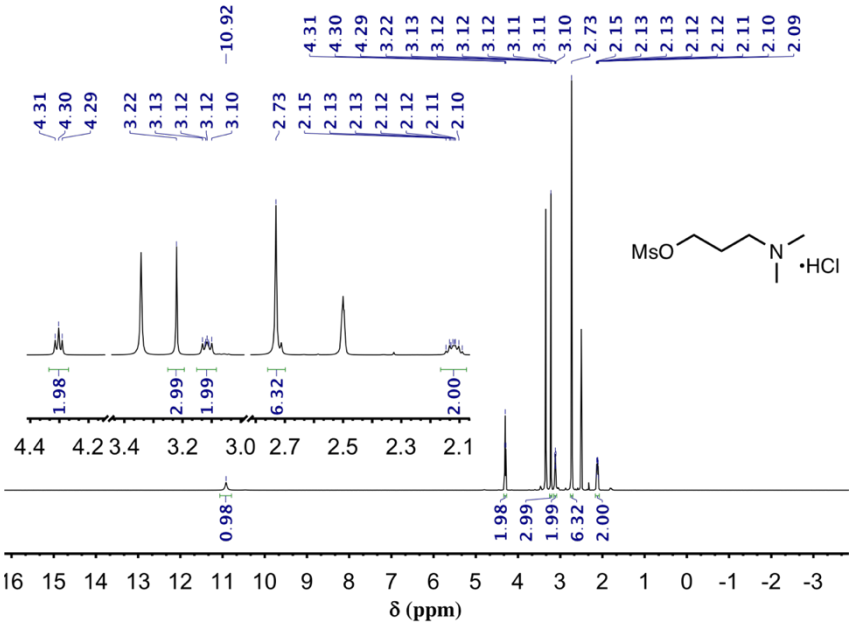

Fig. S3. ^{13}C NMR spectrum of 3-dimethylaminopropyl methanesulfonate (HCl salt) in DMSO-*d*$_6$ (151 MHz)

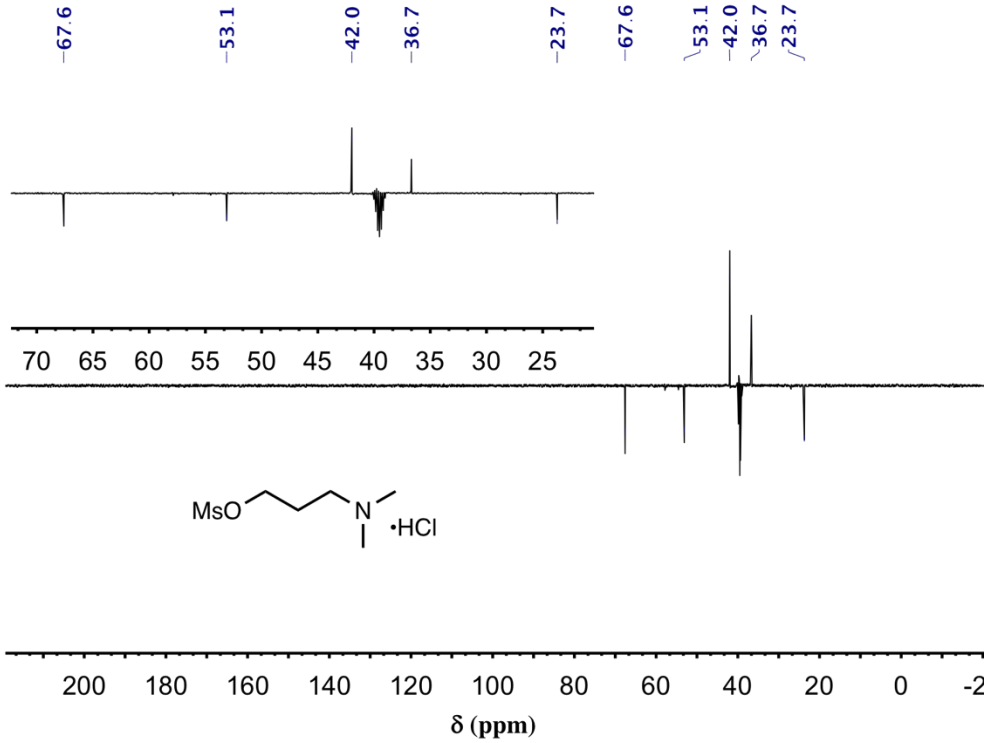

Fig. S4. IR-ATR spectrum of compound 3

Fig. S5. ^{1}H NMR spectrum of compound 3 in $CDCl_3$ (500 MHz)

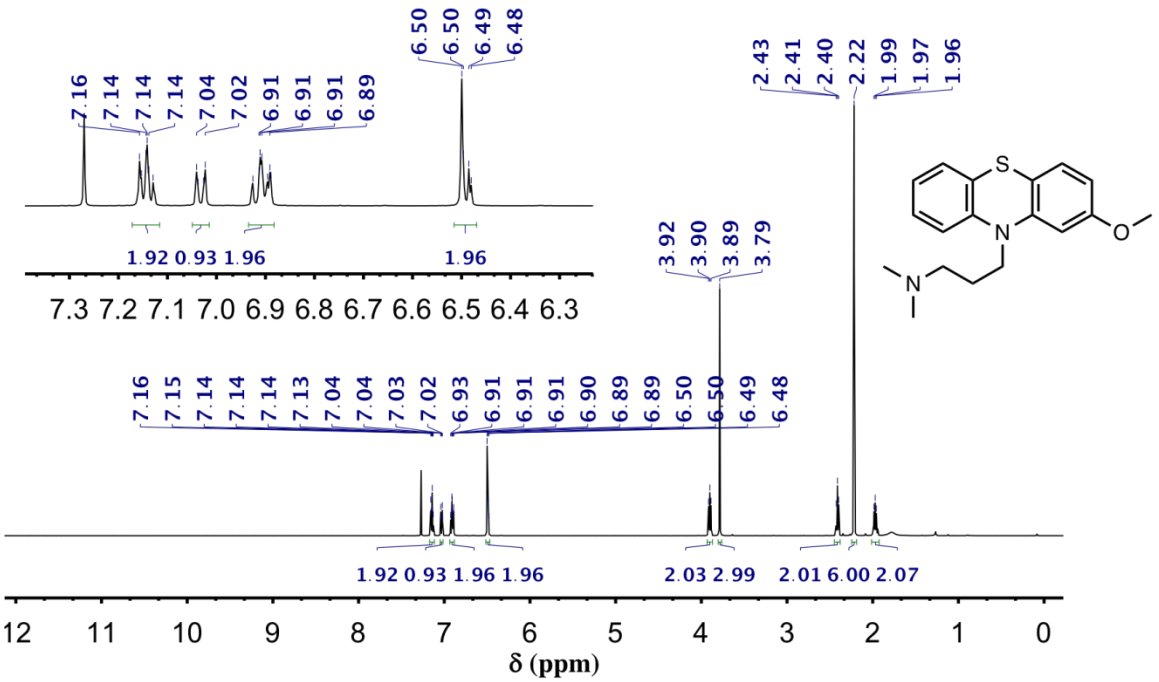

Fig. S6. ^{13}C NMR spectrum of compound 3 in $CDCl_3$ (151 MHz)

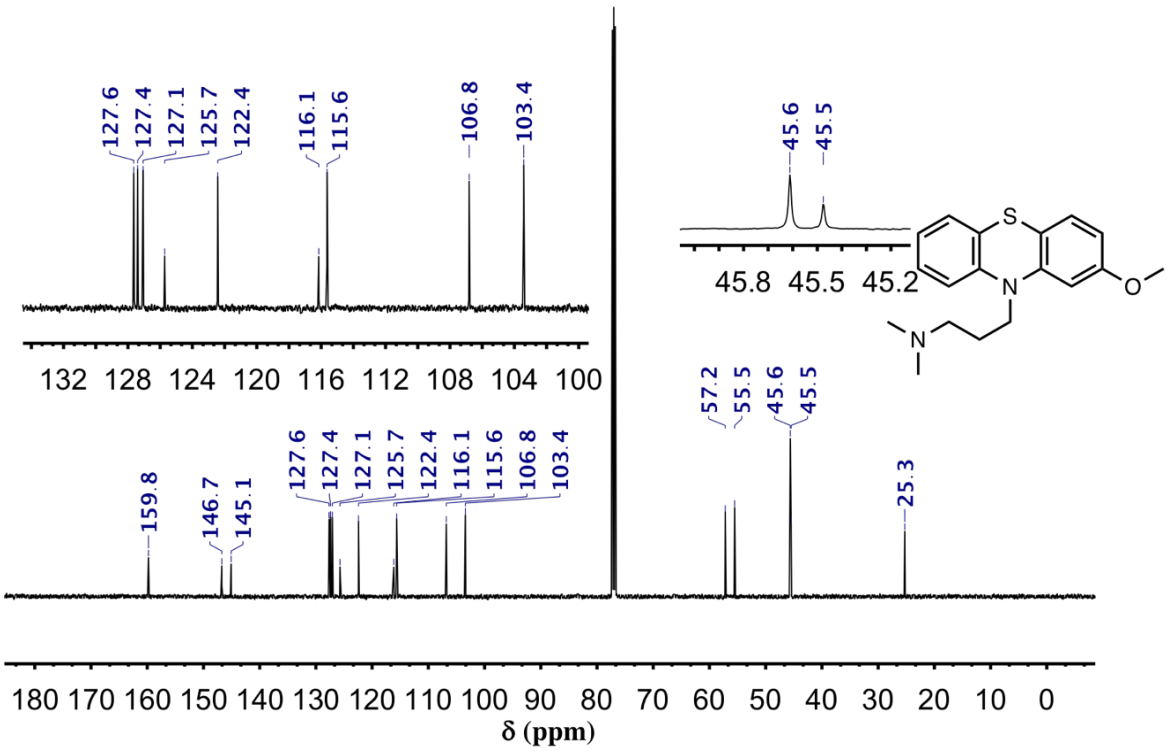

Fig. S7. ESI+ mass spectra (low resolution) of compound 3

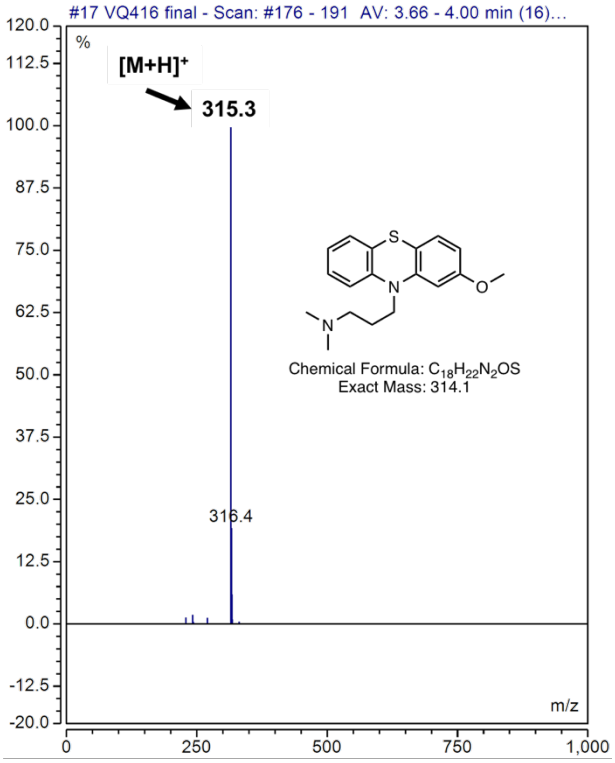

Fig. S8. IR-ATR spectrum of PTZ-coumarin hybrid dye 10

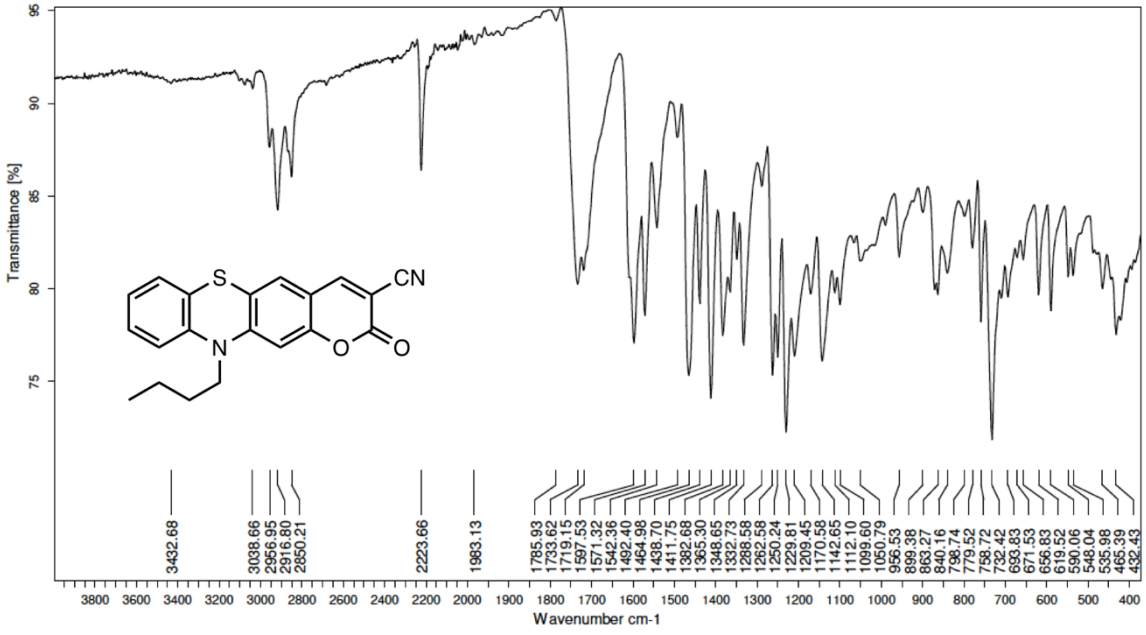

Fig. S9. ^{1}H NMR spectrum of PTZ-coumarin hybrid dye 10 in $CDCl_3$ (600 MHz)

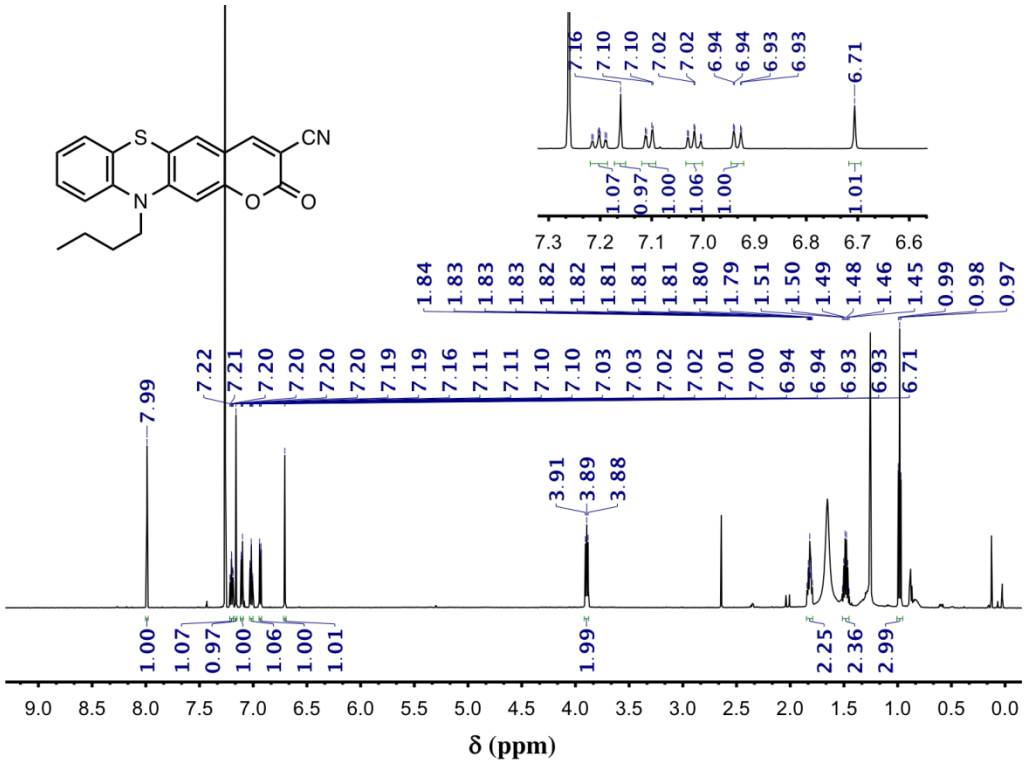

Fig. S10. ^{13}C NMR spectrum of PTZ-coumarin hybrid dye 10 in $CDCl_3$ (151 MHz)

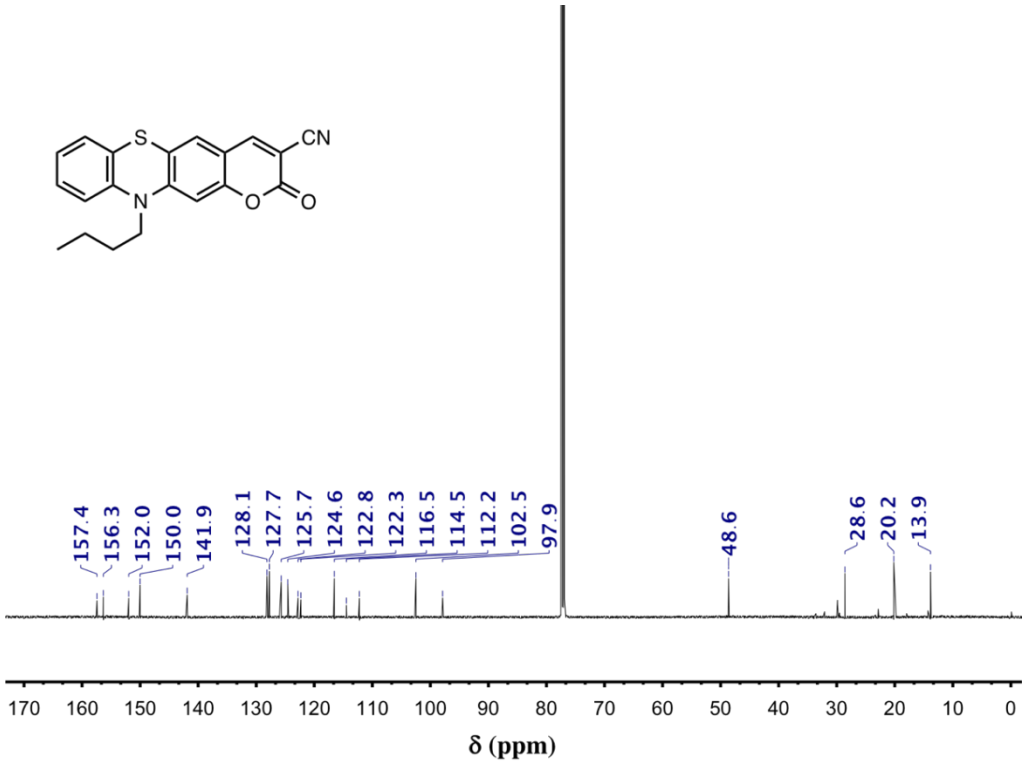

Fig. S11. RP-HPLC elution profile of PTZ-coumarin hybrid dye 10 (system C-QC, detection at 260 nm)

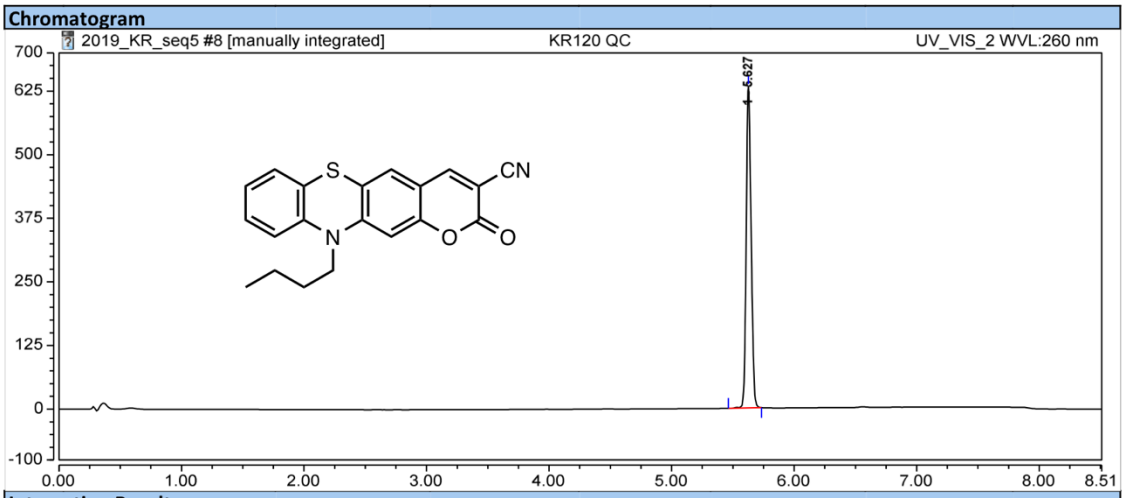

Integration Results

No.	Peak Name	Retention Time min	Area mAU*min	Height mAU	Relative Area %	Relative Height %	Amount n.a.
1		5.627	29.352	631.534	100.00	100.00	n.a.
Total:			**29.352**	**631.534**	**100.00**	**100.00**	

Fig. S12. RP-HPLC elution profile of PTZ-coumarin hybrid dye 10 (system C-QC, detection at 450 nm)

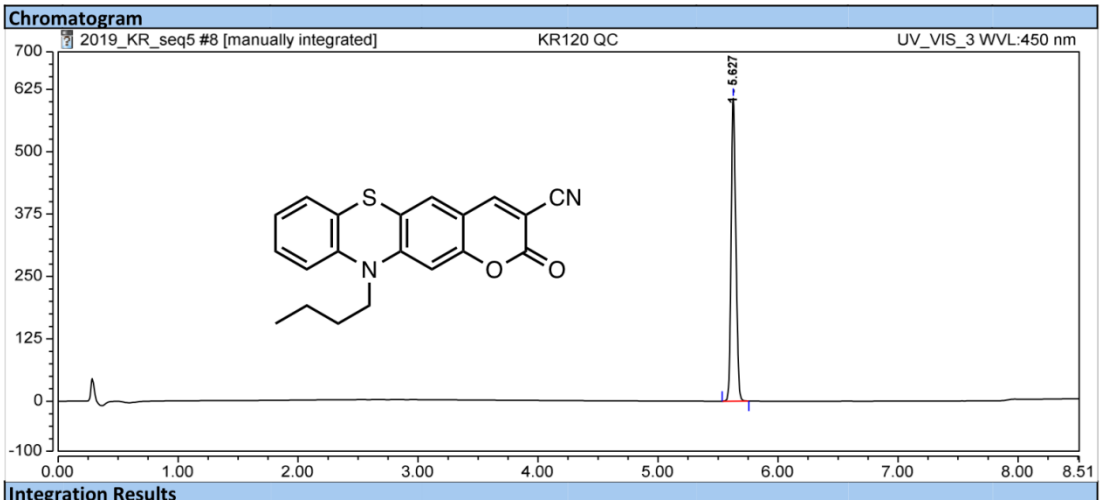

Integration Results

No.	Peak Name	Retention Time min	Area mAU*min	Height mAU	Relative Area %	Relative Height %	Amount n.a.
1		5.627	27.454	606.191	100.00	100.00	n.a.
Total:			**27.454**	**606.191**	**100.00**	**100.00**	

Fig. S13. ESI+ mass spectra (low resolution) of PTZ-coumarin hybrid dye 10

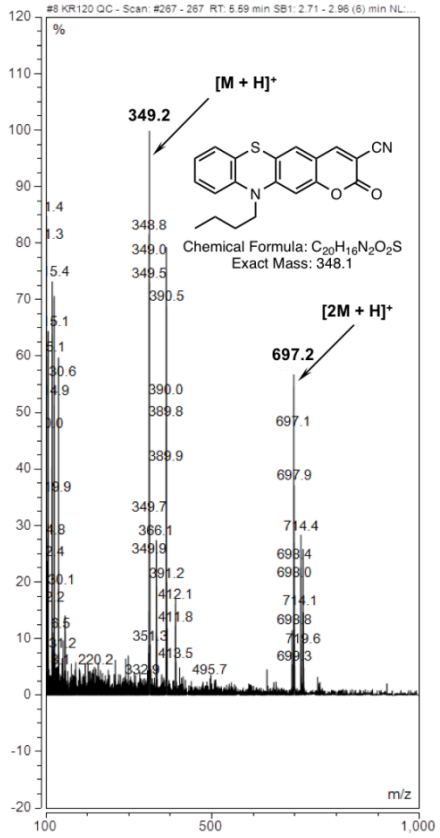

Fig. S14. IR-ATR spectrum of compound 11

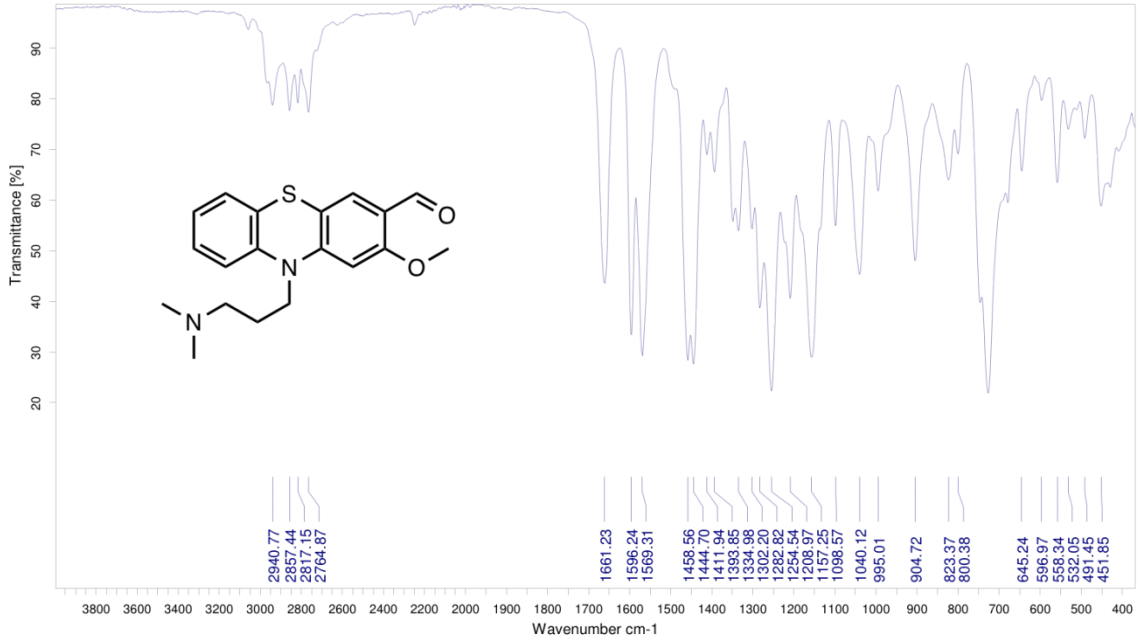

Fig. S15. ^{1}H NMR spectrum of compound 11 in $CDCl_3$ (400 MHz)

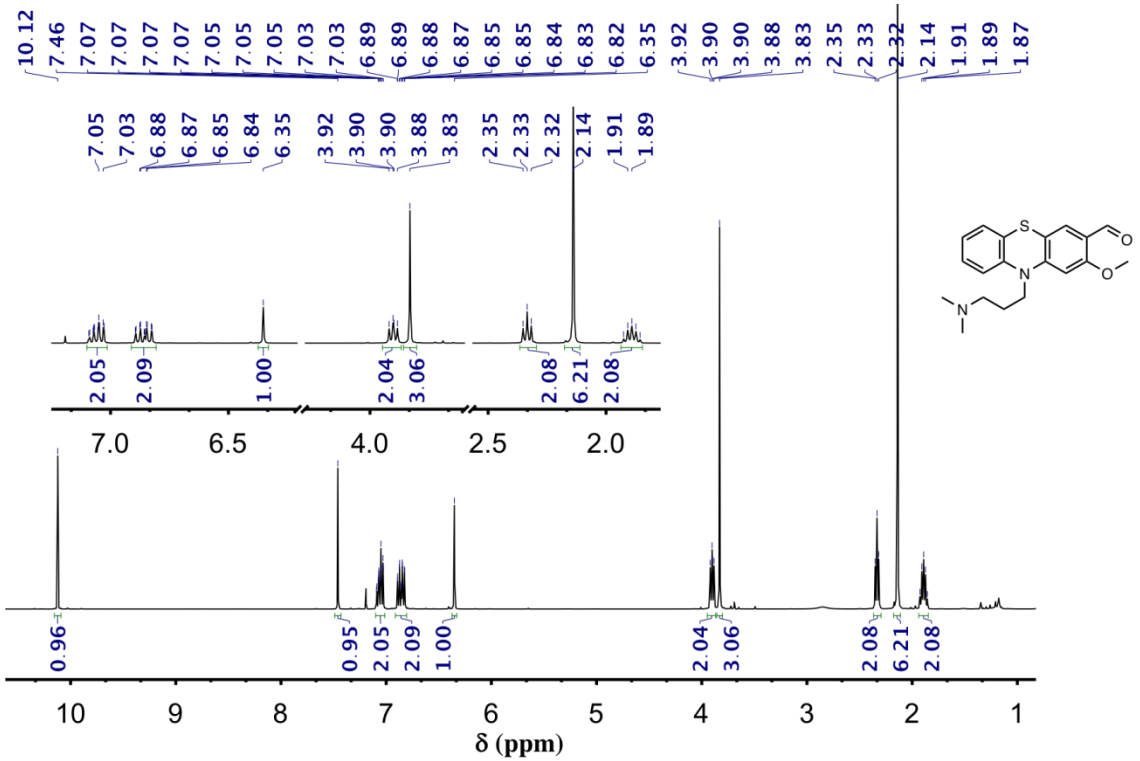

Fig. S16. ^{13}C NMR spectrum of comppound 11 in $CDCl_3$ (101 MHz)

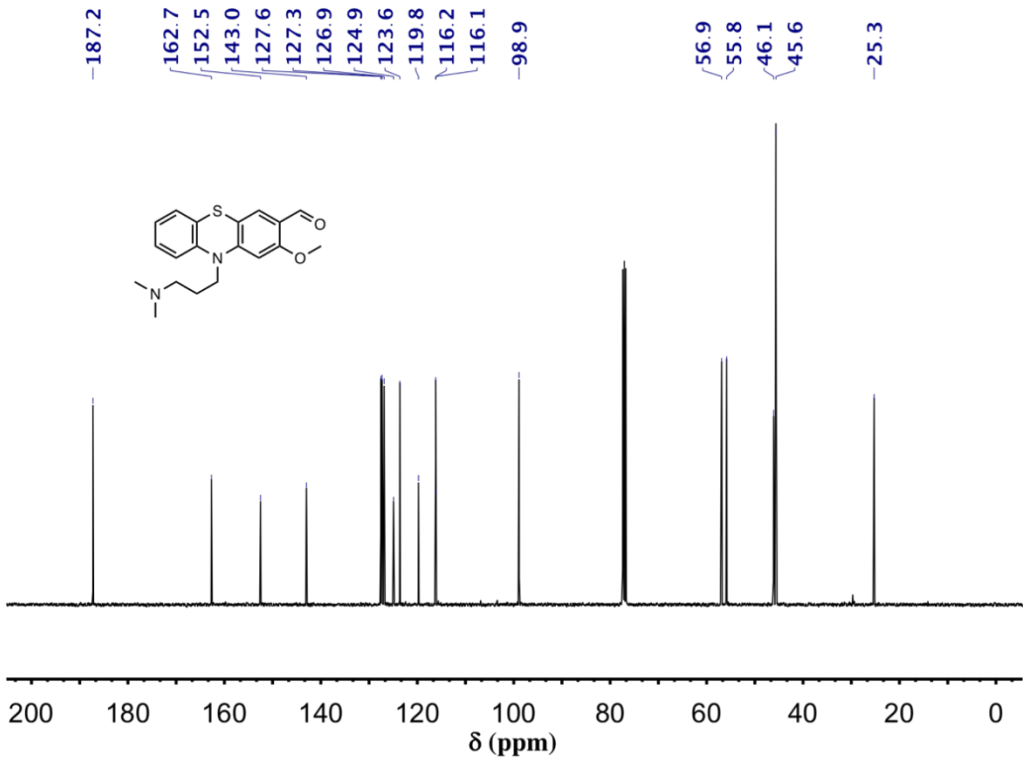

Fig. S17. ESI+ mass spectra (low resolution) of compound 11

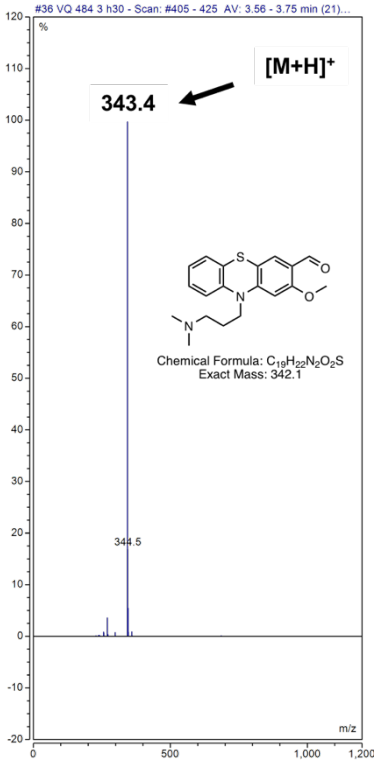

Fig. S18. IR-ATR spectrum of compound 12

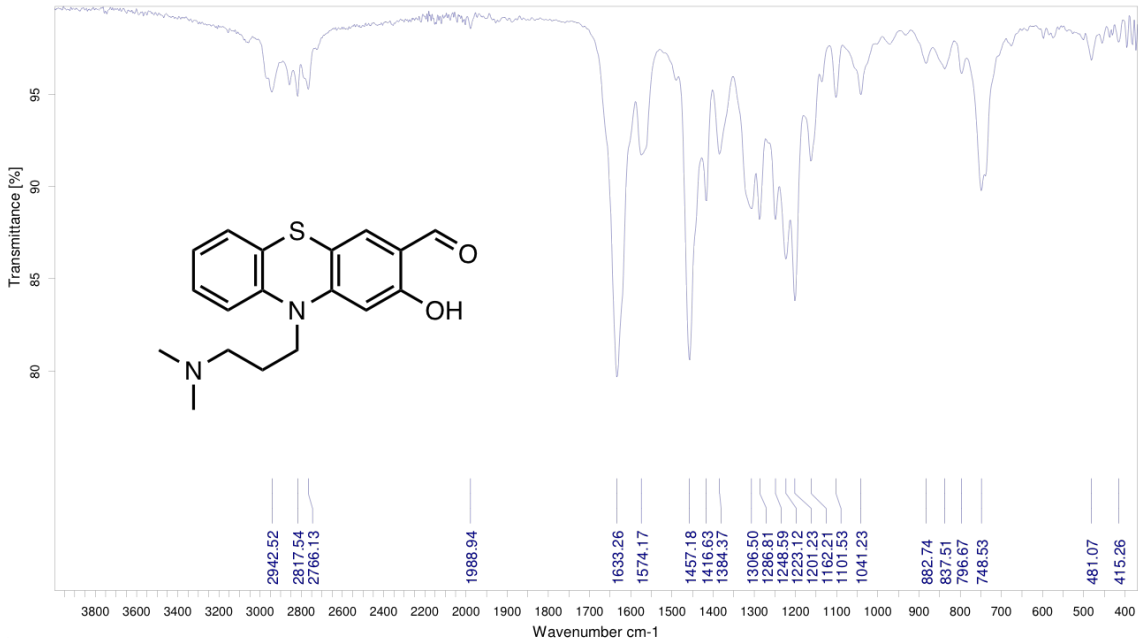

Fig. S19. ^{1}H NMR spectrum of compound 12 in $CDCl_3$ (400 MHz)

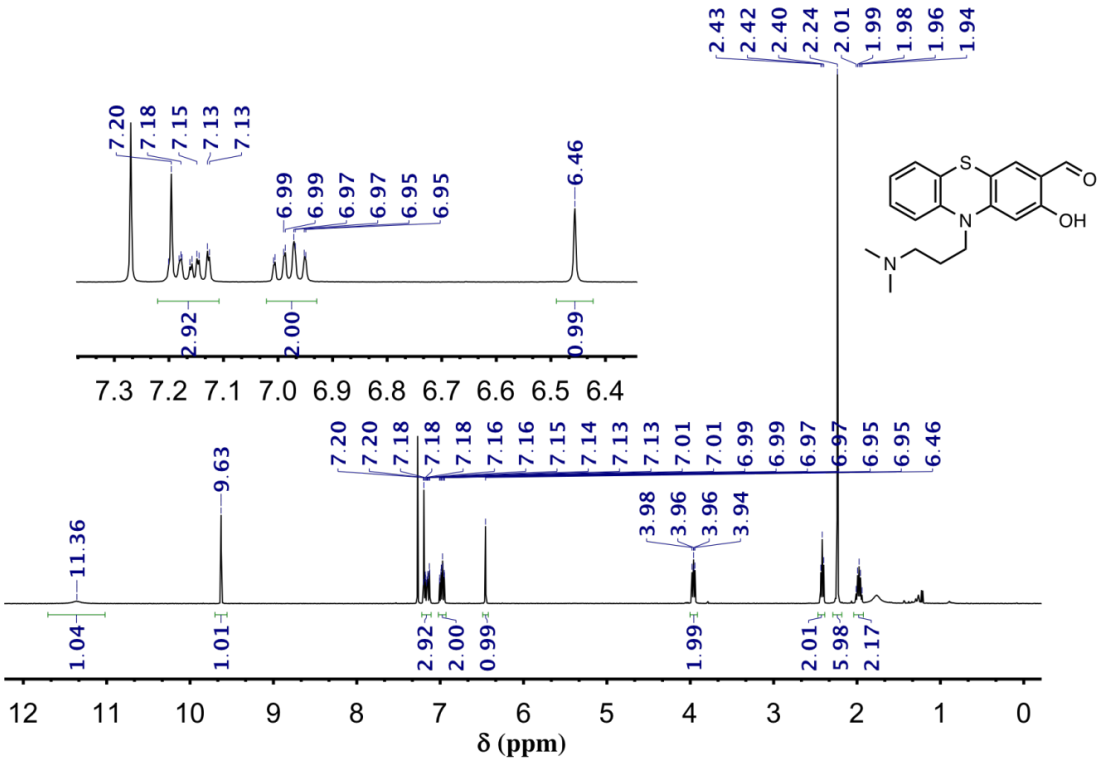

Fig. S20. ^{13}C NMR spectrum of compound 12 in $CDCl_3$ (101 MHz)

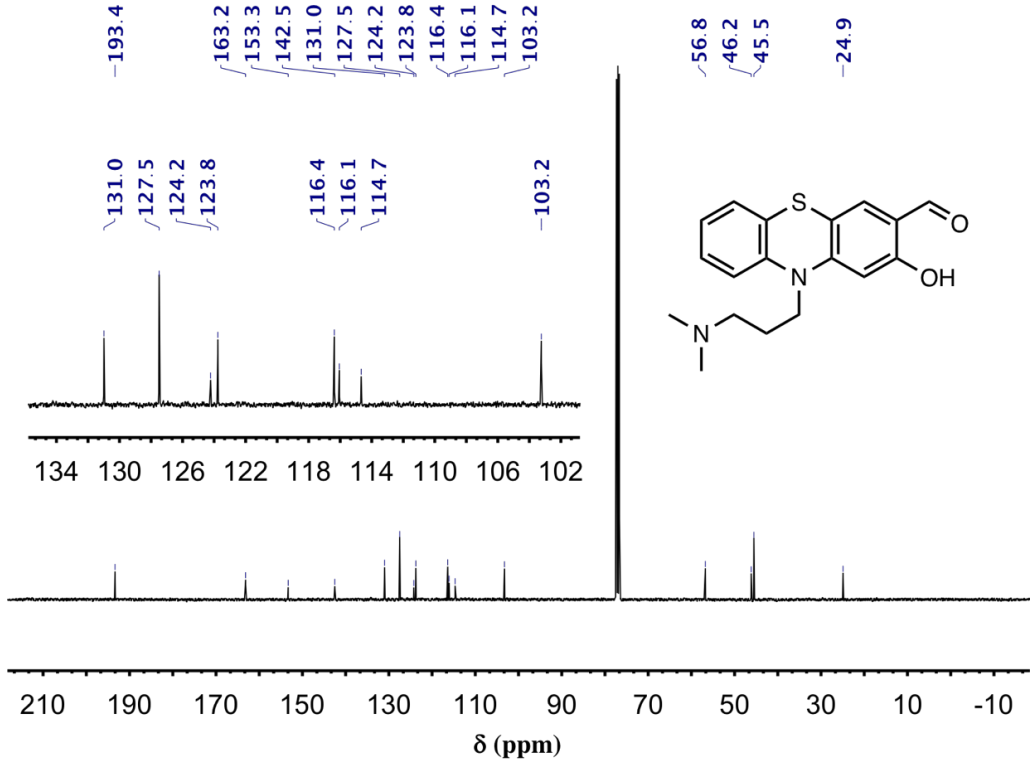

Fig. S21. IR-ATR spectrum of compound 13

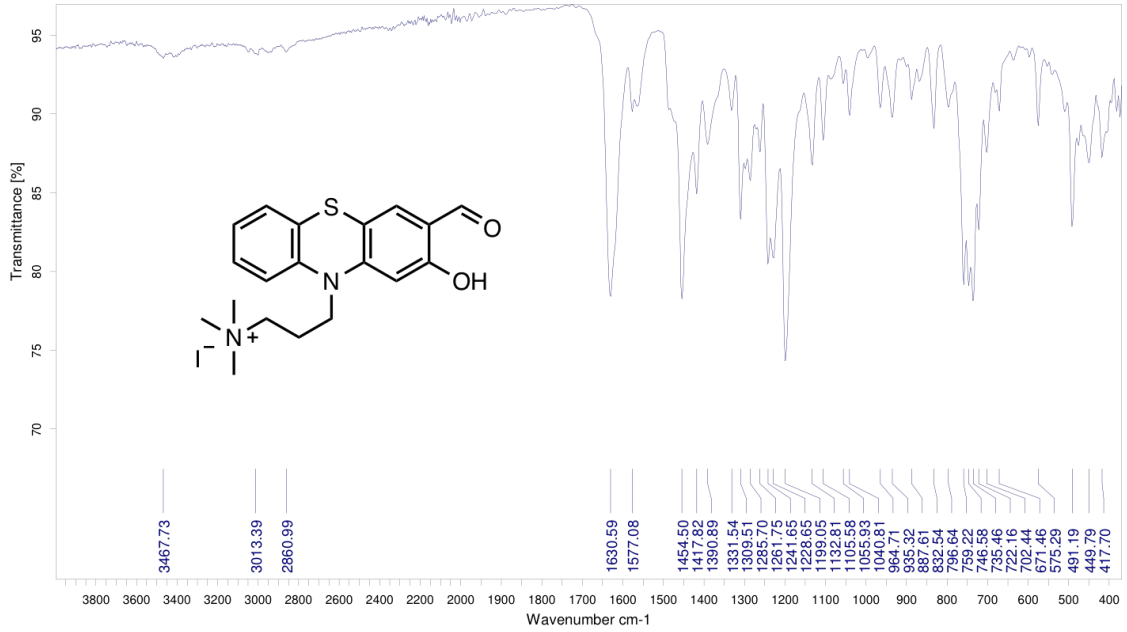

Fig. S22. ^{1}H NMR spectrum of compound 13 in DMSO-d_6 (400 MHz)

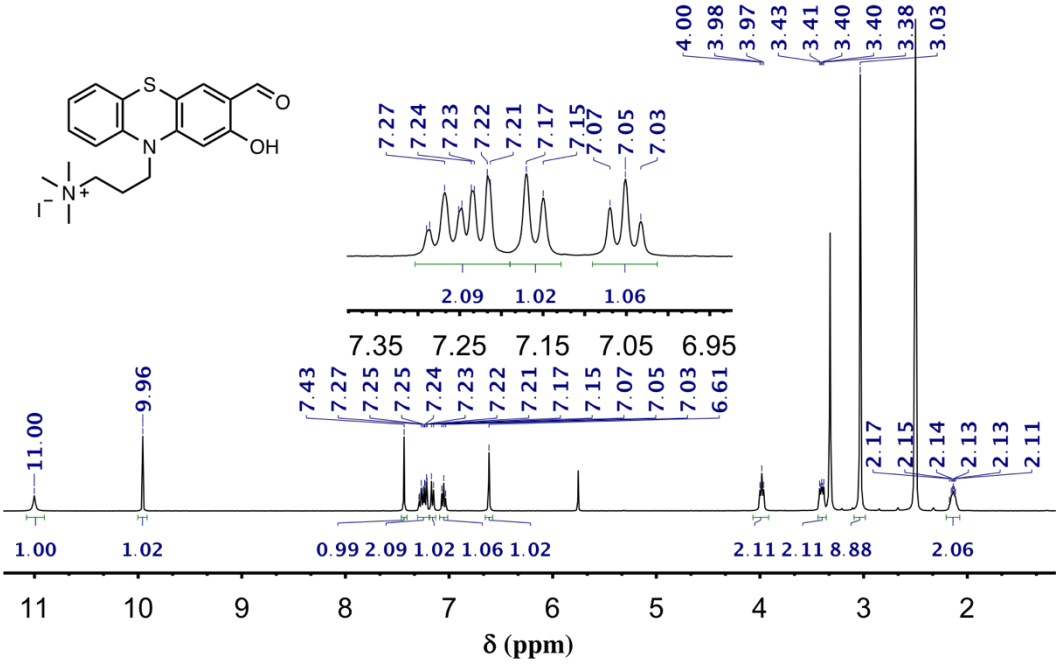

Fig. S23. ^{13}C NMR spectrum of compound 13 in DMSO-d_6 (101 MHz)

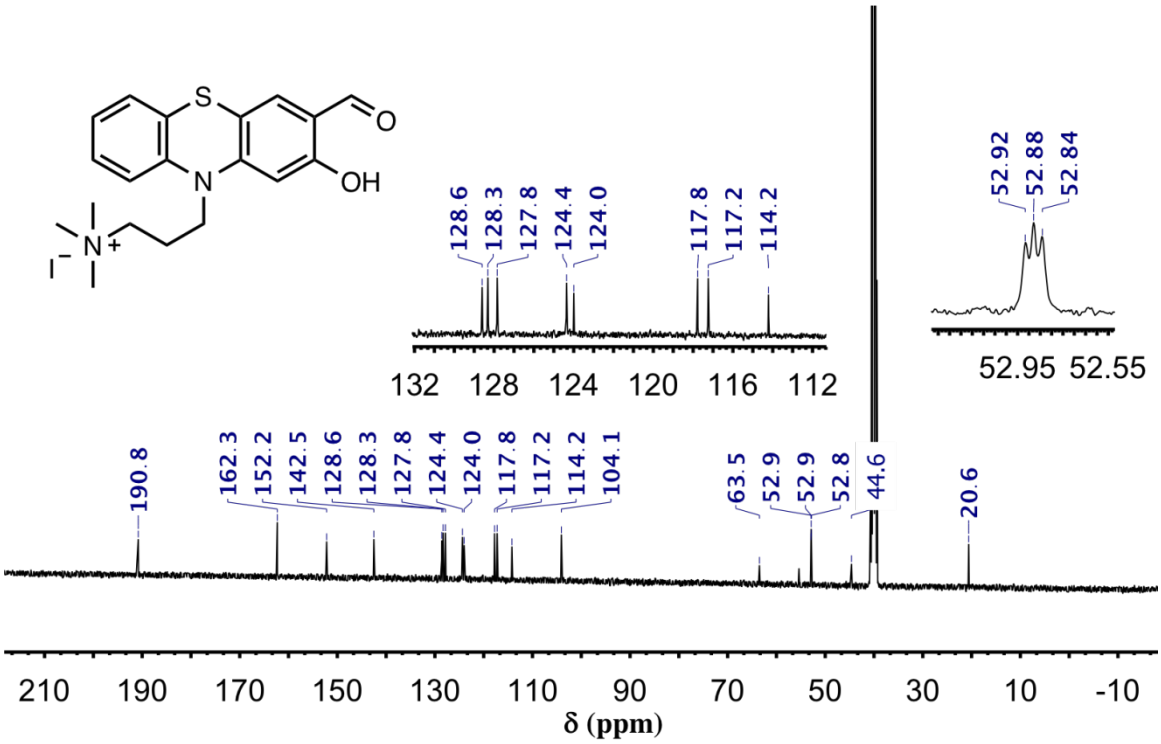

Fig. S24. RP-HPLC elution profile of compound 13 (system A-QC, detection at 280 nm)

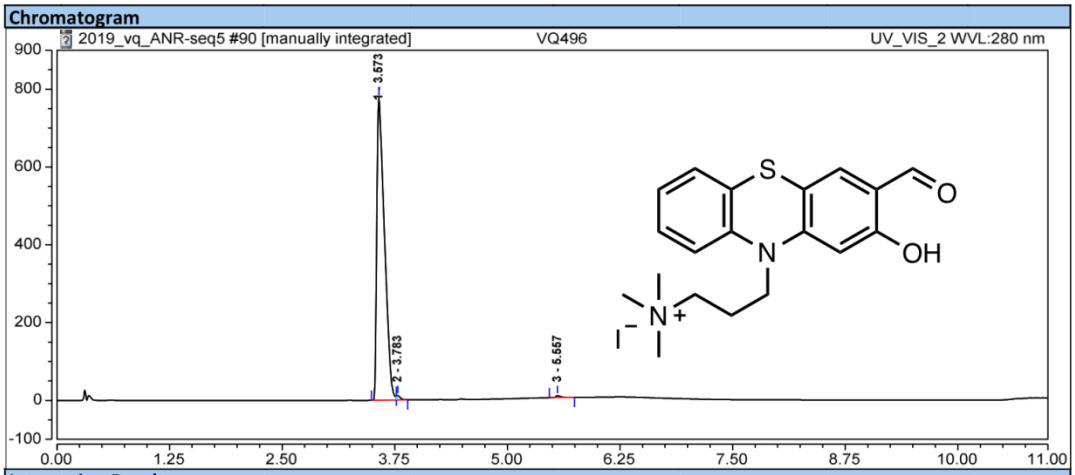

Integration Results

No.	Peak Name	Retention Time min	Area mAU*min	Height mAU	Relative Area %	Relative Height %	Amount n.a.
1		3.573	75.543	776.808	98.86	97.96	n.a.
2		3.783	0.538	10.838	0.70	1.37	n.a.
3		5.557	0.337	5.346	0.44	0.67	n.a.
Total:			**76.418**	**792.993**	**100.00**	**100.00**	

Fig. S25. RP-HPLC elution profile of compound 13 (system A-QC, detection at 350 nm)

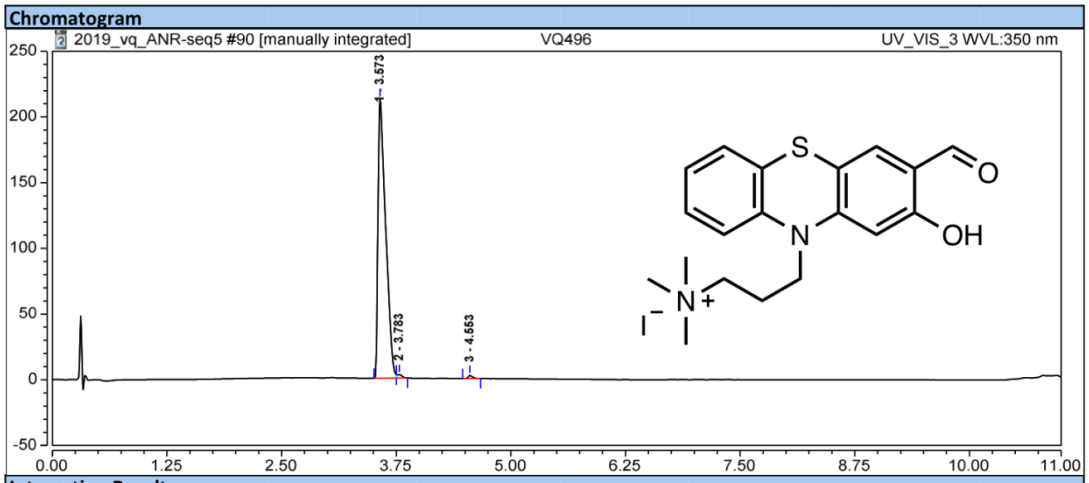

Integration Results

No.	Peak Name	Retention Time min	Area mAU*min	Height mAU	Relative Area %	Relative Height %	Amount n.a.
1		3.573	20.535	212.471	98.57	97.62	n.a.
2		3.783	0.171	2.718	0.82	1.25	n.a.
3		4.553	0.126	2.453	0.60	1.13	n.a.
Total:			**20.832**	**217.642**	**100.00**	**100.00**	

Fig. S26. ESI+ mass spectra (low resolution) of compound 13

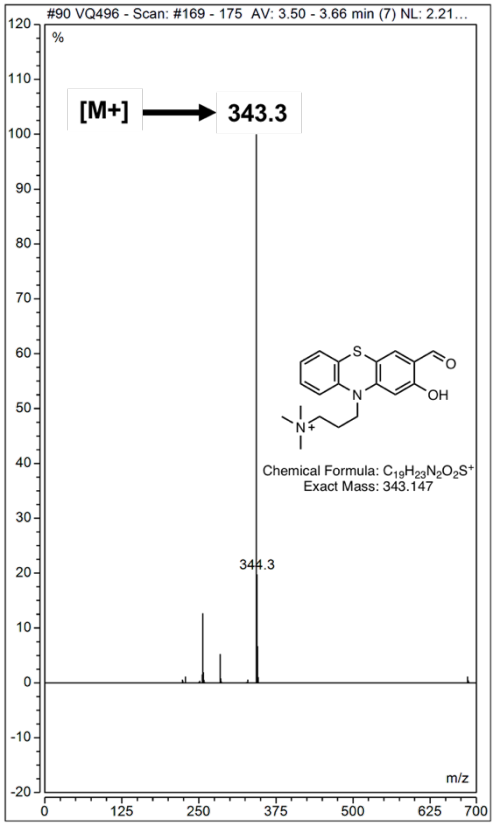

Fig. S27. IR-ATR spectrum of compound 14

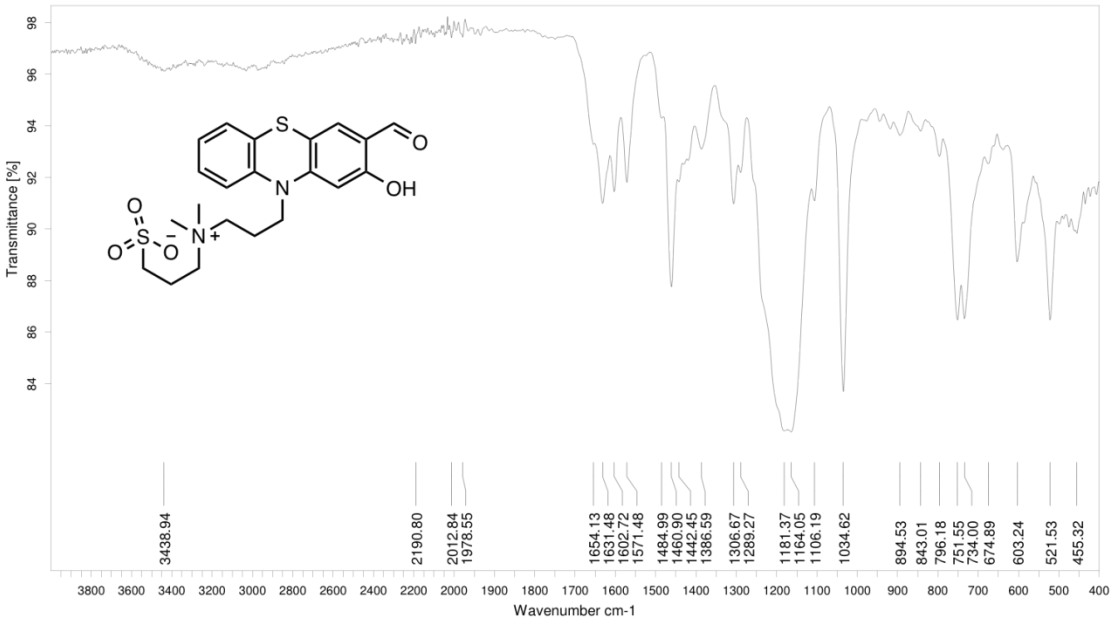

Fig. S28. ^{1}H NMR spectrum of compound 14 in CD_3CN-CD_3OD 5:1, v/v (400 MHz)

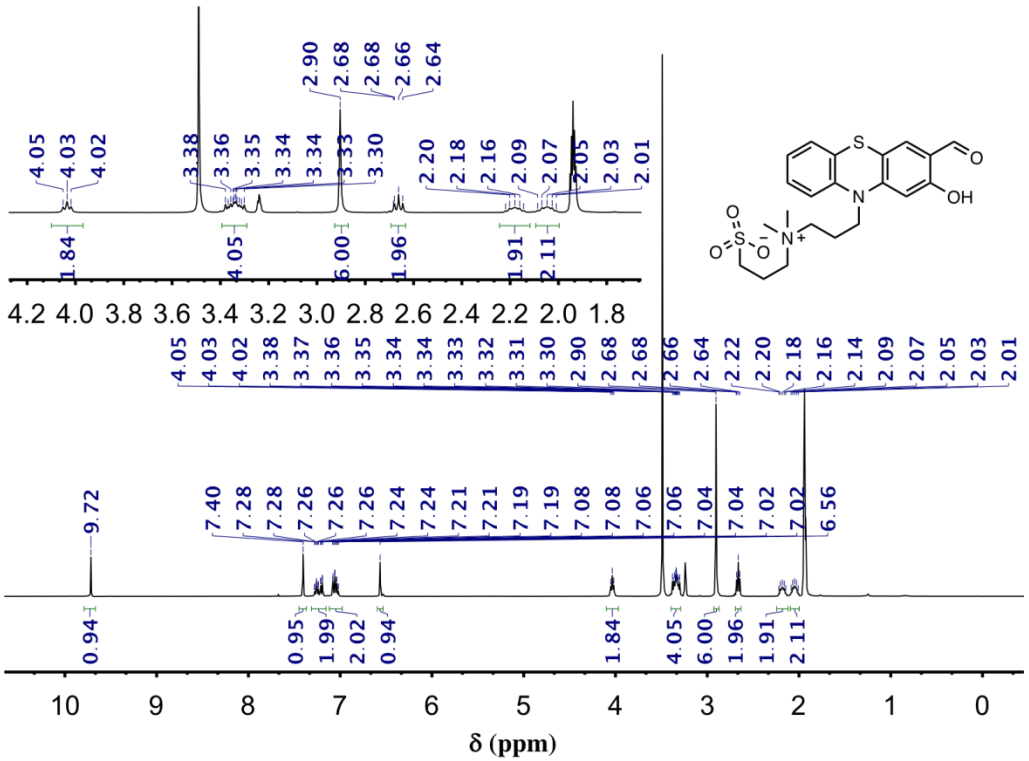

Fig. S29. ^{13}C NMR spectrum of compound 14 in CD_3CN-CD_3OD 5:1, v/v (101 MHz)

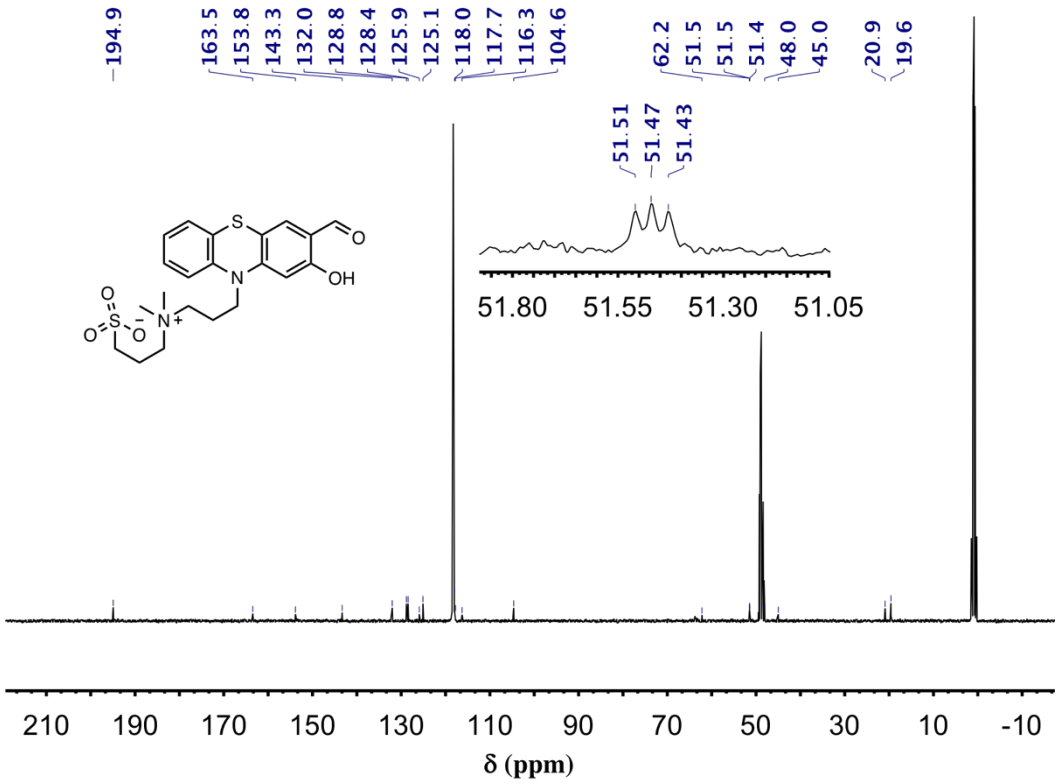

Fig. S30. RP-HPLC elution profile of compound 14 (system A-QC, detection at 280 nm)

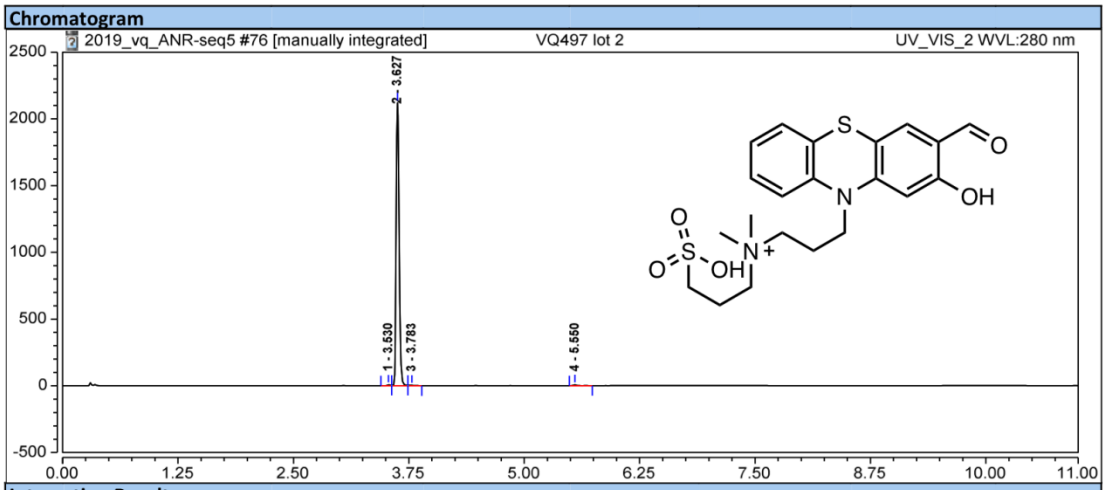

Integration Results

No.	Peak Name	Retention Time min	Area mAU*min	Height mAU	Relative Area %	Relative Height %	Amount n.a.
1		3.530	0.279	6.549	0.34	0.31	n.a.
2		3.627	81.104	2120.378	99.02	99.22	n.a.
3		3.783	0.232	3.593	0.28	0.17	n.a.
4		5.550	0.290	6.563	0.35	0.31	n.a.
Total:			**81.906**	**2137.083**	**100.00**	**100.00**	

Fig. S31. RP-HPLC elution profile of compound 14 (system A-QC, detection at 350 nm)

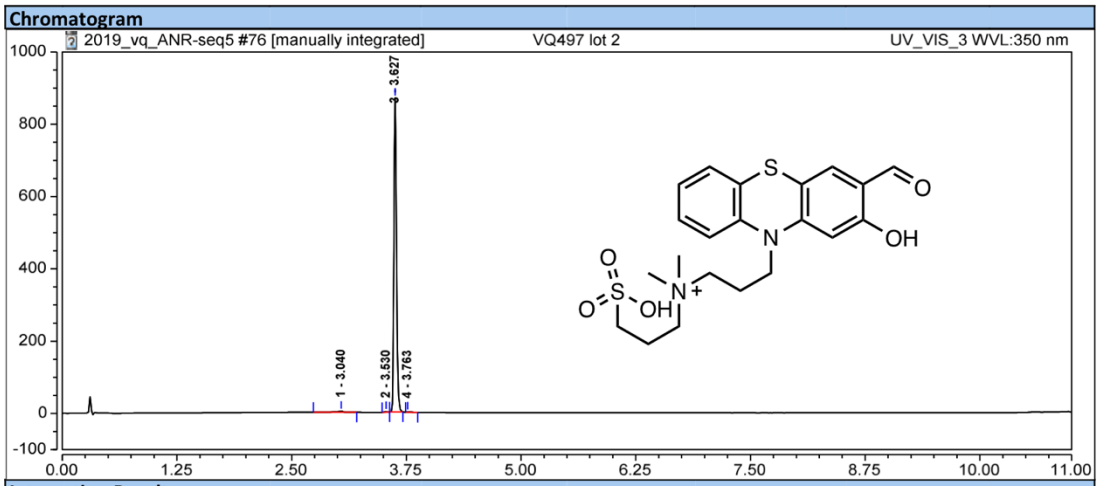

Integration Results

No.	Peak Name	Retention Time min	Area mAU*min	Height mAU	Relative Area %	Relative Height %	Amount n.a.
1		3.040	0.298	3.299	1.02	0.38	n.a.
2		3.530	0.056	1.680	0.19	0.19	n.a.
3		3.627	28.727	868.338	98.66	99.35	n.a.
4		3.763	0.036	0.721	0.12	0.08	n.a.
Total:			**29.117**	**874.038**	**100.00**	**100.00**	

Fig. S32. ESI+ mass spectra (low resolution) of compound 14

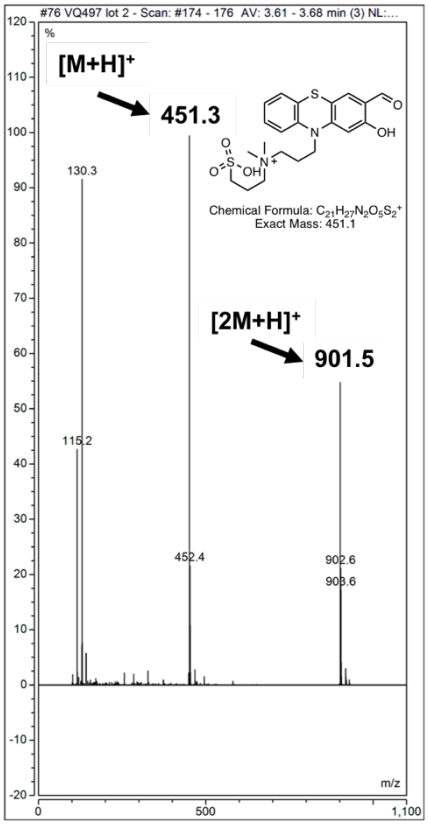

Fig. S33. IR-ATR spectrum of PTZ-coumarin hybrid dye 15 (TFA salt)

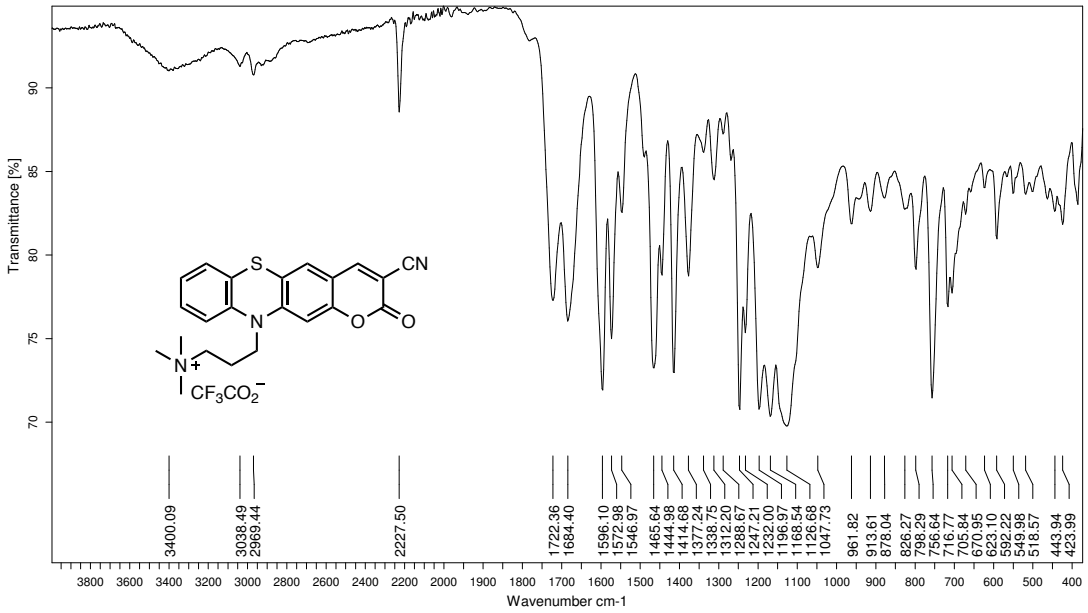

Fig. S34. ^{1}H NMR spectrum of PTZ-coumarin hybrid dye 15 (TFA salt) in CD_3OD (400 MHz)

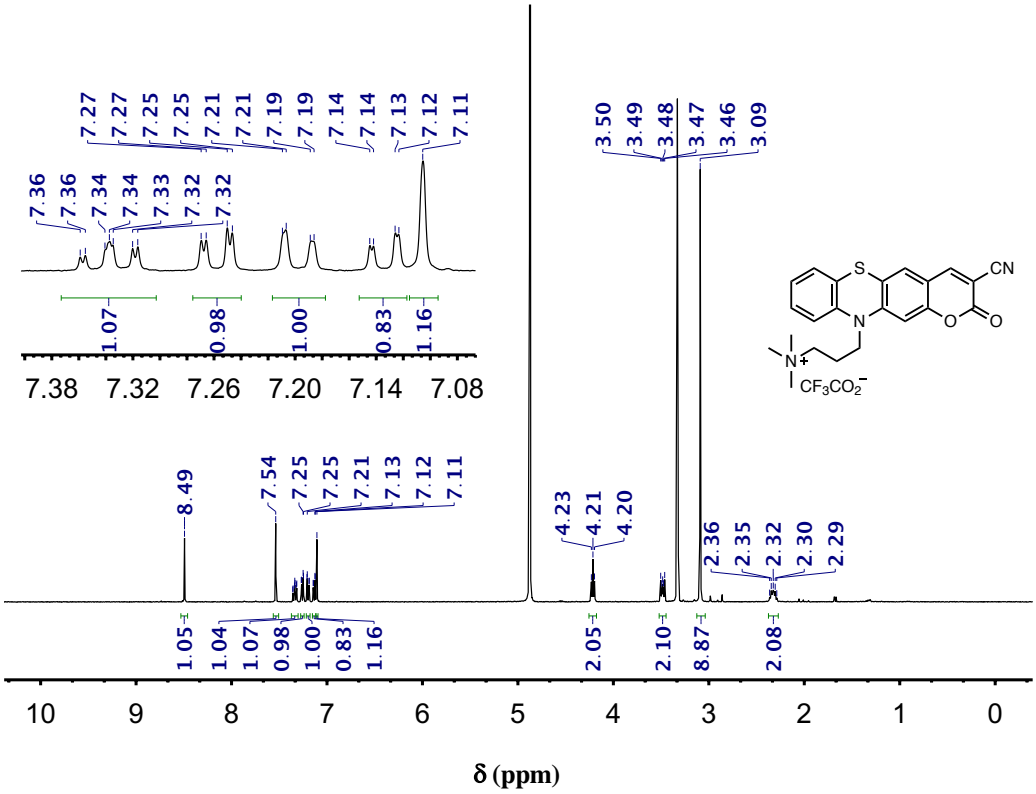

Fig. S35. ^{13}C NMR spectrum of PTZ-coumarin hybrid dye 15 (TFA salt) in CD_3OD (101 MHz)

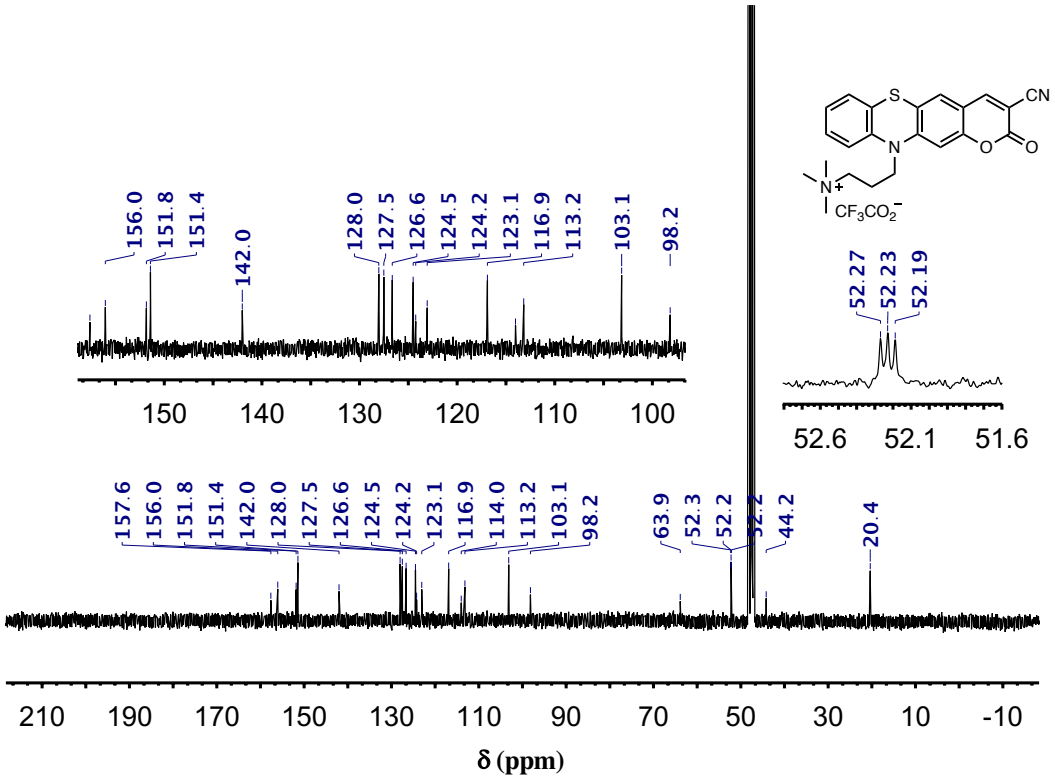

Fig. S36. ^{19}F NMR spectrum of PTZ-coumarin hybrid dye 15 (TFA salt) in CD_3OD (101 MHz)

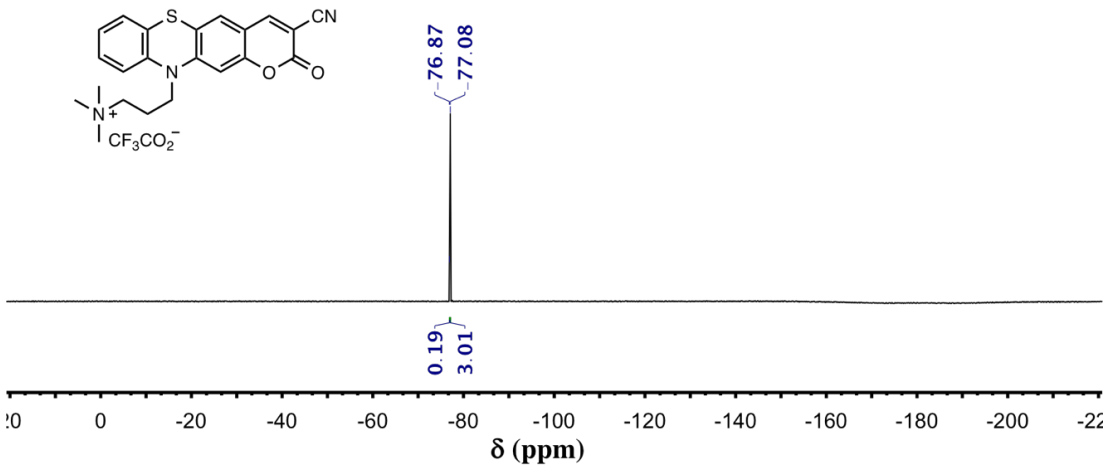

Fig. S37. RP-HPLC elution profile of PTZ-coumarin hybrid dye 15 (system A-QC, detection at 350 nm)

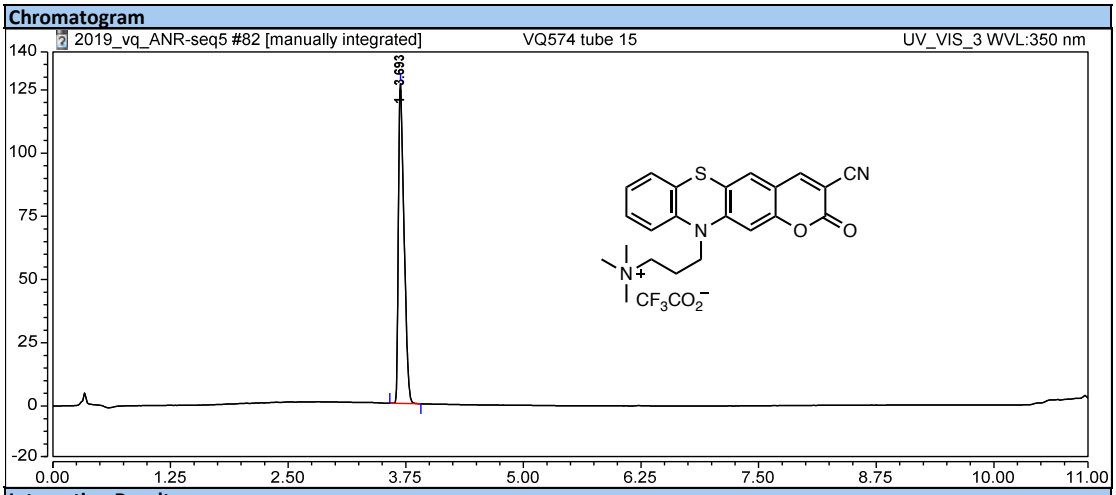

Integration Results

No.	Peak Name	Retention Time min	Area mAU*min	Height mAU	Relative Area %	Relative Height %	Amount n.a.
1		3.693	8.830	126.396	100.00	100.00	n.a.
Total:			**8.830**	**126.396**	**100.00**	**100.00**	

Fig. S38. RP-HPLC elution profile of PTZ-coumarin hybrid dye 15 (system A-QC, detection at 450 nm)

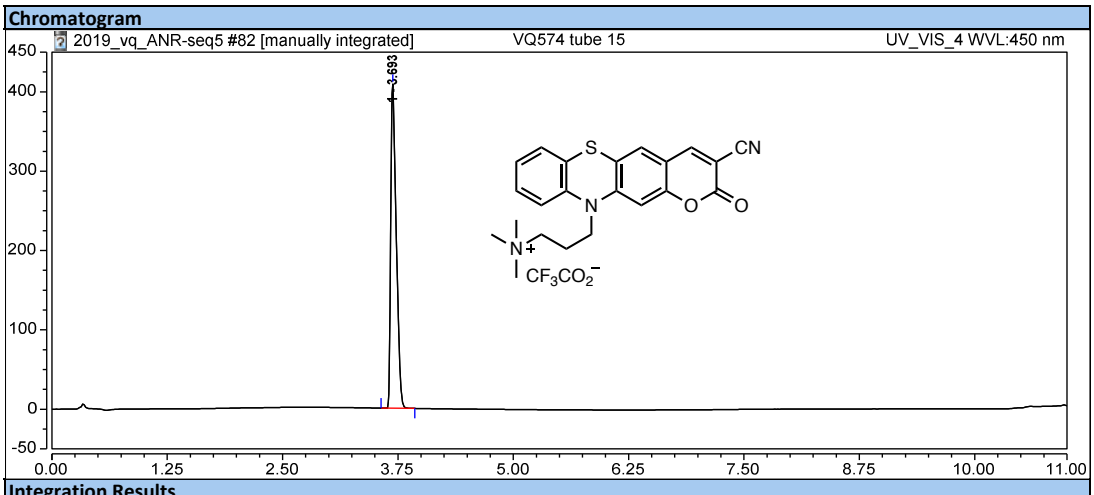

Integration Results

No.	Peak Name	Retention Time min	Area mAU*min	Height mAU	Relative Area %	Relative Height %	Amount n.a.
1		3.693	28.437	408.138	100.00	100.00	n.a.
Total:			**28.437**	**408.138**	**100.00**	**100.00**	

Fig. S39. ESI+ mass spectra (low resolution) of PTZ-coumarin hybrid dye 15

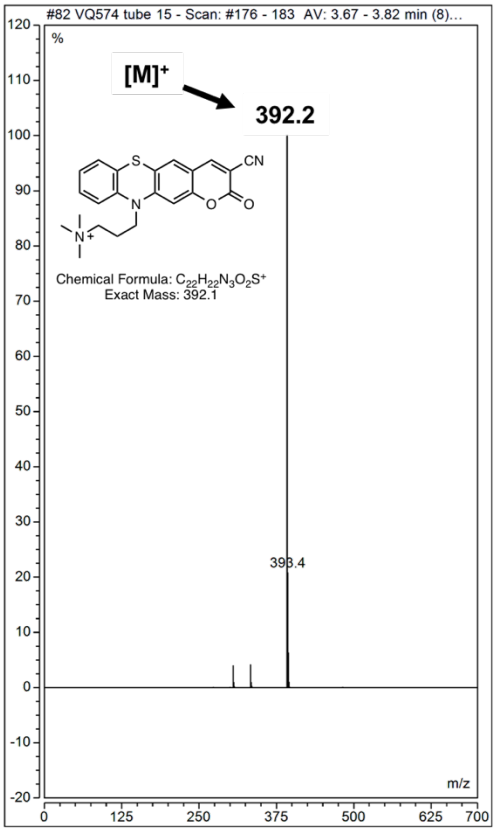

Fig. S40. UV-vis absorption, emission (Ex. at 450 nm, slit 5 nm) and exitation (Em. at 625 nm, slit 5 nm) spectra of PTZ-coumarin hybrid dye 15 in MeOH at 25 °C

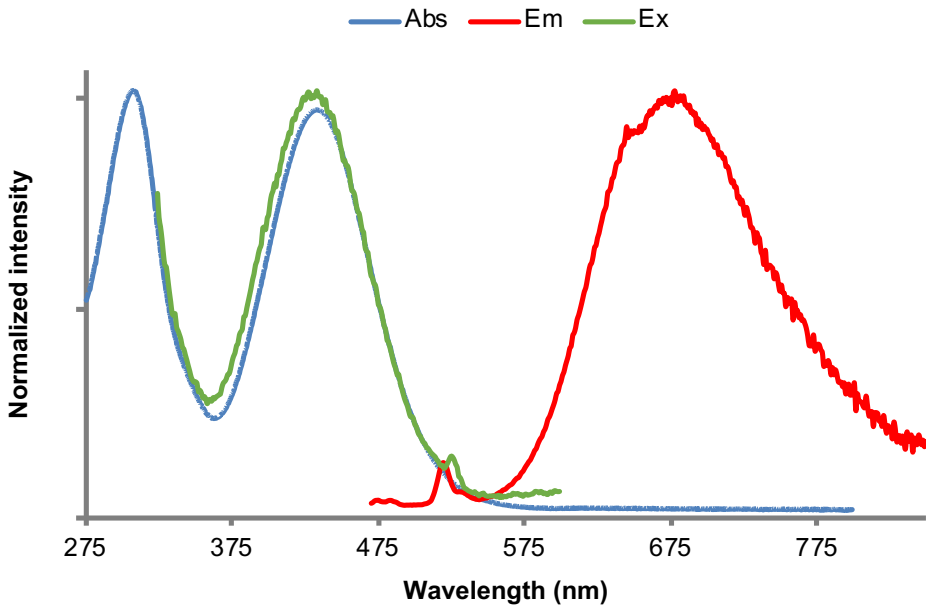

Please note: Em. peak at 519 nm is assigned to Raman scattering.

Fig. S41. UV-vis absorption, emission (Ex. at 450 nm, slit 5 nm) and exitation (Em. at 625 nm, slit 5 nm) spectra of PTZ-coumarin hybrid dye 15 in PBS (pH 7.3) at 25 °C

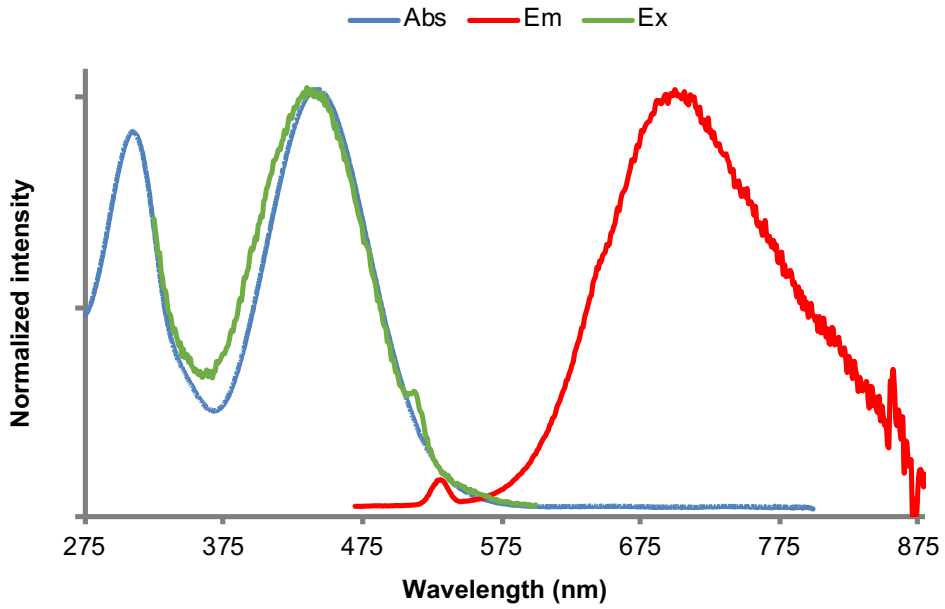

Please note: Em. peak at 531 nm is assigned to Raman scattering; Em. spectrum corrected until 850 nm which explains the artifact observed at this wavelength.

Fig. S42. UV-vis absorption, emission (Ex. at 450 nm, slit 5 nm) and exitation (Em. at 625 nm, slit 5 nm) spectra of PTZ-coumarin hybrid dye 15 in PBS (pH 7.3) + 300 µM Tween® 80 at 25 °C

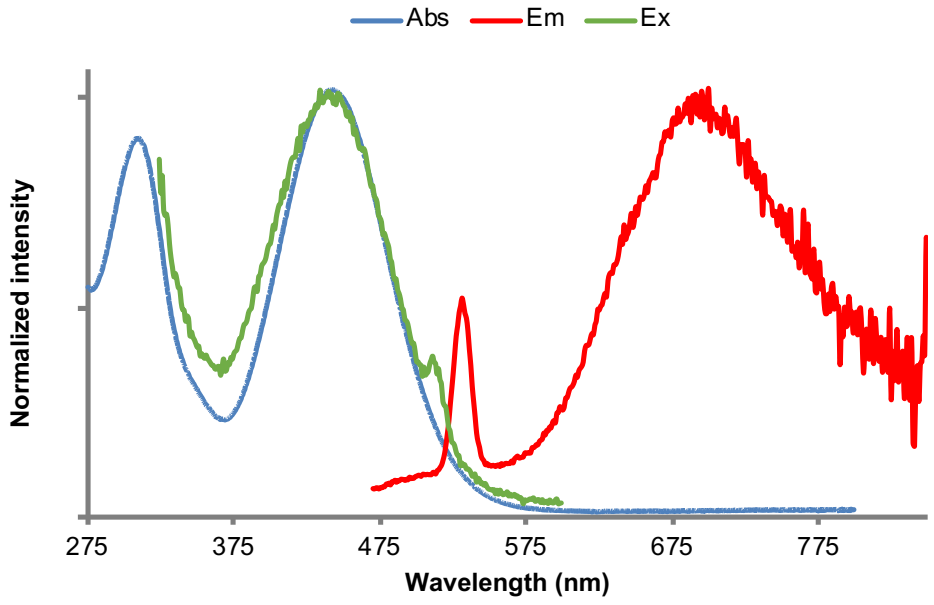

Please note: Em. peak at 531 nm is assigned to Raman scattering; Em. spectrum corrected until 850 nm which explains the artifact observed at this wavelength.

Fig. S43. IR-ATR spectrum of PTZ-coumarin hybrid dye 16 (TEA salt)

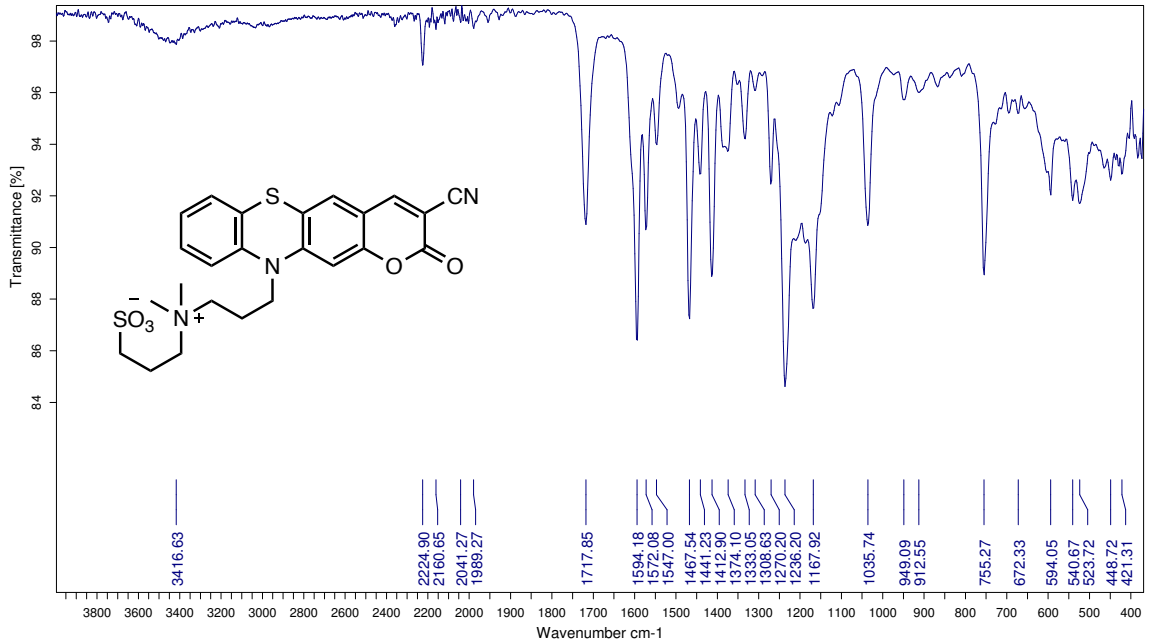

Fig. S44. ^{1}H NMR spectrum of PTZ-coumarin hybrid dye 16 (TEA salt) in DMF-d_7-D_2O 5:3, v/v with water signal suppression sequence (600 MHz, 325 K)

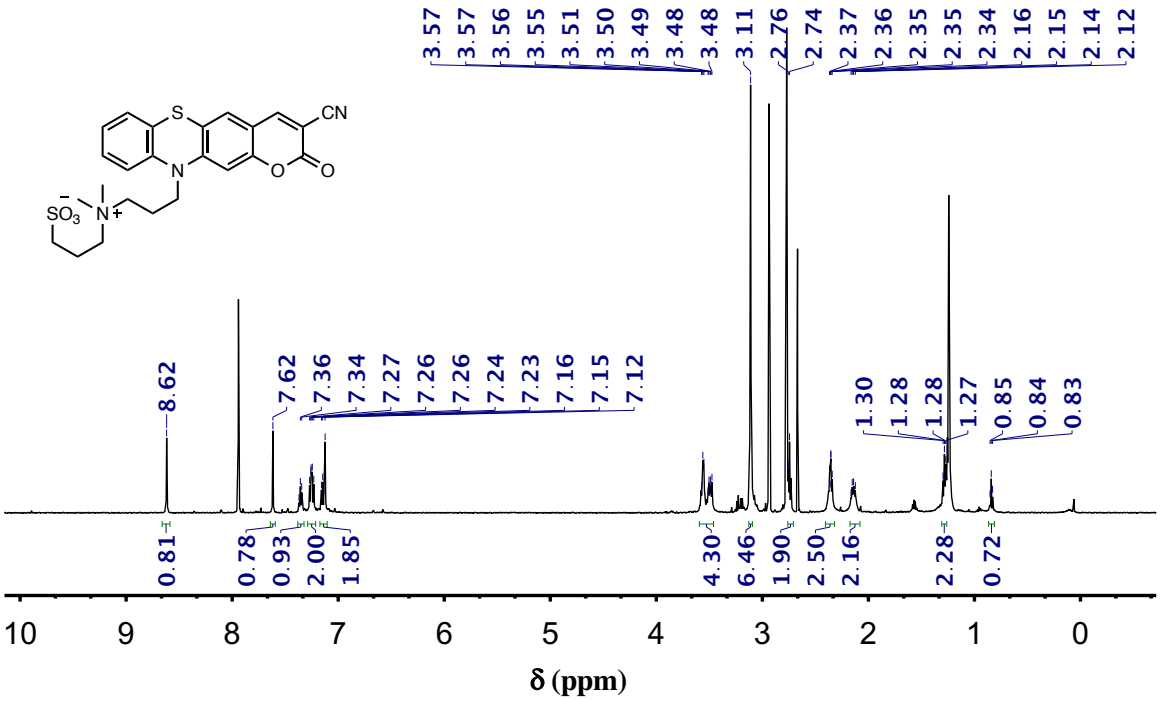

Fig. S45. RP-HPLC elution profile of PTZ-coumarin hybrid dye 16 (system A-QC, detection at 350 nm)

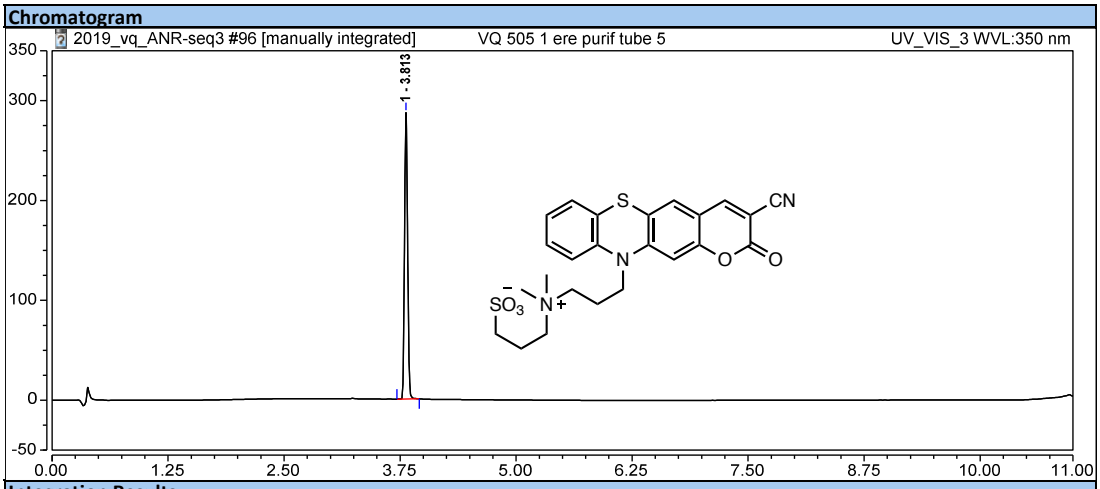

Integration Results

No.	Peak Name	Retention Time min	Area mAU*min	Height mAU	Relative Area %	Relative Height %	Amount n.a.
1		3.813	11.204	286.747	100.00	100.00	n.a.
Total:			**11.204**	**286.747**	**100.00**	**100.00**	

Fig. S46. RP-HPLC elution profile of PTZ-coumarin hybrid dye 16 (system A-QC, detection at 450 nm)

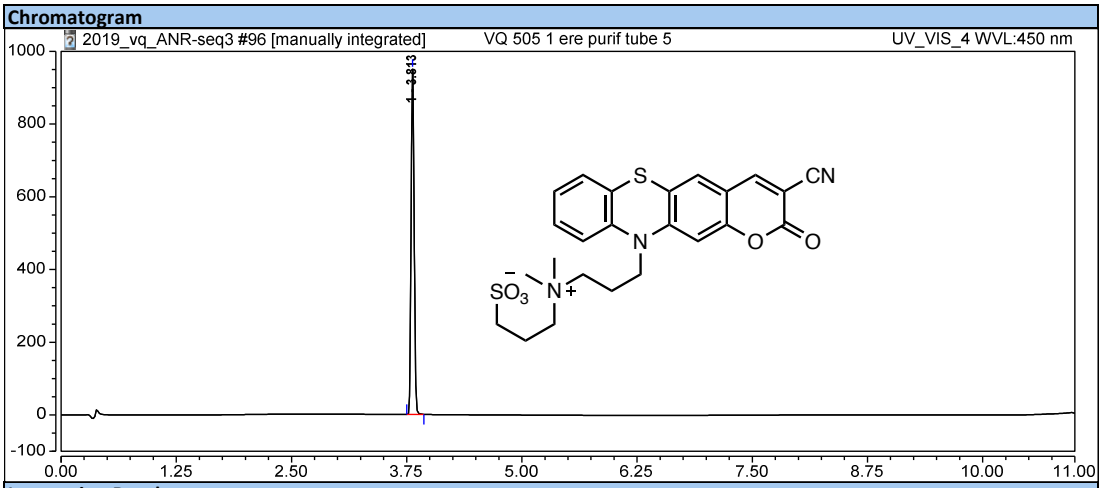

Integration Results

No.	Peak Name	Retention Time min	Area mAU*min	Height mAU	Relative Area %	Relative Height %	Amount n.a.
1		3.813	36.819	949.226	100.00	100.00	n.a.
Total:			**36.819**	**949.226**	**100.00**	**100.00**	

Fig. S47. ESI+ mass spectra (low resolution) of PTZ-coumarin hybrid dye 16

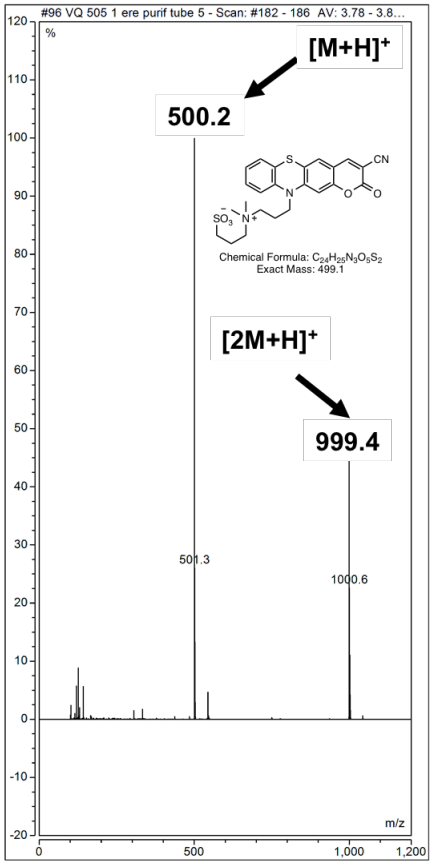

Fig. S48. UV-vis absorption, emission (Ex. at 450 nm, slit 5 nm) and exitation (Em. at 625 nm, slit 5 nm) spectra of PTZ-coumarin hybrid dye 16 in MeOH at 25 °C

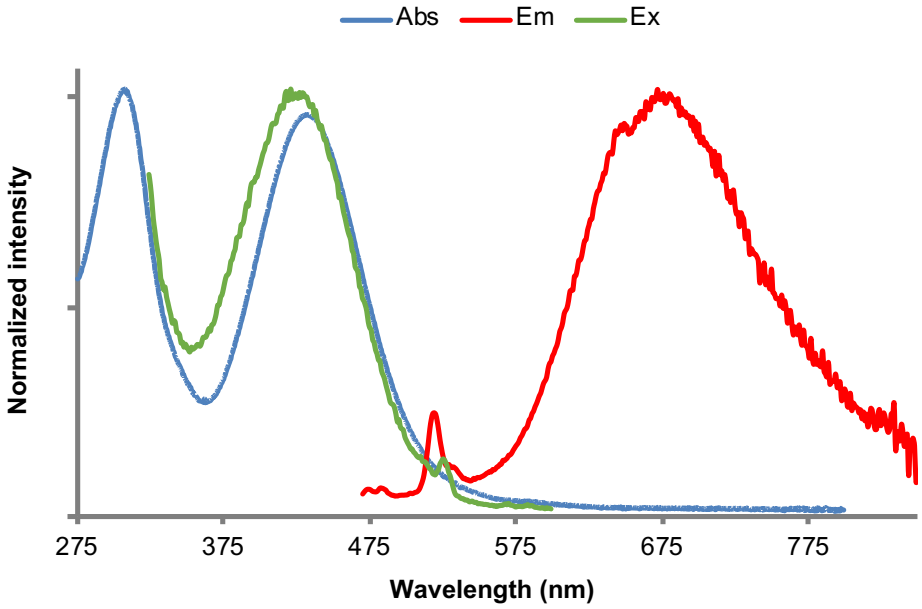

Please note: Em. peak at 519 nm is assigned to Raman scattering.

Fig. S49. UV-vis absorption, emission (Ex. at 450 nm, slit 5 nm) and exitation (Em. at 710 nm, slit 10 nm, Ex. 380-650 nm, slit 12 nm) spectra of PTZ-coumarin hybrid dye 16 in PBS (pH 7.3) at 25 °C

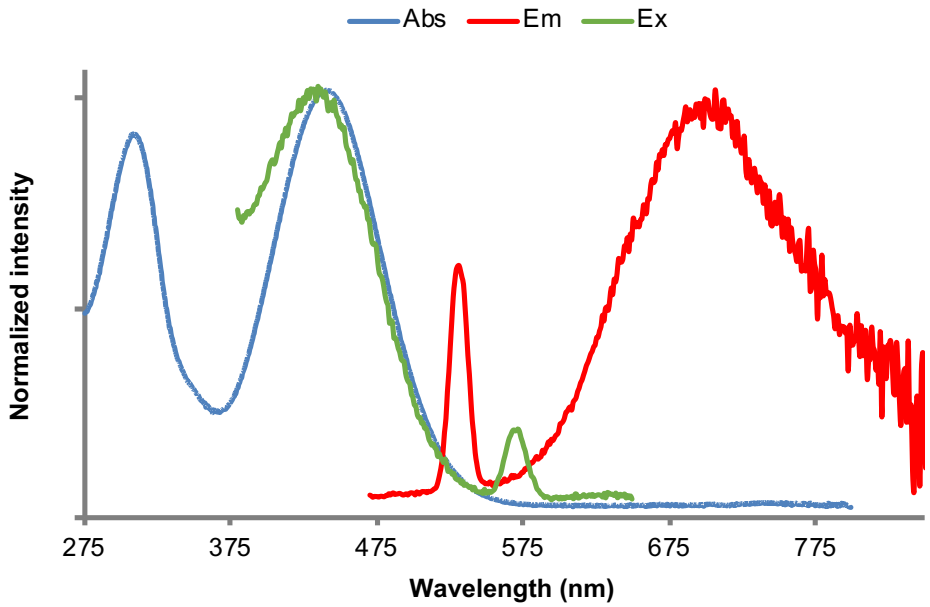

Please note: Em. peak at 531 nm is assigned to Raman scattering.

Fig. S50. UV-vis absorption, emission (Ex. at 450 nm, slit 5 nm) and exitation (Em. at 710 nm, slit 10 nm, Ex. 380-650 nm, slit 12 nm) spectra of PTZ-coumarin hybrid dye 16 in PBS (pH 7.3) + 300 μM Tween® 80 at 25 °C

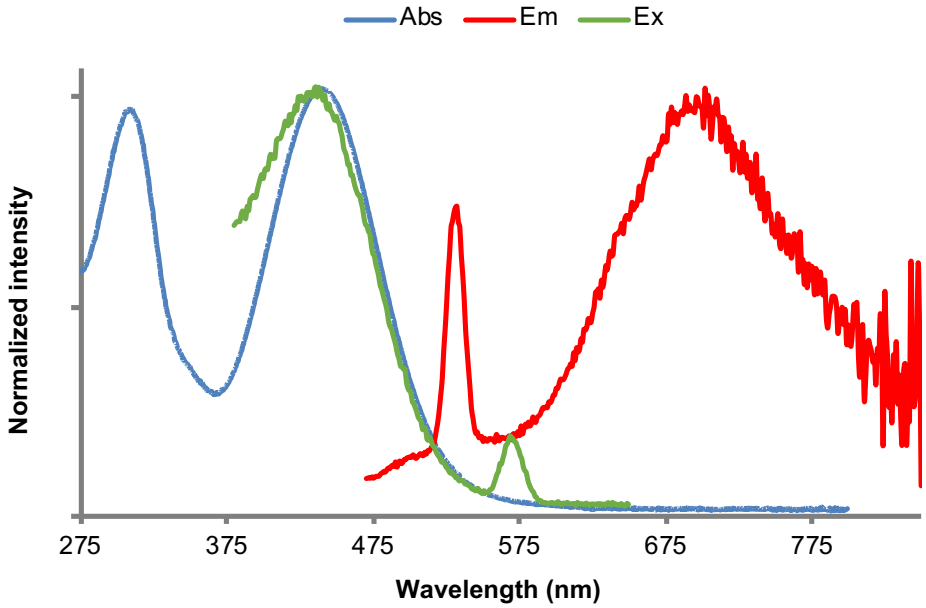

Please note: Em. peak at 532 nm is assigned to Raman scattering.

Fig. S51. Fluorescence emission time course (Ex./Em. 400/520 nm, slit 2 nm) of PTZ-coumarin hybrid dye 10 (concentration: 2.0 μM) in the presence of hypochlorite anion (1 equiv.) in PBS (pH 7.3) at 25 °C

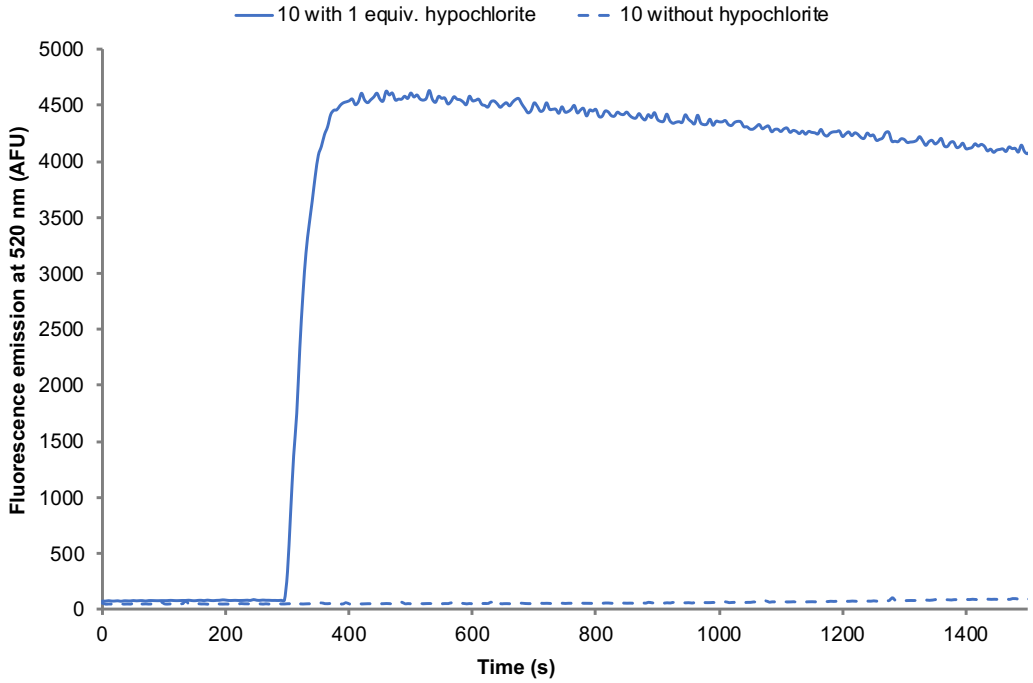

Please note: addition of NaOCl after 5 min of incubation in PBS.

Fig. S1. Overlayed fluorescence emission spectra (Ex. 400 nm, slit 5 nm) of PTZ-coumarin hybrid dye 10 (concentration: 2.0 μM) in PBS (pH 7.3), before and after incubation with hypochlorite anion (1 equiv.)

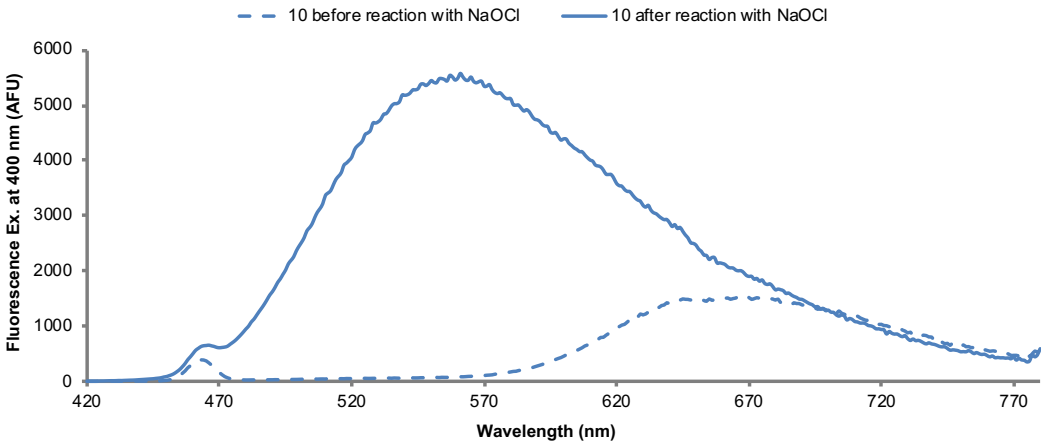

Please note: Em. peak at 463-466 nm is assigned to Raman scattering.

Fig. S53. Overlayed fluorescence emission spectra (Ex. 400 nm, slit 5 nm) of PTZ-coumarin hybrid dye 10 (concentration: 2.0 μM) before and after incubation in PBS (pH 7.3)

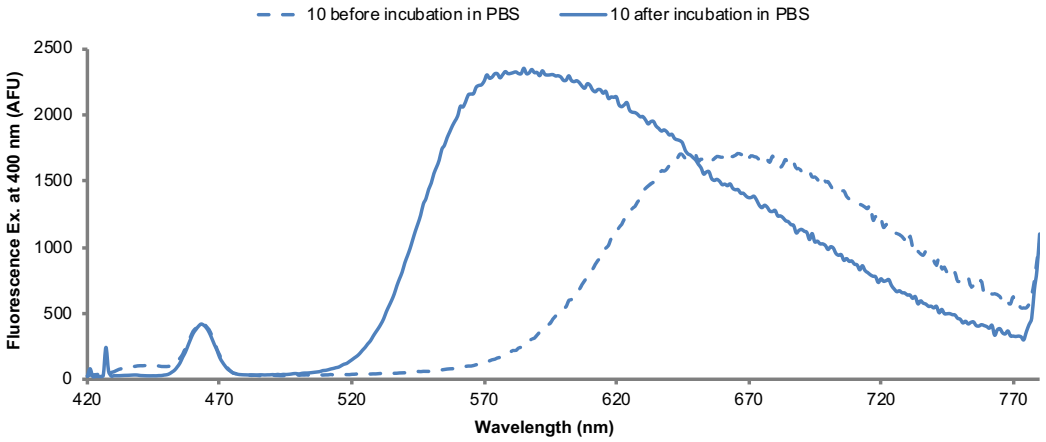

*Please note: Em. peak at 463 nm is assigned to Raman scattering. Em spectrum (after incubation in PBS) is the sum of Em spectra of starting PTZ-coumarin hybrid dye **10** and sulfoxide derivative (more fluorescent) whose formation in minor amount arises from a photooxidation reaction.*

Fig. S54. Fluorescence emission time course (Ex./Em. 400/520 nm, slit 2 nm) of PTZ-coumarin hybrid dye 10 (concentration: 2.0 μM) in the presence of hypochlorite anion (1, 10 and 100 equiv.) in PBS (pH 7.3) at 25 °C

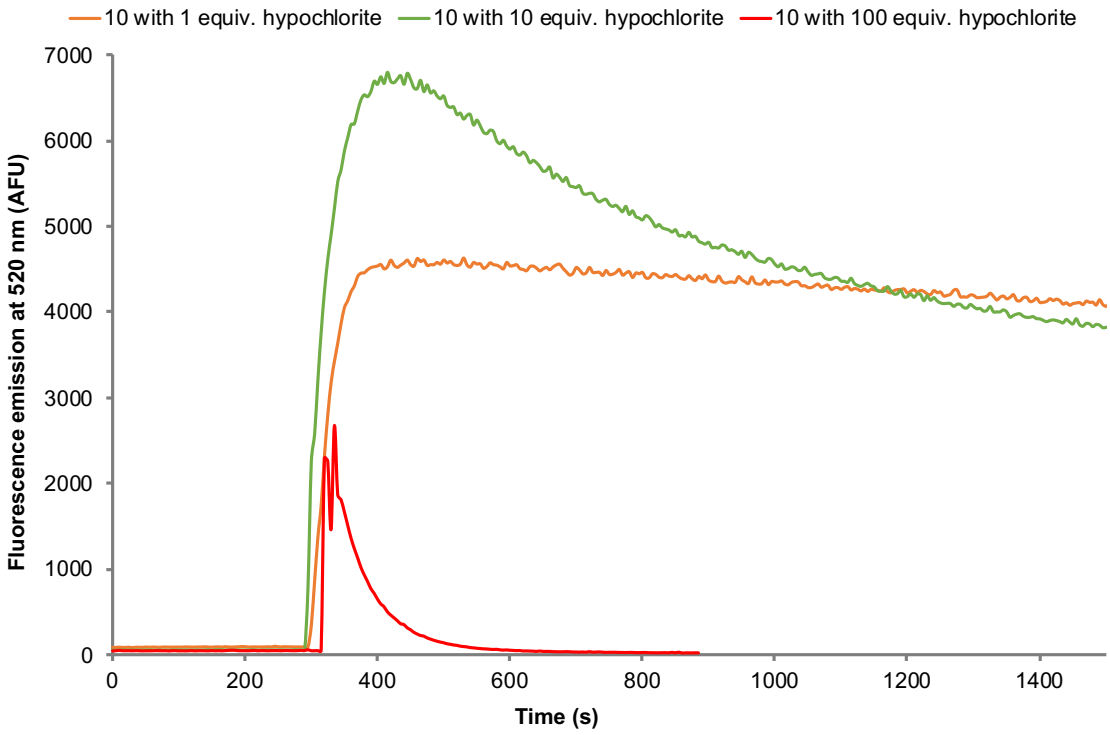

Please note: addition of NaOCl after 5 min of incubation in PBS.

Fig. S55. Overlayed fluorescence emission spectra (Ex. 400 nm, slit 5 nm) of PTZ-coumarin hybrid dye 10 (concentration: 2.0 μM) in PBS (pH 7.3), before and after incubation with hypochlorite anion (10 equiv.)

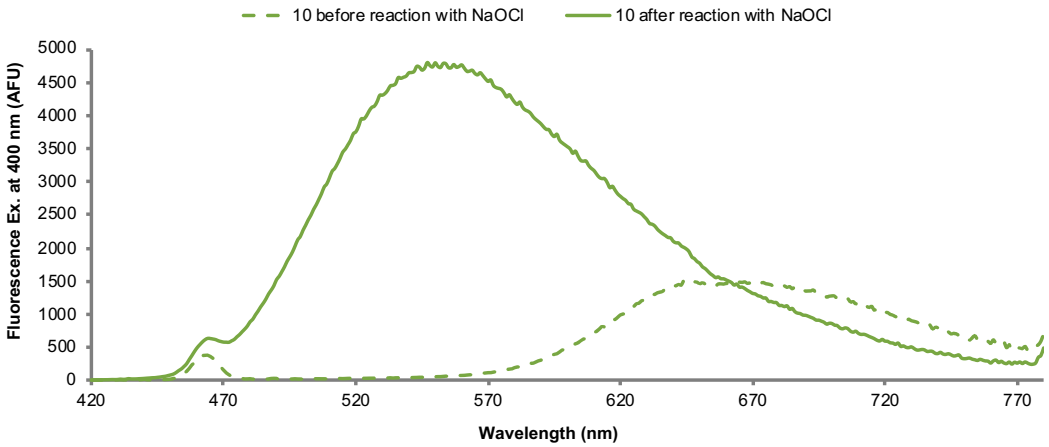

Please note: Em. peak at 464 nm is assigned to Raman scattering.

Fig. S56. Overlayed fluorescence emission spectra (Ex. 400 nm, slit 5 nm) of PTZ-coumarin hybrid dye 10 (concentration: 2.0 μM) in PBS (pH 7.3), before and after incubation with hypochlorite anion (100 equiv.)

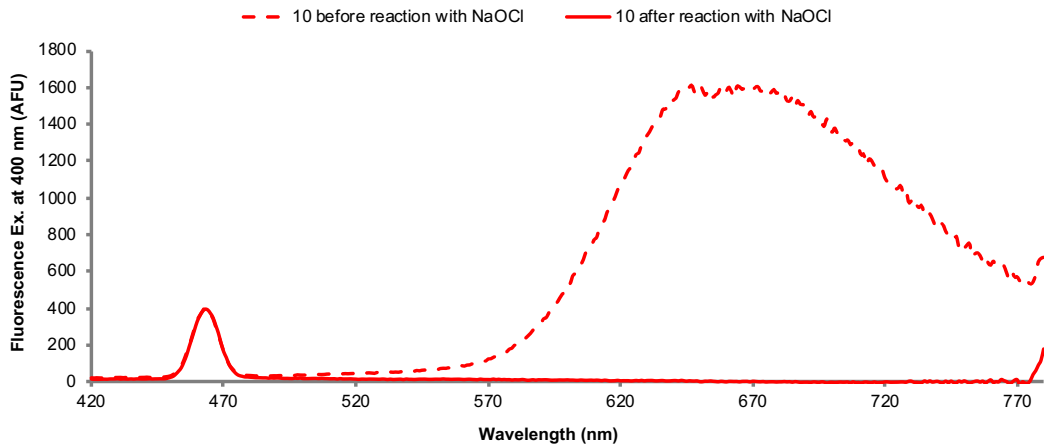

Please note: Em. peak at 463 nm is assigned to Raman scattering. The lack of detectable Em. upon Ex. at 400 nm suggests that sulfoxide derivative may undergone over-oxidation (formation of sulfone derivative?) and subsequent degradation of PTZ heterocycle.

Fig. S57. Fluorescence emission time course (Ex./Em. 400/520 nm, slit 2 nm) of PTZ-coumarin hybrid dye 15 (concentration: 2.0 μM) in the presence of hypochlorite anion (1 equiv.) in PBS (pH 7.3) at 25 °C

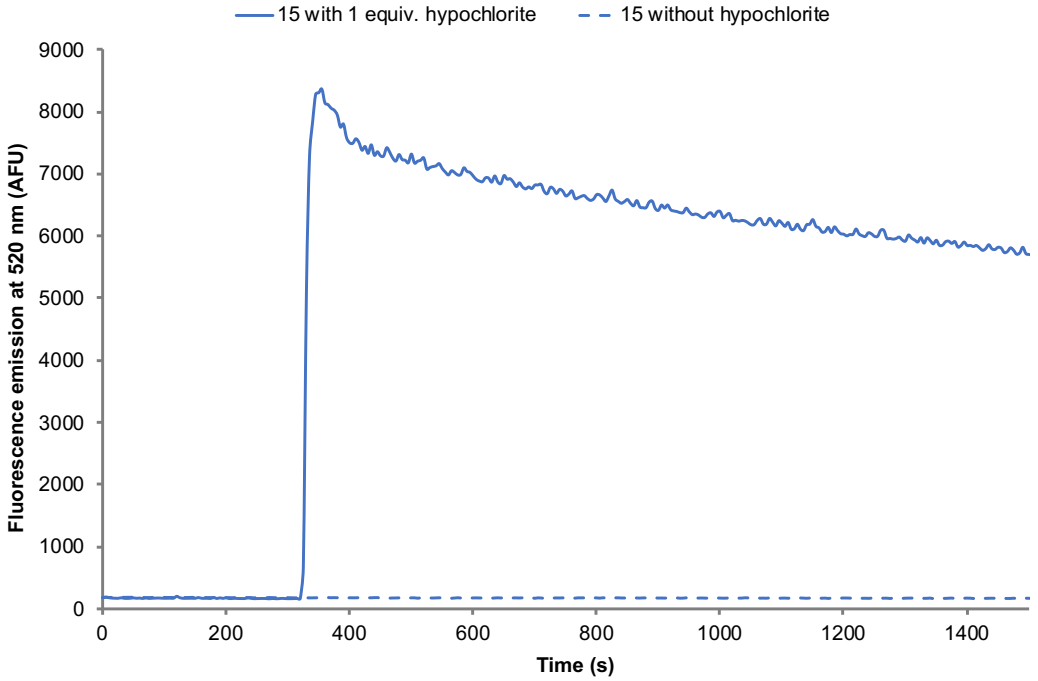

Fig. S58. Overlayed fluorescence emission spectra (Ex. 400 nm, slit 5 nm) of PTZ-coumarin hybrid dye 15 (concentration: 2.0 μM) in PBS (pH 7.3), before and after incubation with hypochlorite anion (1 equiv.)

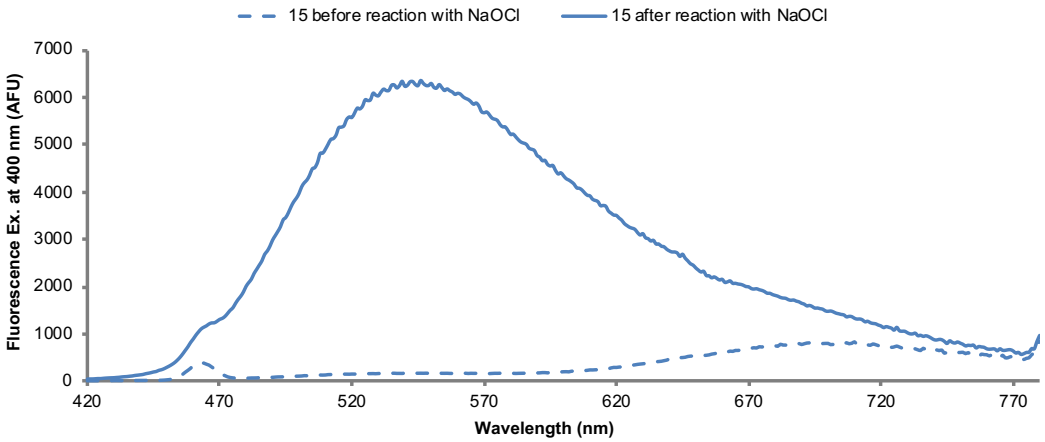

Please note: Em. peak at 463 nm is assigned to Raman scattering.

Fig. S59. Overlayed fluorescence emission spectra (Ex. 400 nm, slit 5 nm) of PTZ-coumarin hybrid dye 15 (concentration: 2.0 μM) before and after incubation in PBS (pH 7.3)

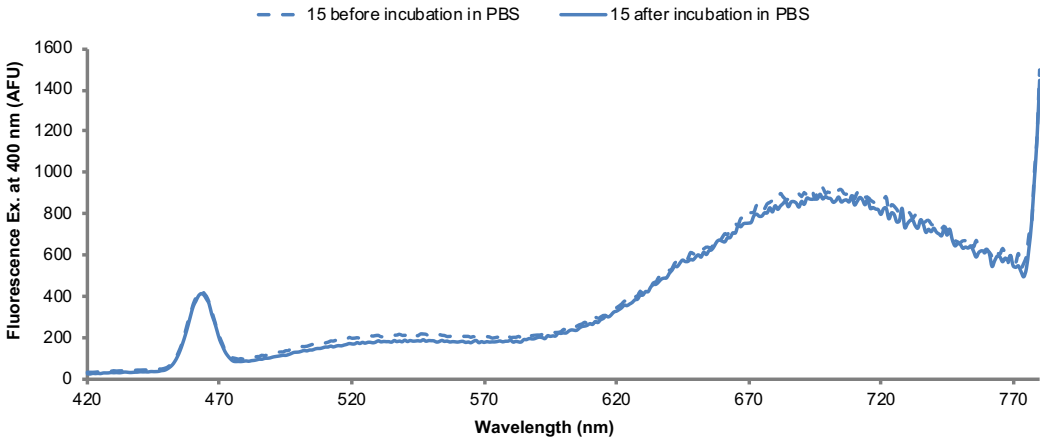

Please note: Em. peak at 463 nm is assigned to Raman scattering.

Fig. S60. Fluorescence emission time course (Ex./Em. 400/520 nm, slit 2 nm) of PTZ-coumarin hybrid dye 16 (concentration: 2.0 μM) in the presence of hypochlorite anion (1 equiv.) in PBS (pH 7.3) at 25 °C

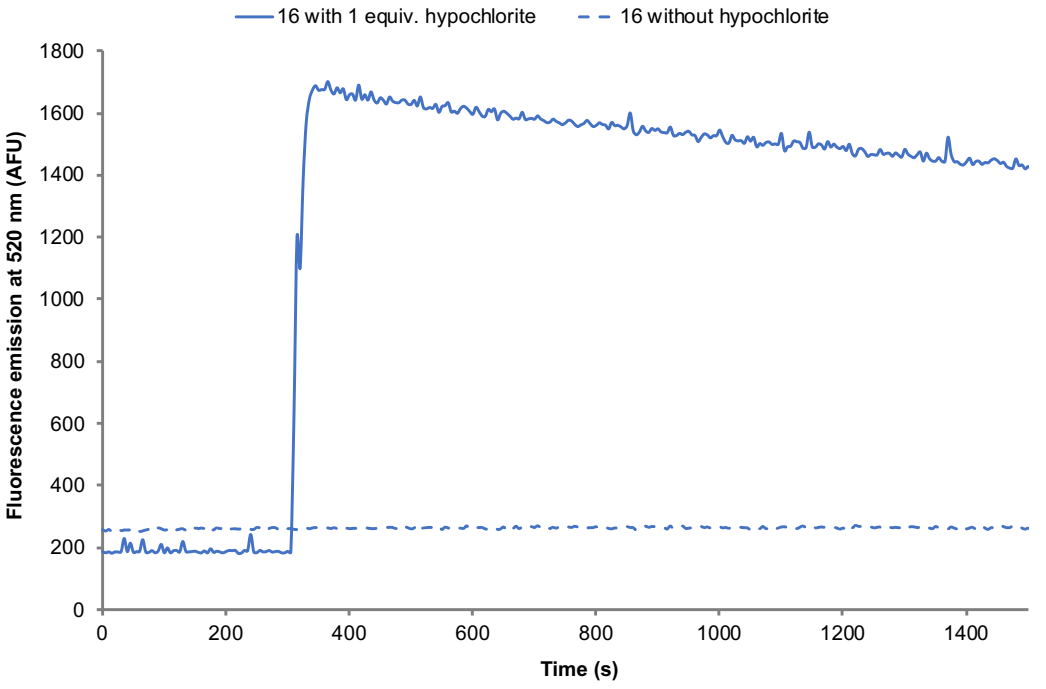

Fig. S61. Overlayed fluorescence emission spectra (Ex. 400 nm, slit 5 nm) of PTZ-coumarin hybrid dye 16 (concentration: 2.0 μM) in PBS (pH 7.3), before and after incubation with hypochlorite anion (1 equiv.)

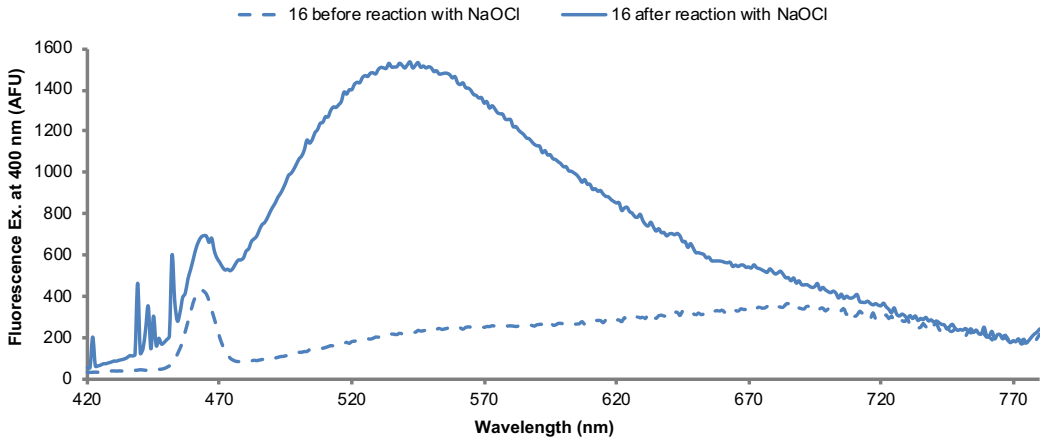

Please note: Em. peak at 463-464 nm is assigned to Raman scattering.

Fig. S62. Overlayed fluorescence emission spectra (Ex. 400 nm, slit 5 nm) of PTZ-coumarin hybrid dye 16 (concentration: 2.0 μM) before and after incubation in PBS (pH 7.3)

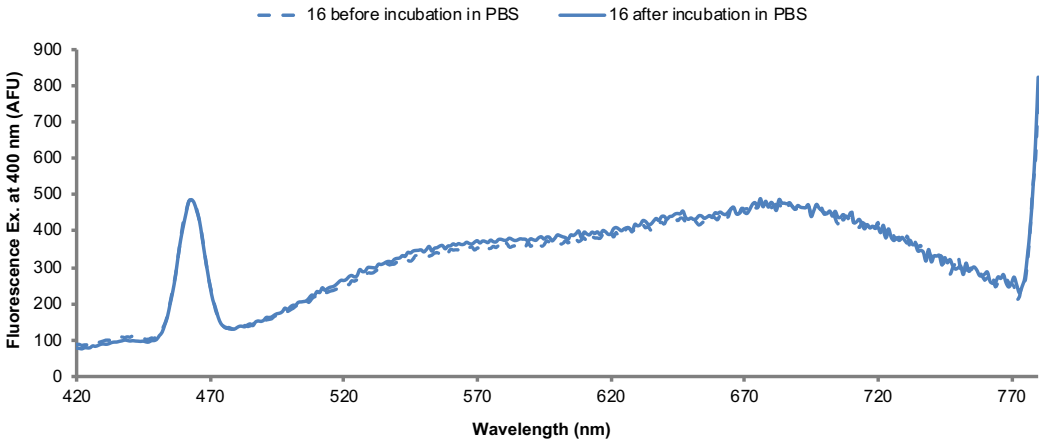

Please note: Em. peak at 463 nm is assigned to Raman scattering.

Fig. S63. RP-HPLC elution profile (system D-Fluo, fluorescence detection Ex./Em. 400/520 nm (top) and 450/700 nm (bottom)) of PTZ-coumarin hybrid dye 10 (concentration: 2.0 μM in PBS)

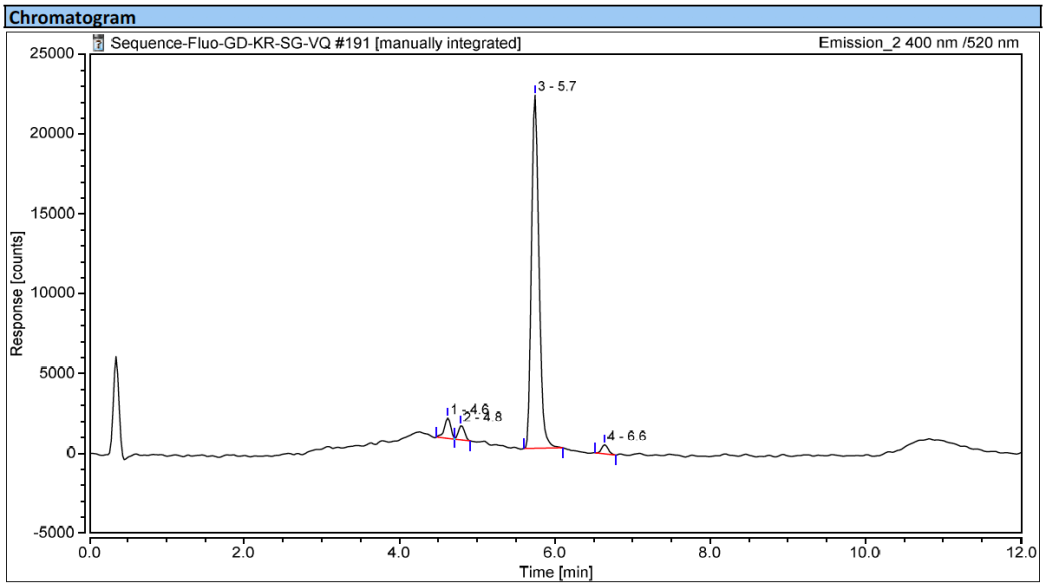

No.	Peak Name	Retention Time min	Area counts*min	Height counts	Relative Area %	Relative Height %	Amount n.a.
1		4.622	121.671	1274.981	4.42	5.13	n.a.
2		4.788	83.914	884.563	3.05	3.56	n.a.
3		5.747	2488.759	22126.293	90.50	89.04	n.a.
4		6.643	55.605	565.335	2.02	2.27	n.a.
Total:			**2749.949**	**24851.173**	**100.00**	**100.00**	

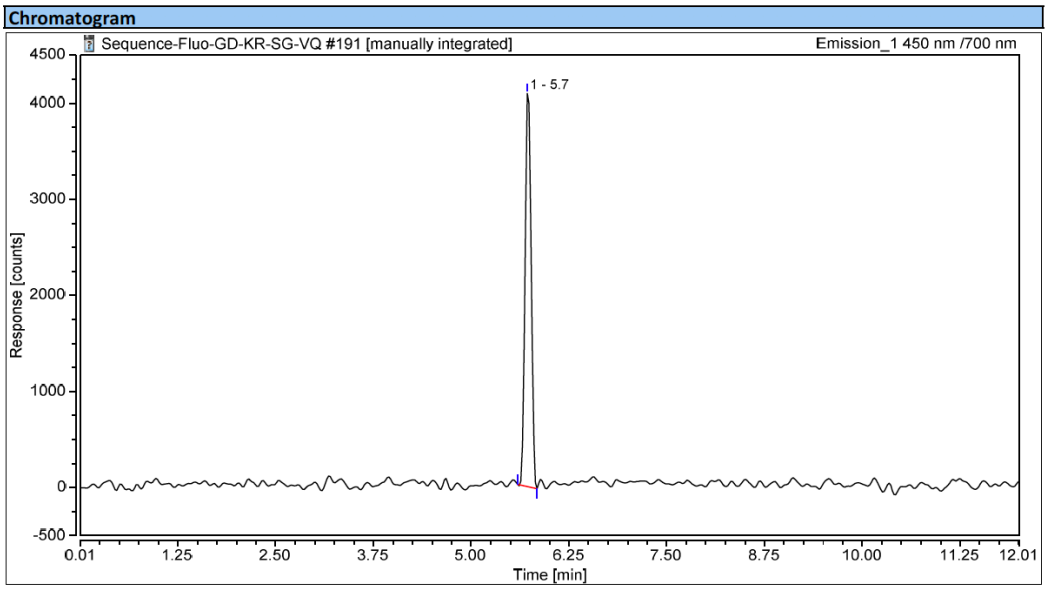

No.	Peak Name	Retention Time min	Area counts*min	Height counts	Relative Area %	Relative Height %	Amount n.a.
1		5.718	371.521	4091.000	100.00	100.00	n.a.
Total:			**371.521**	**4091.000**	**100.00**	**100.00**	

Fig. S64. RP-HPLC elution profile (system D-Fluo, fluorescence detection Ex./Em. 400/520 nm (top) and 450/700 nm (bottom)) of PTZ-coumarin hybrid dye 10 (concentration: 2.0 μM in PBS) after incubation in PBS (pH 7.3)

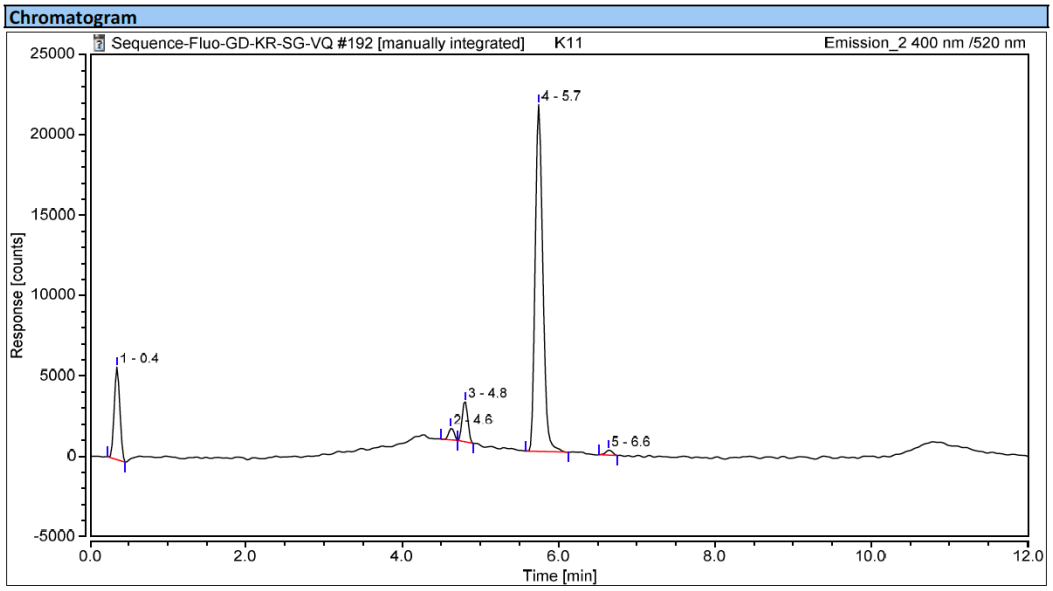

No.	Peak Name	Retention Time min	Area counts*min	Height counts	Relative Area %	Relative Height %	Amount n.a.
1		0.351	481.389	5755.909	14.91	18.67	n.a.
2		4.622	58.598	707.800	1.82	2.30	n.a.
3		4.809	214.969	2485.500	6.66	8.06	n.a.
4		5.747	2441.639	21575.154	75.65	69.98	n.a.
5		6.643	31.103	306.545	0.96	0.99	n.a.
Total:			**3227.698**	**30830.908**	**100.00**	**100.00**	

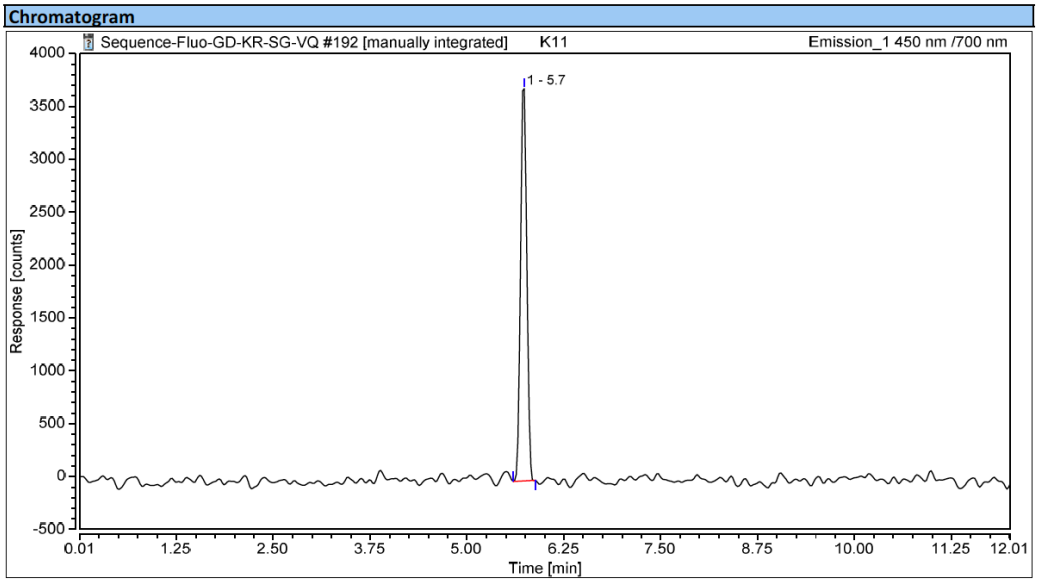

No.	Peak Name	Retention Time min	Area counts*min	Height counts	Relative Area %	Relative Height %	Amount n.a.
1		5.739	350.385	3708.500	100.00	100.00	n.a.
Total:			**350.385**	**3708.500**	**100.00**	**100.00**	

Fig. S65. RP-HPLC elution profile (system D-Fluo, fluorescence detection Ex./Em. 400/520 nm (top) and 450/700 nm (bottom)) of PTZ-coumarin hybrid dye 10 (concentration: 2.0 μM in PBS) after incubation with hypochlorite anion (1 equiv.) in PBS (pH 7.3)

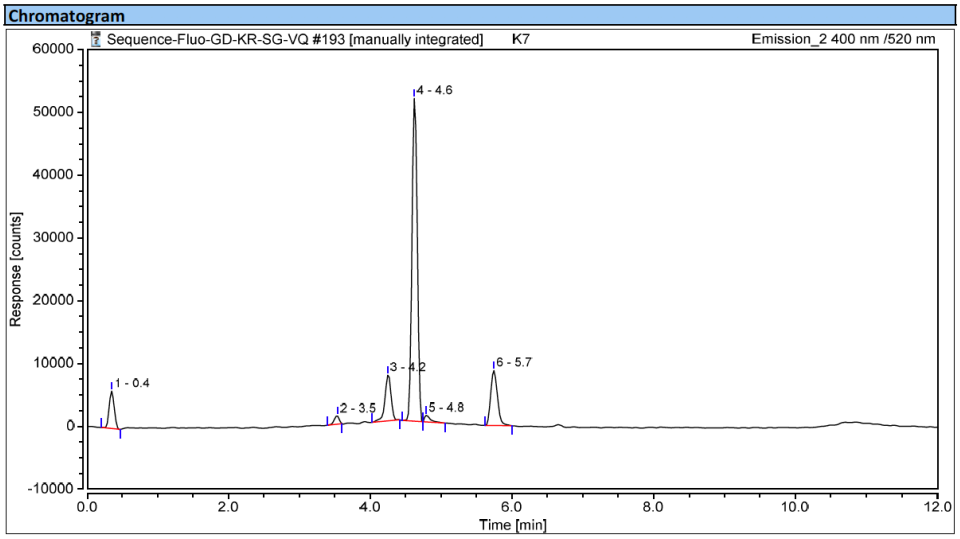

No.	Peak Name	Retention Time min	Area counts*min	Height counts	Relative Area %	Relative Height %	Amount n.a.
1		0.351	495.559	5951.050	7.21	7.86	n.a.
2		3.538	108.723	1289.055	1.58	1.70	n.a.
3		4.247	728.944	7292.842	10.60	9.63	n.a.
4		4.622	4478.623	51416.843	65.16	67.88	n.a.
5		4.788	97.500	1034.600	1.42	1.37	n.a.
6		5.747	964.367	8759.333	14.03	11.56	n.a.
Total:			**6873.717**	**75743.724**	**100.00**	**100.00**	

Please note: peak at t_R = 4.6 min assigned to fluorescent sulfoxide derivative.

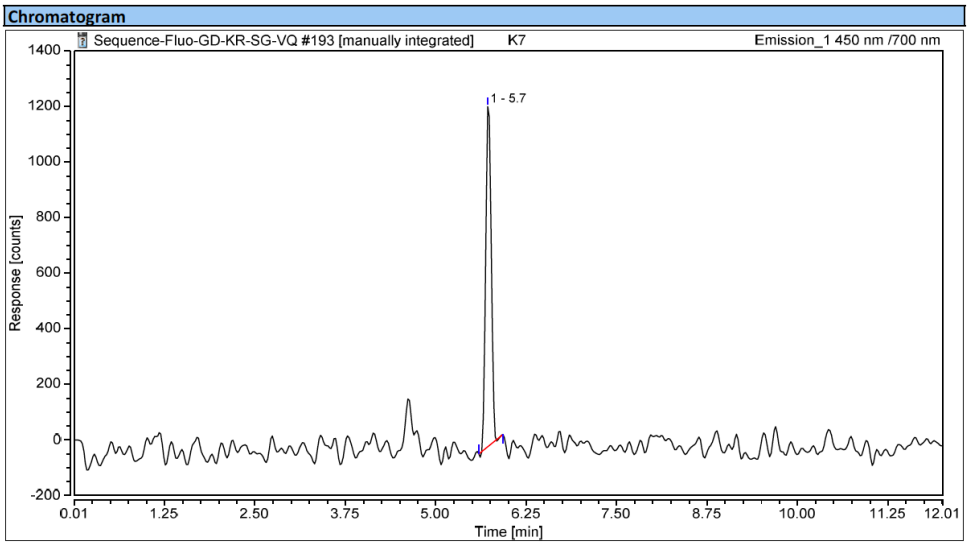

No.	Peak Name	Retention Time min	Area counts*min	Height counts	Relative Area %	Relative Height %	Amount n.a.
1		5.718	108.458	1223.750	100.00	100.00	n.a.
Total:			**108.458**	**1223.750**	**100.00**	**100.00**	

Fig. S66. RP-HPLC elution profile (system D-Fluo, fluorescence detection Ex./Em. 400/520 nm (top) and 450/700 nm (bottom)) of PTZ-coumarin hybrid dye 10 (concentration: 2.0 µM in PBS) after incubation with hypochlorite anion (10 equiv.) in PBS (pH 7.3)

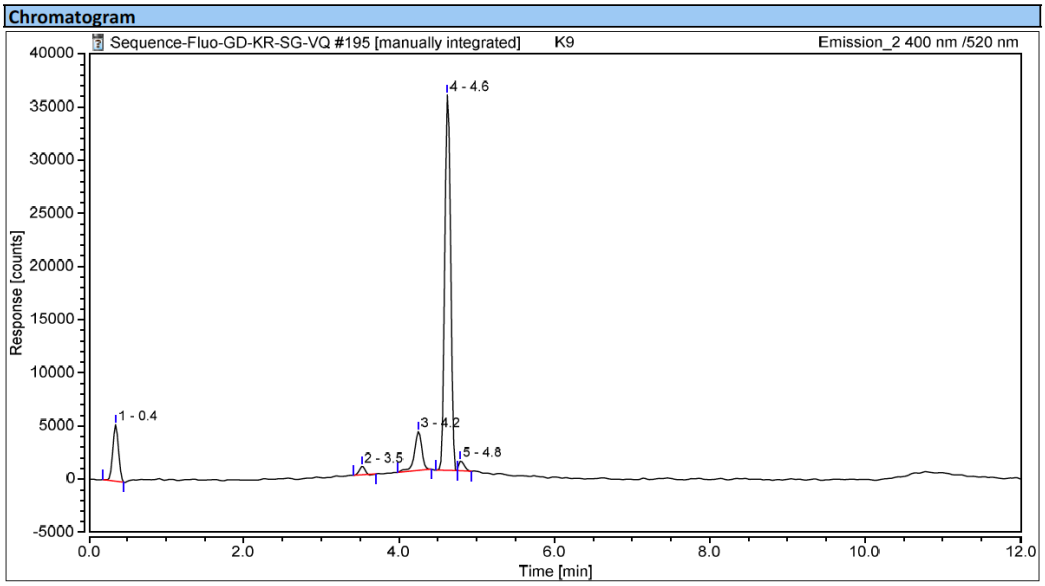

No.	Peak Name	Retention Time min	Area counts*min	Height counts	Relative Area %	Relative Height %	Amount n.a.
1		0.351	455.583	5332.000	11.19	11.61	n.a.
2		3.518	61.647	771.429	1.51	1.68	n.a.
3		4.247	404.875	3652.571	9.94	7.95	n.a.
4		4.622	3075.351	35300.534	75.53	76.84	n.a.
5		4.788	74.383	883.319	1.83	1.92	n.a.
Total:			**4071.839**	**45939.854**	**100.00**	**100.00**	

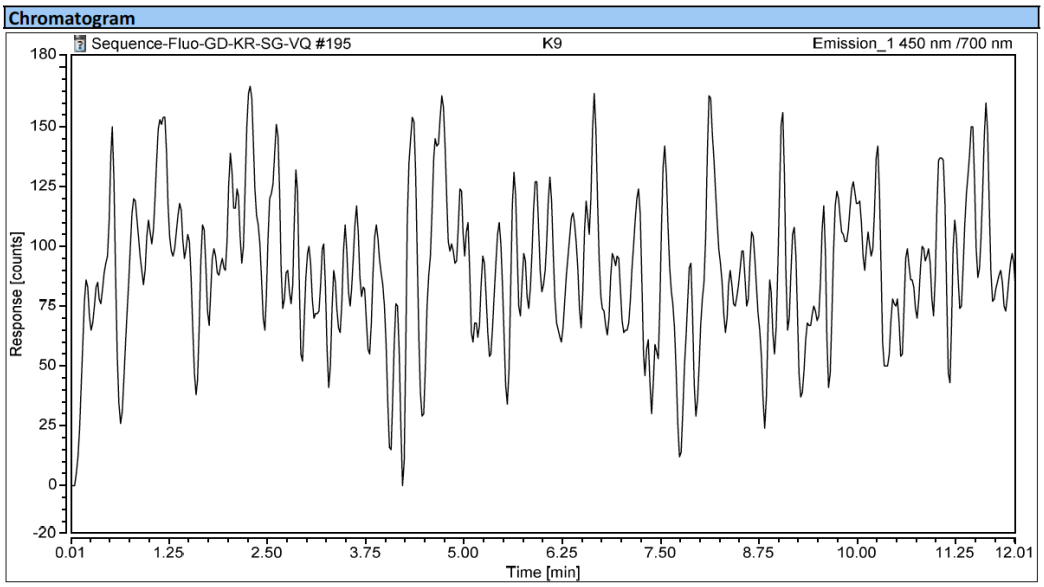

No.	Peak Name	Retention Time min	Area counts*min	Height counts	Relative Area %	Relative Height %	Amount n.a.
Total:			**0.000**	**0.000**	**0.00**	**0.00**	

Fig. S67. RP-HPLC elution profile (system D-Fluo, fluorescence detection Ex./Em. 400/520 nm (top) and 450/700 nm (bottom)) of PTZ-coumarin hybrid dye 10 (concentration: 2.0 μM in PBS) after incubation with hypochlorite anion (100 equiv.) in PBS (pH 7.3)

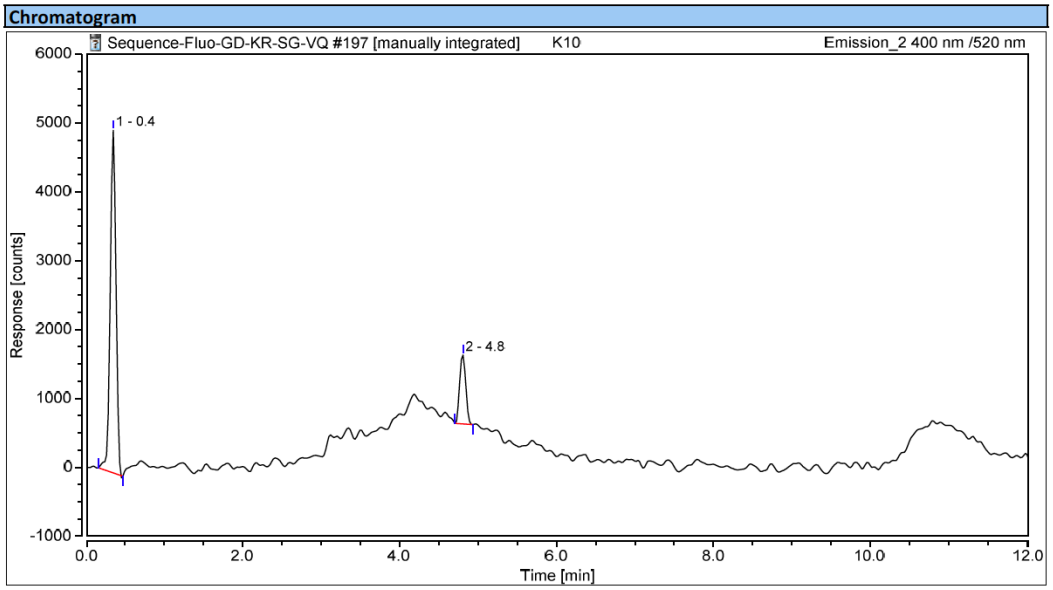

No.	Peak Name	Retention Time min	Area counts*min	Height counts	Relative Area %	Relative Height %	Amount n.a.
1		0.351	425.900	4973.400	82.62	83.25	n.a.
2		4.809	89.605	1000.636	17.38	16.75	n.a.
Total:			**515.506**	**5974.036**	**100.00**	**100.00**	

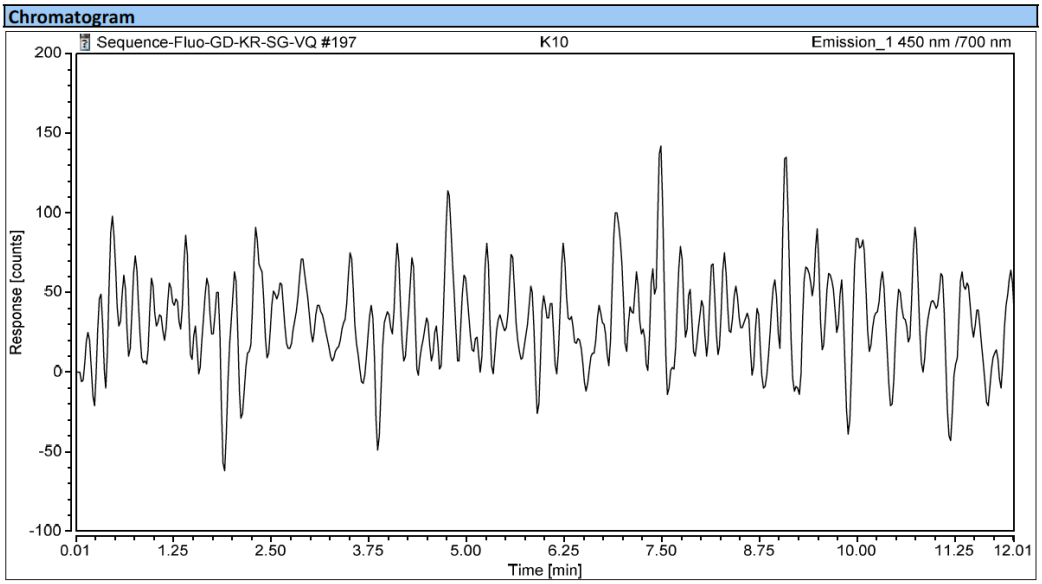

No.	Peak Name	Retention Time min	Area counts*min	Height counts	Relative Area %	Relative Height %	Amount n.a.
Total:			**0.000**	**0.000**	**0.00**	**0.00**	

Please note: the lack of peak at t_R = 4.6 min upon Ex. at 400 nm suggests that sulfoxide derivative may undergone over-oxidation (formation of sulfone derivative?) and subsequent degradation of PTZ heterocycle.

Fig. S68. RP-HPLC elution profile (system D-Fluo, fluorescence detection Ex./Em. 400/520 nm (top) and 450/700 nm (bottom)) of PTZ-coumarin hybrid dye 15 (concentration: 2.0 µM in PBS)

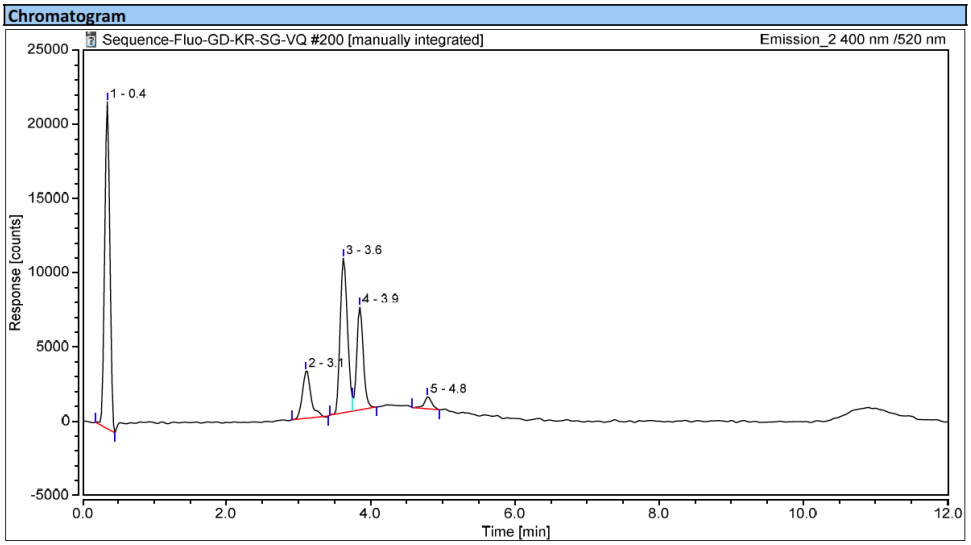

No.	Peak Name	Retention Time min	Area counts*min	Height counts	Relative Area %	Relative Height %	Amount n.a.
1		0.351	1838.331	22037.642	42.37	50.81	n.a.
2		3.101	437.867	3172.625	10.09	7.31	n.a.
3		3.622	1219.113	10419.742	28.10	24.02	n.a.
4		3.851	743.277	6932.871	17.13	15.98	n.a.
5		4.789	100.513	812.576	2.32	1.87	n.a.
Total:			**4339.101**	**43375.456**	**100.00**	**100.00**	

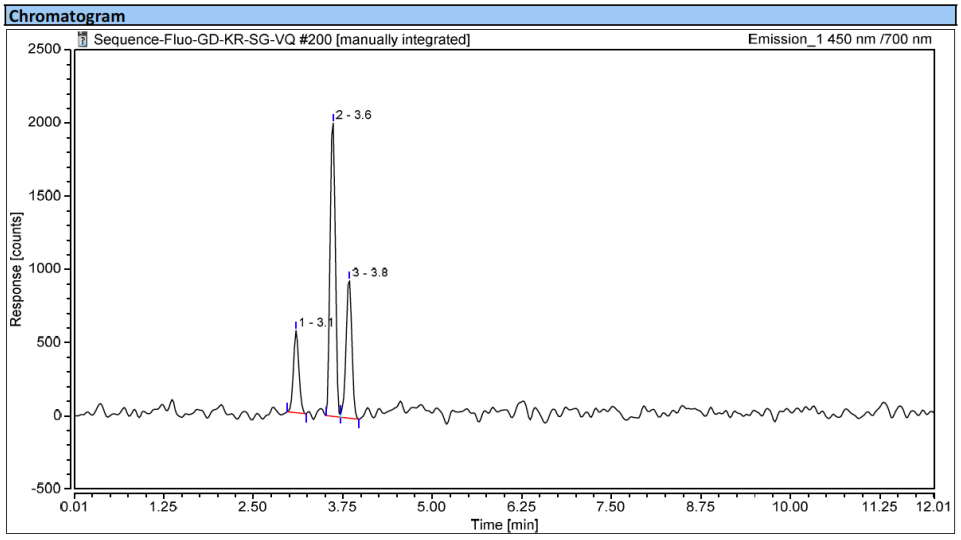

No.	Peak Name	Retention Time min	Area counts*min	Height counts	Relative Area %	Relative Height %	Amount n.a.
1		3.093	49.667	562.000	16.12	16.04	n.a.
2		3.614	170.044	2002.909	55.18	57.16	n.a.
3		3.843	88.477	938.909	28.71	26.80	n.a.
Total:			**308.188**	**3503.818**	**100.00**	**100.00**	

*Please note: several hypotheses may explain the presence of several peaks in pure sample of **15**, counter-ion effect for quaternary ammonium of pendant arm (chloride, formate and phosphate), fluorescent impurities (present in minute amounts) not detectable by NMR and RP-HPLC coupled to UV-vis detection.*

Fig. S69. RP-HPLC elution profile (system D-Fluo, fluorescence detection Ex./Em. 400/520 nm (top) and 450/700 nm (bottom)) of PTZ-coumarin hybrid dye 15 (concentration: 2.0 μM in PBS) after incubation in PBS (pH 7.3)

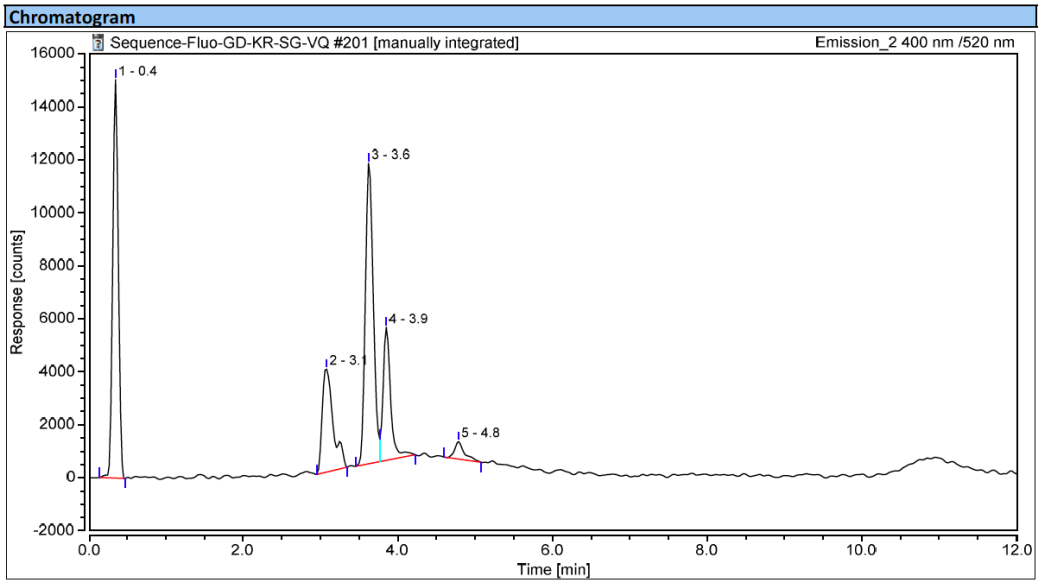

No.	Peak Name	Retention Time min	Area counts*min	Height counts	Relative Area %	Relative Height %	Amount n.a.
1		0.351	1262.669	15039.000	32.14	41.81	n.a.
2		3.080	642.601	3884.316	16.36	10.80	n.a.
3		3.622	1354.139	11356.216	34.47	31.58	n.a.
4		3.851	572.830	5024.514	14.58	13.97	n.a.
5		4.788	96.555	661.696	2.46	1.84	n.a.
Total:			**3928.795**	**35965.741**	**100.00**	**100.00**	

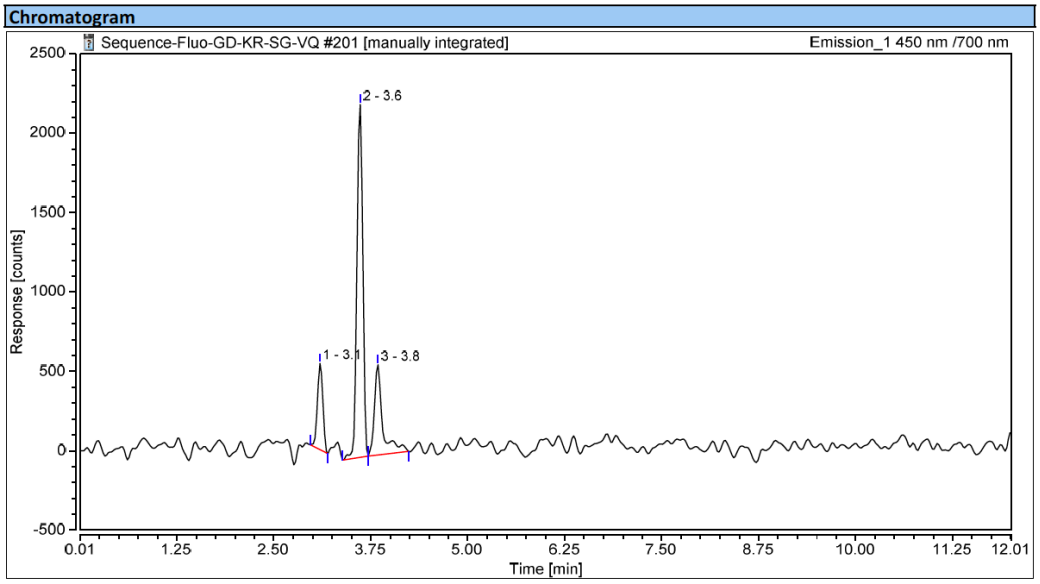

No.	Peak Name	Retention Time min	Area counts*min	Height counts	Relative Area %	Relative Height %	Amount n.a.
1		3.093	44.458	542.091	14.42	16.26	n.a.
2		3.614	193.906	2222.813	62.87	66.69	n.a.
3		3.843	70.042	568.040	22.71	17.04	n.a.
Total:			**308.406**	**3332.943**	**100.00**	**100.00**	

Fig. S70. RP-HPLC elution profile (system D-Fluo, fluorescence detection Ex./Em. 400/520 nm (top) and 450/700 nm (bottom)) of PTZ-coumarin hybrid dye 15 (concentration: 2.0 μM in PBS) after incubation with hypochlorite anion (1 equiv.) in PBS (pH 7.3)

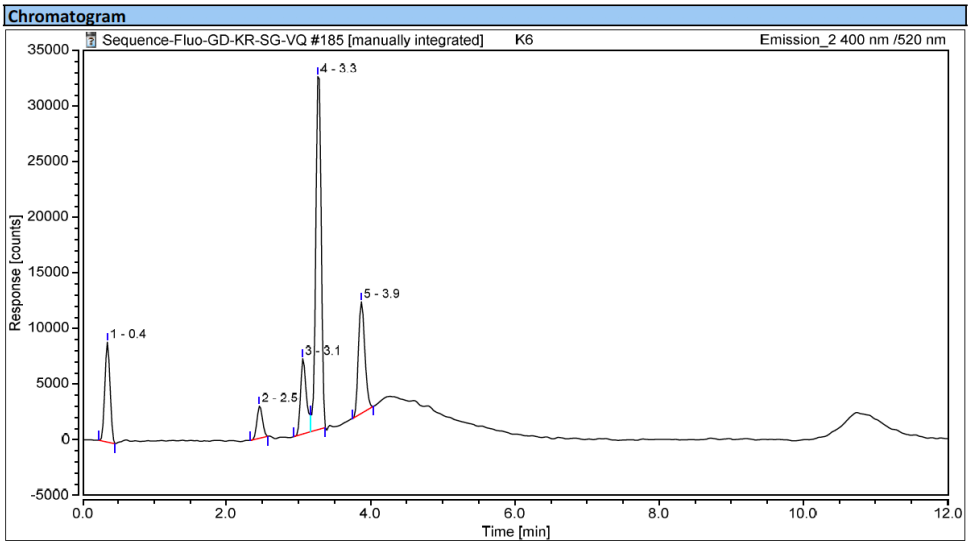

No.	Peak Name	Retention Time min	Area counts*min	Height counts	Relative Area %	Relative Height %	Amount n.a.
1		0.351	754.286	8992.959	13.74	14.88	n.a.
2		2.455	257.003	2895.000	4.68	4.79	n.a.
3		3.059	631.893	6775.892	11.51	11.21	n.a.
4		3.268	2801.269	31751.713	51.04	52.53	n.a.
5		3.872	1044.182	10033.143	19.02	16.60	n.a.
Total:			**5488.633**	**60448.707**	**100.00**	**100.00**	

Please note: peak at t_R = 3.3 min assigned to fluorescent sulfoxide derivative.

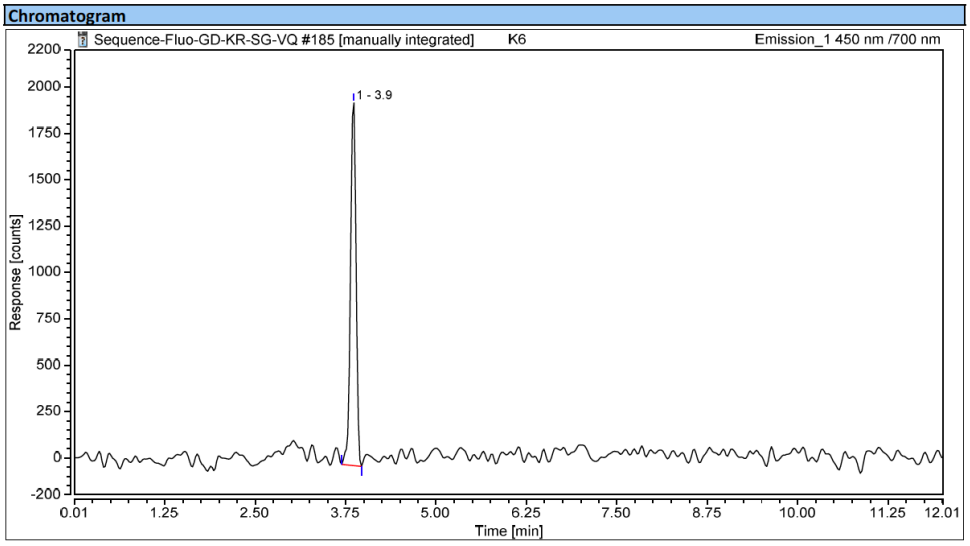

No.	Peak Name	Retention Time min	Area counts*min	Height counts	Relative Area %	Relative Height %	Amount n.a.
1		3.864	174.667	1957.154	100.00	100.00	n.a.
Total:			**174.667**	**1957.154**	**100.00**	**100.00**	

Fig. S71. RP-HPLC elution profile (system D-Fluo, fluorescence detection Ex./Em. 400/520 nm (top) and 450/700 nm (bottom)) of PTZ-coumarin hybrid dye 16 (concentration: 2.0 μM in PBS)

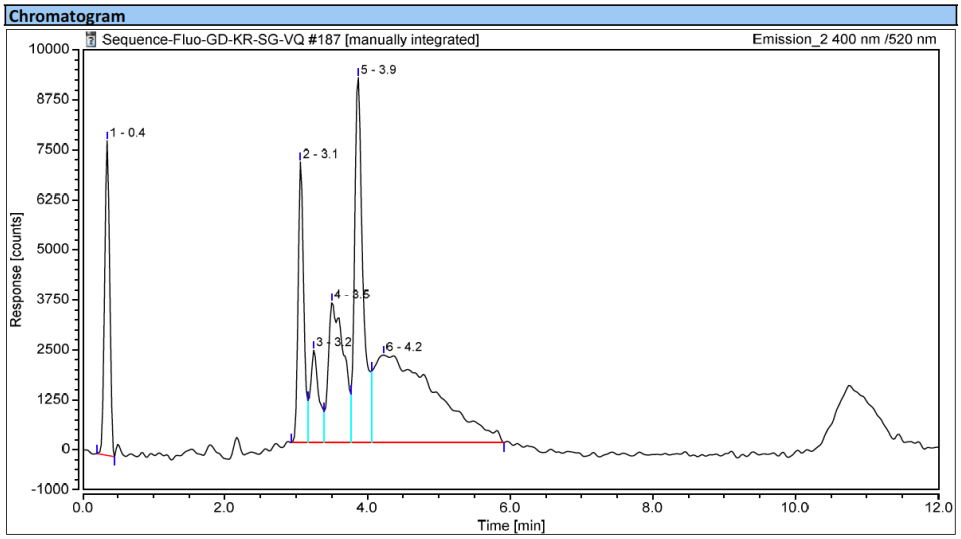

No.	Peak Name	Retention Time min	Area counts*min	Height counts	Relative Area %	Relative Height %	Amount n.a.
1		0.351	647.761	7870.099	10.82	24.57	n.a.
2		3.059	639.546	7023.874	10.68	21.93	n.a.
3		3.247	328.417	2314.685	5.49	7.23	n.a.
4		3.497	884.753	3503.434	14.78	10.94	n.a.
5		3.872	1262.335	9130.056	21.09	28.50	n.a.
6		4.226	2223.374	2192.699	37.14	6.84	n.a.
Total:			**5986.186**	**32034.847**	**100.00**	**100.00**	

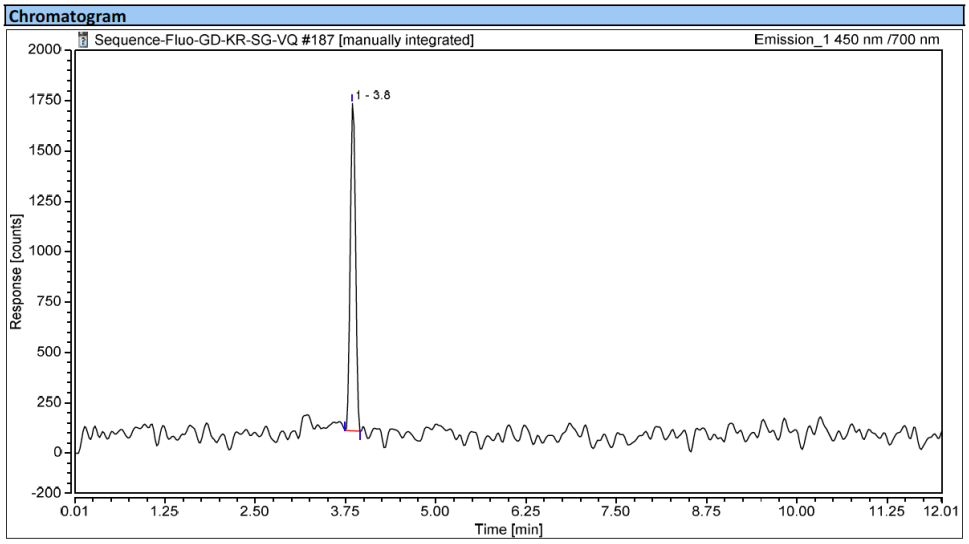

No.	Peak Name	Retention Time min	Area counts*min	Height counts	Relative Area %	Relative Height %	Amount n.a.
1		3.843	136.458	1625.000	100.00	100.00	n.a.
Total:			**136.458**	**1625.000**	**100.00**	**100.00**	

*Please note: several hypotheses may explain the presence of several peaks in pure sample of **16**, counter-ion effect for sulfobetain pendant arm (chloride, formate and phosphate), fluorescent impurities (present in minute amounts) not detectable by NMR and RP-HPLC coupled to UV-vis detection.*

Fig. S72. RP-HPLC elution profile (system D-Fluo, fluorescence detection Ex./Em. 400/520 nm (top) and 450/700 nm (bottom)) of PTZ-coumarin hybrid dye 16 (concentration: 2.0 μM in PBS) after incubation in PBS (pH 7.3)

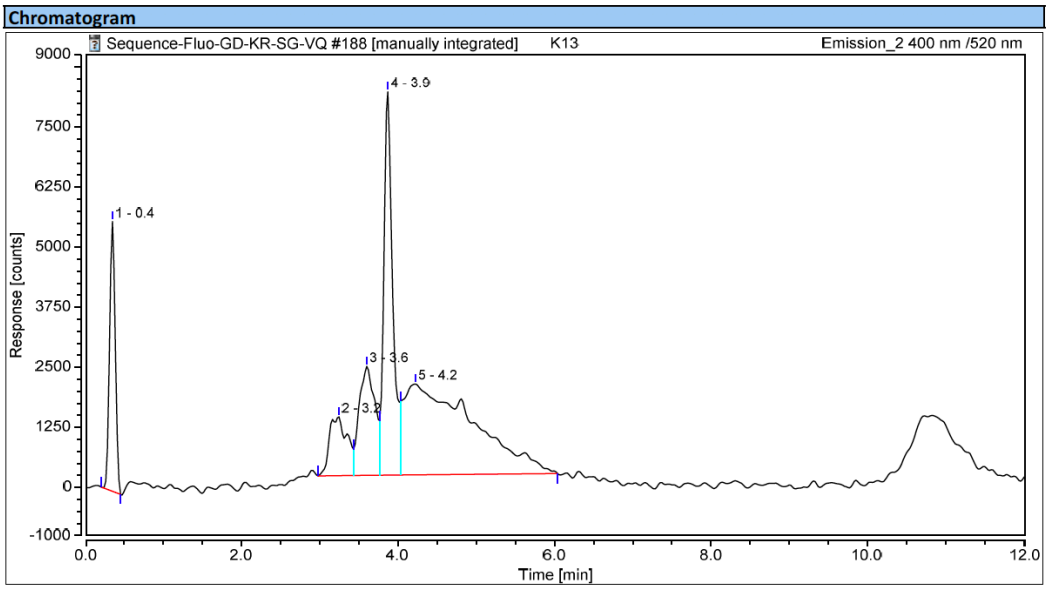

No.	Peak Name	Retention Time min	Area counts*min	Height counts	Relative Area %	Relative Height %	Amount n.a.
1		0.351	475.238	5607.874	10.97	29.57	n.a.
2		3.247	323.668	1222.578	7.47	6.45	n.a.
3		3.601	530.976	2268.796	12.25	11.96	n.a.
4		3.872	1050.705	7976.374	24.25	42.05	n.a.
5		4.226	1952.520	1891.592	45.06	9.97	n.a.
Total:			**4333.106**	**18967.215**	**100.00**	**100.00**	

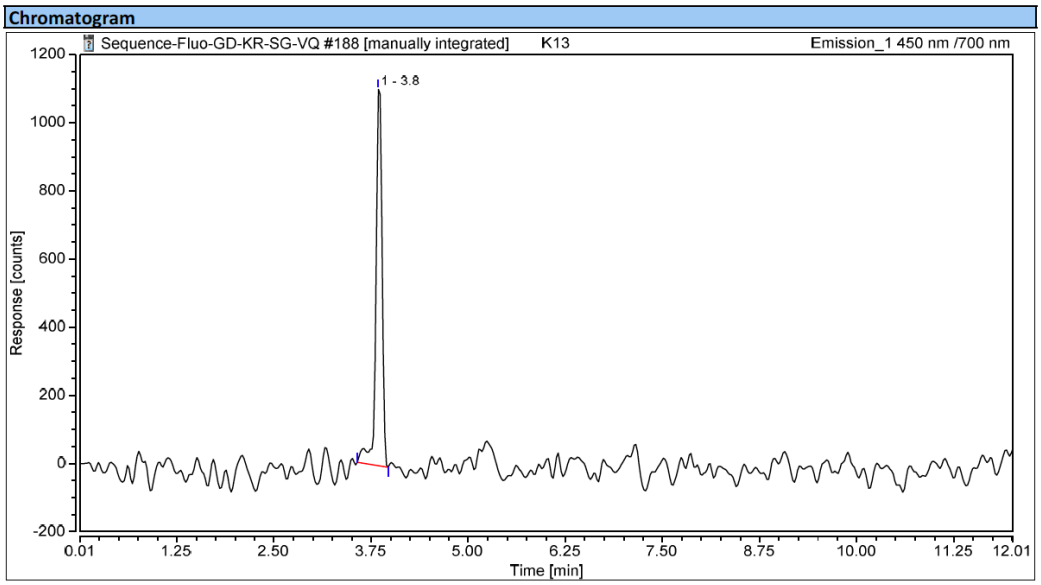

No.	Peak Name	Retention Time min	Area counts*min	Height counts	Relative Area %	Relative Height %	Amount n.a.
1		3.843	101.021	1104.263	100.00	100.00	n.a.
Total:			**101.021**	**1104.263**	**100.00**	**100.00**	

Fig. S73. RP-HPLC elution profile (system D-Fluo, fluorescence detection Ex./Em. 400/520 nm (top) and 450/700 nm (bottom)) of PTZ-coumarin hybrid dye 16 (concentration: 2.0 μM in PBS) after incubation with hypochlorite anion (1 equiv.) in PBS (pH 7.3)

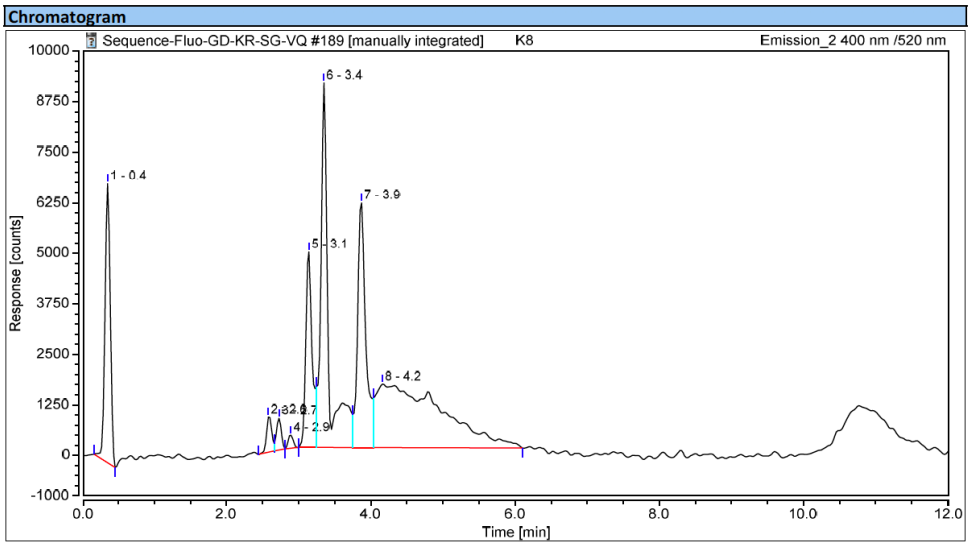

No.	Peak Name	Retention Time min	Area counts*min	Height counts	Relative Area %	Relative Height %	Amount n.a.
1		0.351	587.911	6903.786	12.11	22.75	n.a.
2		2.580	73.955	869.944	1.52	2.87	n.a.
3		2.726	61.361	782.889	1.26	2.58	n.a.
4		2.893	26.070	323.556	0.54	1.07	n.a.
5		3.143	499.053	4834.799	10.28	15.93	n.a.
6		3.351	1117.949	9012.940	23.03	29.70	n.a.
7		3.872	806.231	6051.792	16.61	19.94	n.a.
8		4.164	1680.966	1570.390	34.63	5.17	n.a.
Total:			**4853.497**	**30350.095**	**100.00**	**100.00**	

Please note: peak at t_R = 3.4 min assigned to fluorescent sulfoxide derivative.

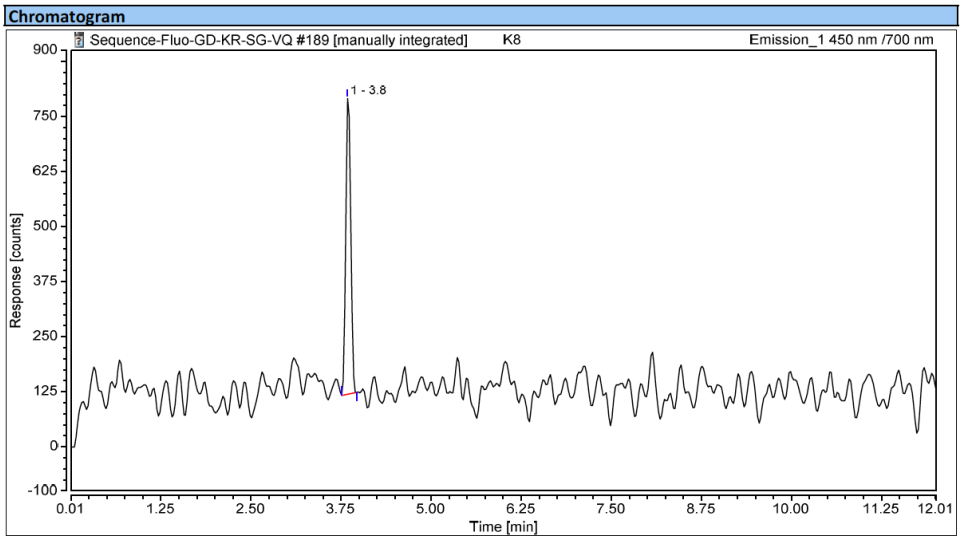

No.	Peak Name	Retention Time min	Area counts*min	Height counts	Relative Area %	Relative Height %	Amount n.a.
1		3.843	54.385	671.200	100.00	100.00	n.a.
Total:			**54.385**	**671.200**	**100.00**	**100.00**	

Fig. S74. RP-HPLC elution profile (system D-Fluo, fluorescence detection Ex./Em. 400/520 nm (top) and 450/700 nm (bottom)) of PBS (blank)

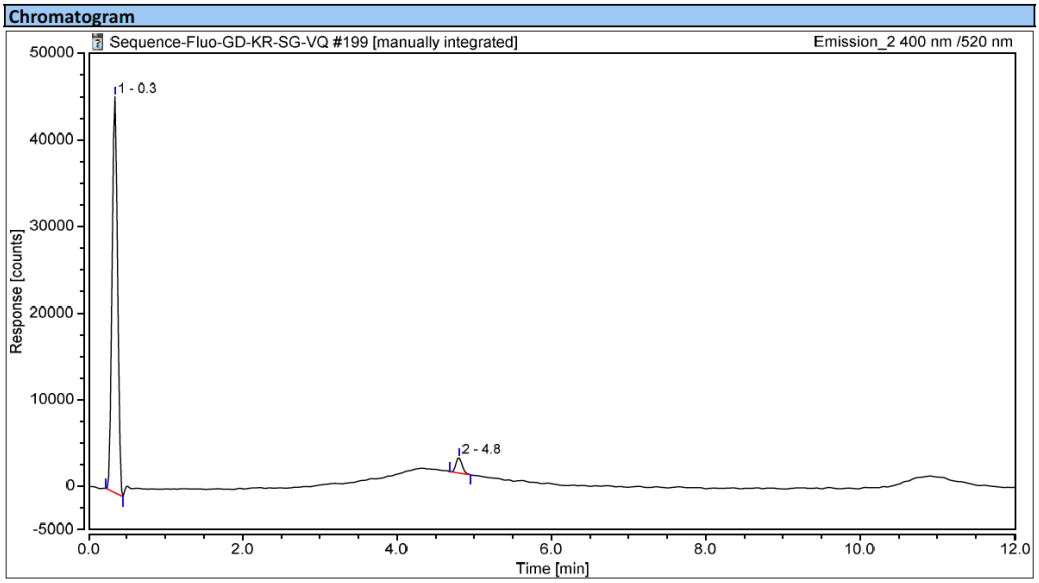

No.	Peak Name	Retention Time min	Area counts*min	Height counts	Relative Area %	Relative Height %	Amount n.a.
1		0.349	3771.336	45726.974	95.81	96.36	n.a.
2		4.808	165.072	1728.231	4.19	3.64	n.a.
Total:			**3936.408**	**47455.205**	**100.00**	**100.00**	

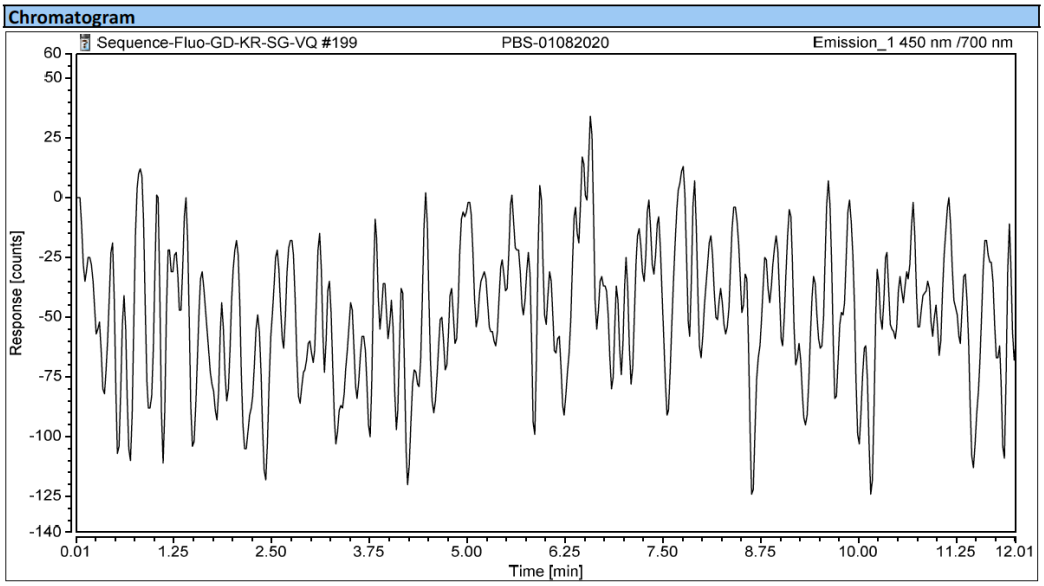

No.	Peak Name	Retention Time min	Area counts*min	Height counts	Relative Area %	Relative Height %	Amount n.a.
Total:			**0.000**	**0.000**	**0.00**	**0.00**	

Fig. S75. RP-HPLC elution profile (system D-Fluo, fluorescence detection Ex./Em. 400/520 nm (top) and 450/700 nm (bottom)) of MeCN (column blank)

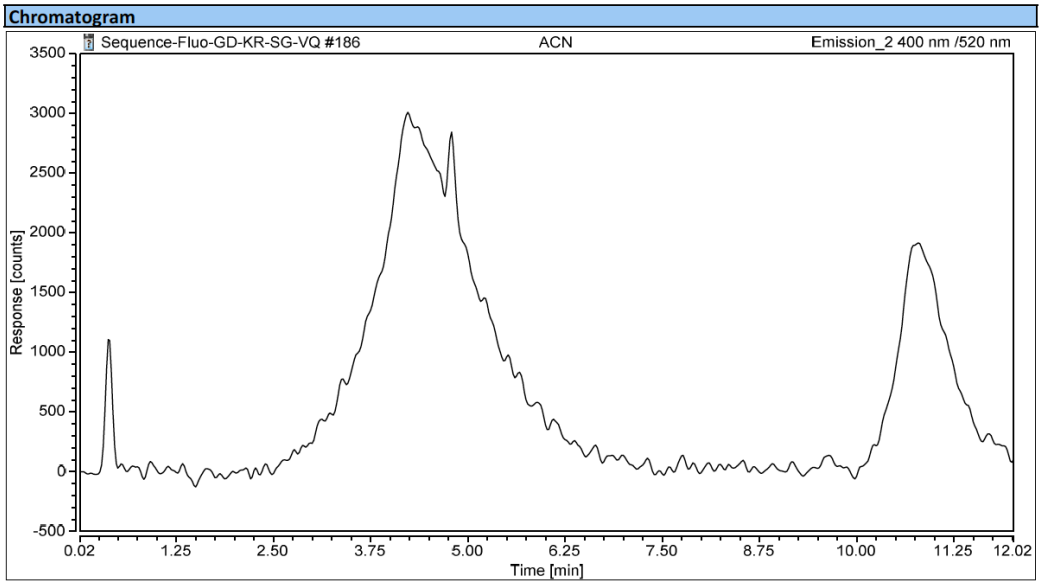

No.	Peak Name	Retention Time min	Area counts*min	Height counts	Relative Area %	Relative Height %	Amount n.a.
Total:			**0.000**	**0.000**	**0.00**	**0.00**	

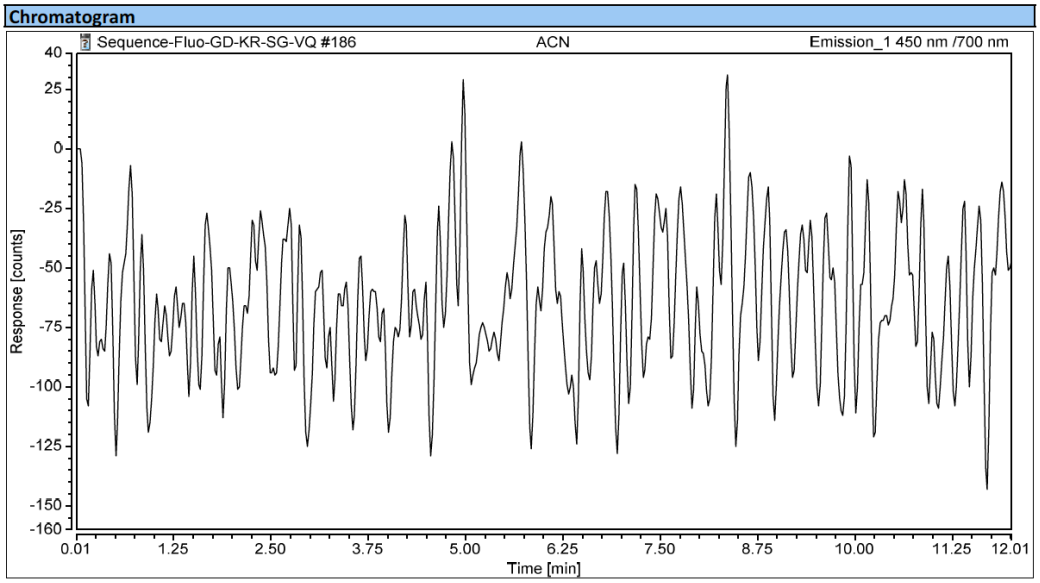

No.	Peak Name	Retention Time min	Area counts*min	Height counts	Relative Area %	Relative Height %	Amount n.a.
Total:			**0.000**	**0.000**	**0.00**	**0.00**	

Fig. S76. RP-HPLC elution profile (system E-MS) of blank (injection of PBS alone). UV detection at 250 nm; UV detection at 300 nm; Visible detection at 425 nm; ESI+ mass detection (SIM1 mode at *m/z* 349.4 ± 0.5); ESI+ mass detection (SIM2 mode at *m/z* 365.4 ± 0.5) (top-down)

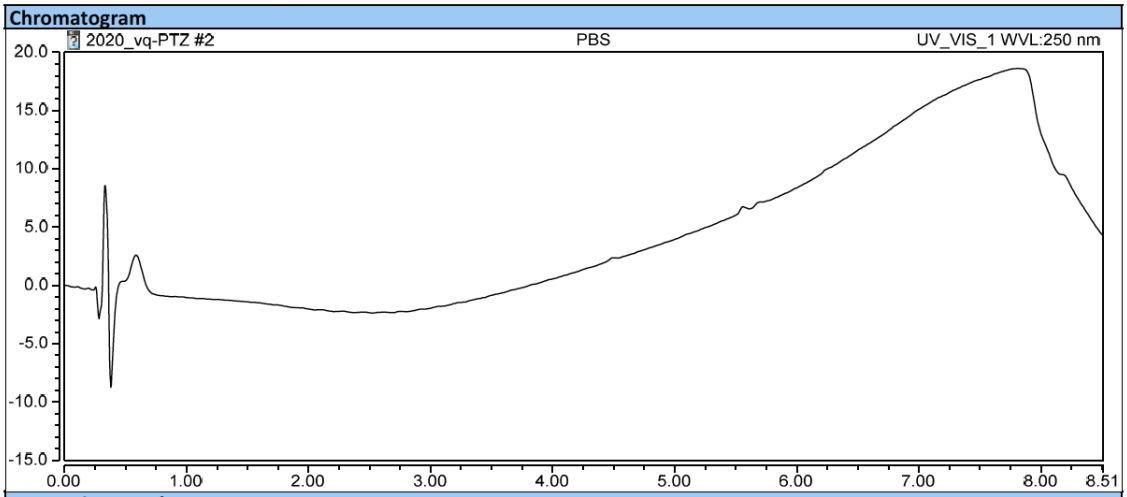

Integration Results

No.	Peak Name	Retention Time min	Area mAU*min	Height mAU	Relative Area %	Relative Height %	Amount n.a.
Total:			**0.000**	**0.000**	**0.00**	**0.00**	

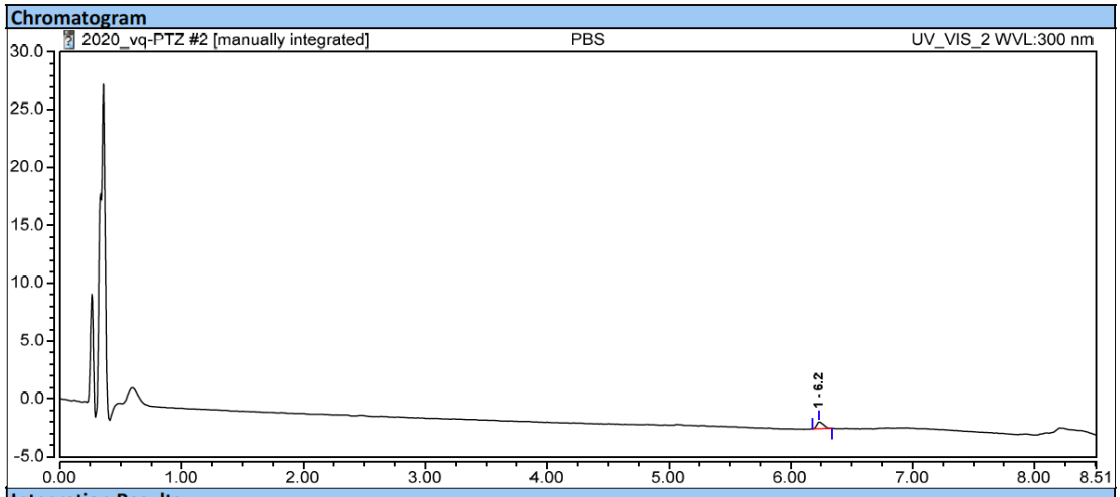

Integration Results

No.	Peak Name	Retention Time min	Area mAU*min	Height mAU	Relative Area %	Relative Height %	Amount n.a.
1		6.233	0.036	0.594	100.00	100.00	n.a.
Total:			**0.036**	**0.594**	**100.00**	**100.00**	

Chromatogram

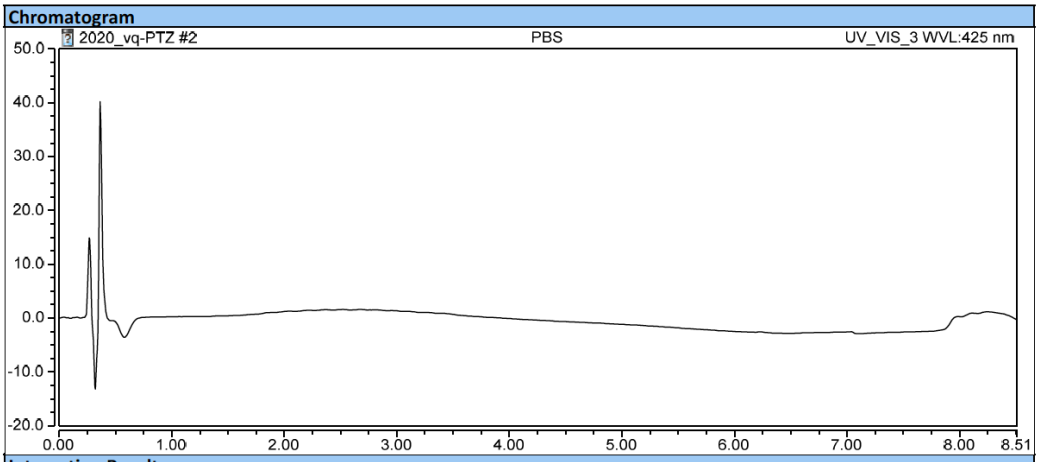

Integration Results

No.	Peak Name	Retention Time min	Area mAU*min	Height mAU	Relative Area %	Relative Height %	Amount n.a.
Total:			**0.000**	**0.000**	**0.00**	**0.00**	

Chromatogram

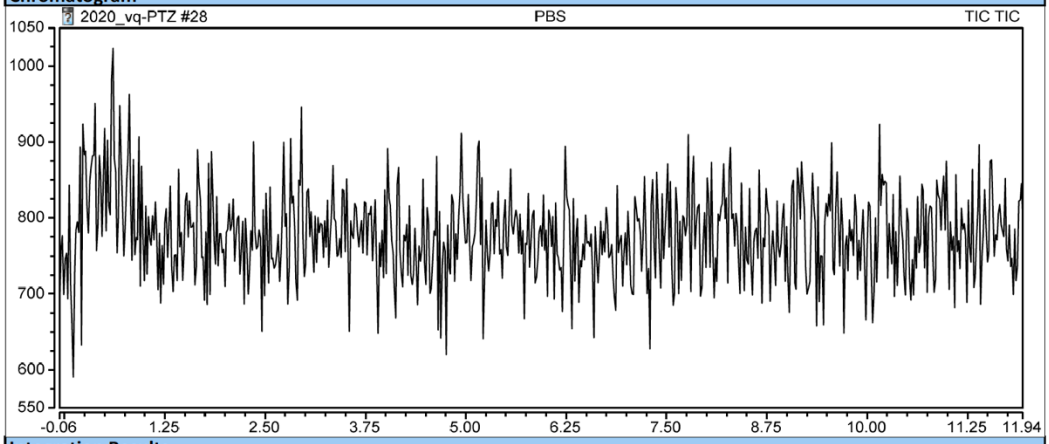

Integration Results

No.	Peak Name	Retention Time min	Area counts*min	Height counts	Relative Area %	Relative Height %	Amount n.a.
Total:			**0.000**	**0.000**	**0.00**	**0.00**	

Chromatogram

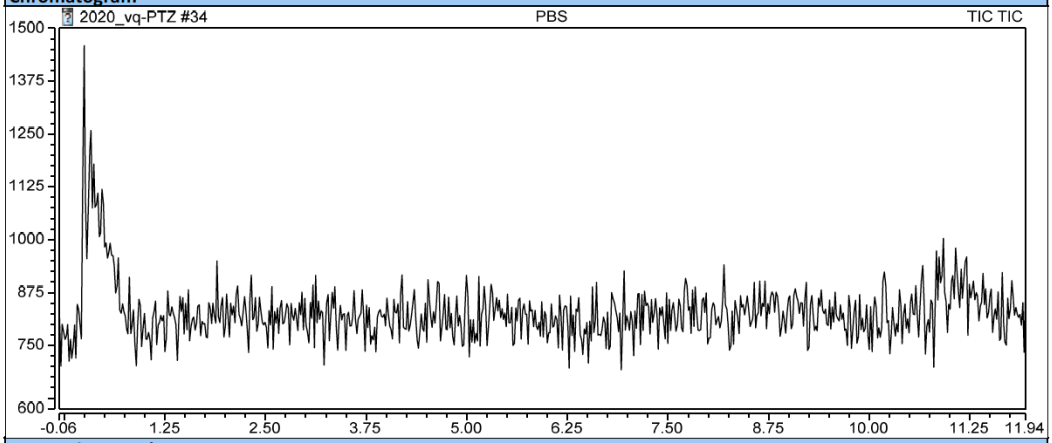

Integration Results

No.	Peak Name	Retention Time min	Area counts*min	Height counts	Relative Area %	Relative Height %	Amount n.a.
Total:			**0.000**	**0.000**	**0.00**	**0.00**	

Fig. S77. RP-HPLC elution profile (system E-MS) of PTZ-coumarin hybrid dye 10. ESI+ mass detection (SIM1 mode at *m/z* 349.4 ± 0.5); ESI+ mass detection (SIM2 mode at *m/z* 365.4 ± 0.5); ESI+ mass detection (SIM3 mode at *m/z* 381.4 ± 0.5) (top-down)

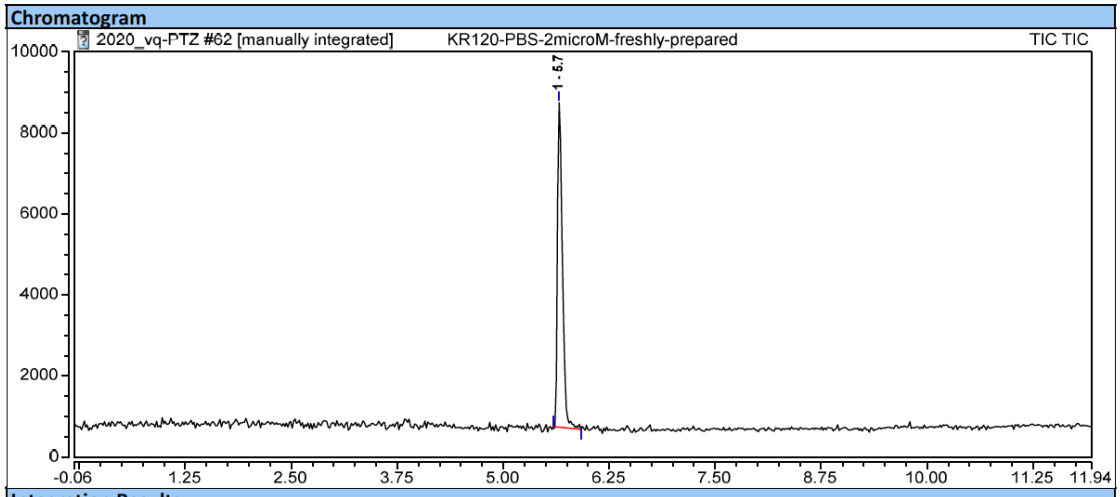

Integration Results

No.	Peak Name	Retention Time min	Area counts*min	Height counts	Relative Area %	Relative Height %	Amount n.a.
1		5.659	550.064	8017.458	100.00	100.00	n.a.
Total:			**550.064**	**8017.458**	**100.00**	**100.00**	

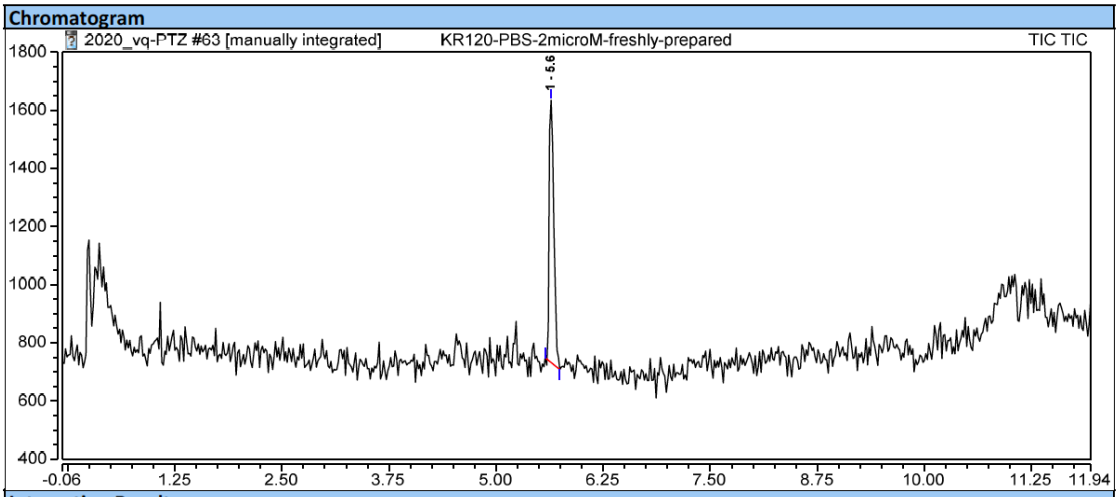

Integration Results

No.	Peak Name	Retention Time min	Area counts*min	Height counts	Relative Area %	Relative Height %	Amount n.a.
1		5.642	56.903	902.099	100.00	100.00	n.a.
Total:			**56.903**	**902.099**	**100.00**	**100.00**	

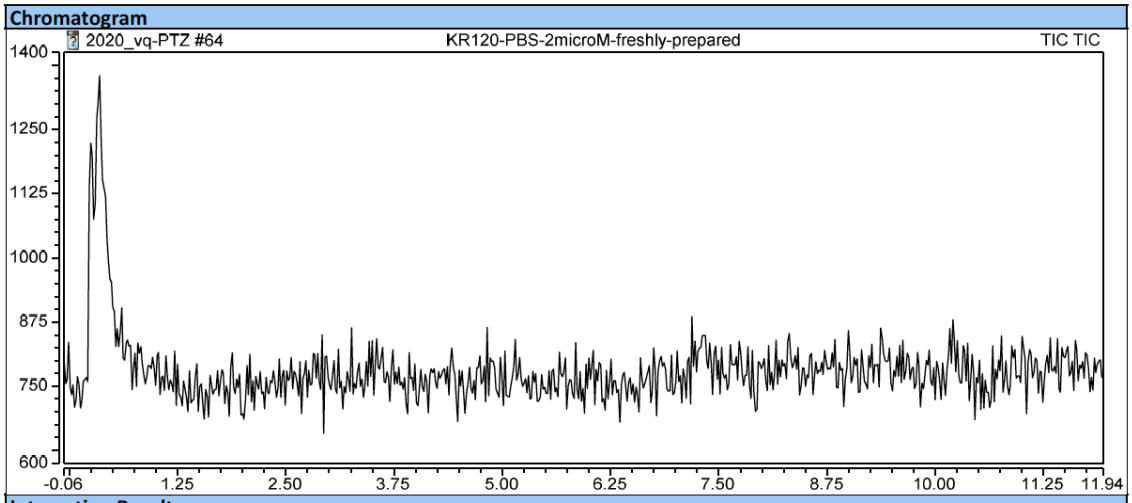

Integration Results

No.	Peak Name	Retention Time min	Area counts*min	Height counts	Relative Area %	Relative Height %	Amount n.a.
Total:			**0.000**	**0.000**	**0.00**	**0.00**	

Fig. S78. RP-HPLC elution profile (system E-MS) of PTZ-coumarin hybrid dye 10 after incubation in PBS. UV detection at 250 nm; UV detection at 300 nm; Visible detection at 425 nm; ESI+ mass detection (SIM1 mode at *m/z* 349.4 ± 0.5); ESI+ mass detection (SIM2 mode at *m/z* 365.4 ± 0.5) (top-down)

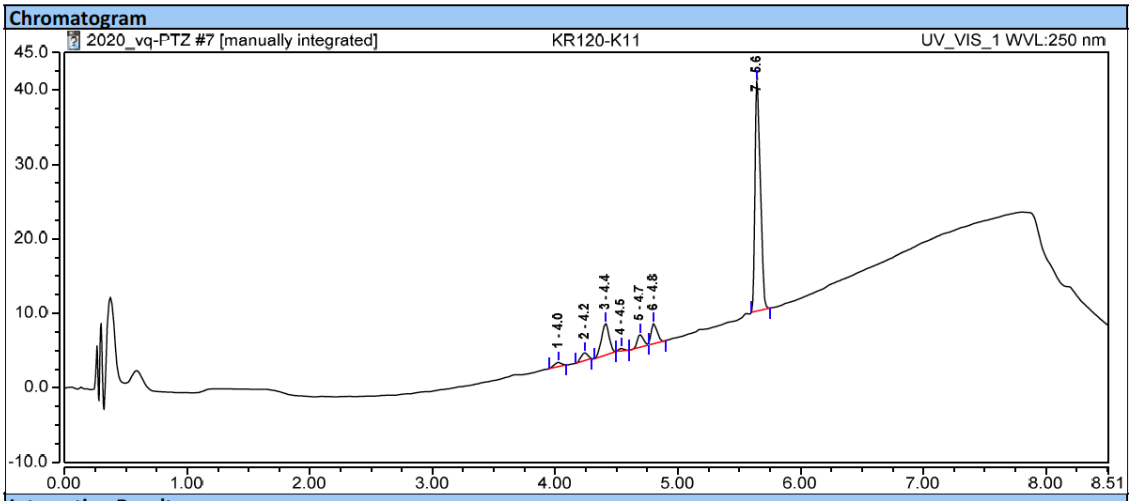

Integration Results

No.	Peak Name	Retention Time min	Area mAU*min	Height mAU	Relative Area %	Relative Height %	Amount n.a.
1		4.027	0.041	0.569	1.82	1.37	n.a.
2		4.240	0.064	1.019	2.87	2.46	n.a.
3		4.410	0.307	4.227	13.70	10.20	n.a.
4		4.537	0.016	0.332	0.70	0.80	n.a.
5		4.690	0.100	1.715	4.48	4.14	n.a.
6		4.800	0.153	2.727	6.85	6.58	n.a.
7		5.643	1.557	30.854	69.58	74.45	n.a.
Total:			**2.238**	**41.443**	**100.00**	**100.00**	

Chromatogram

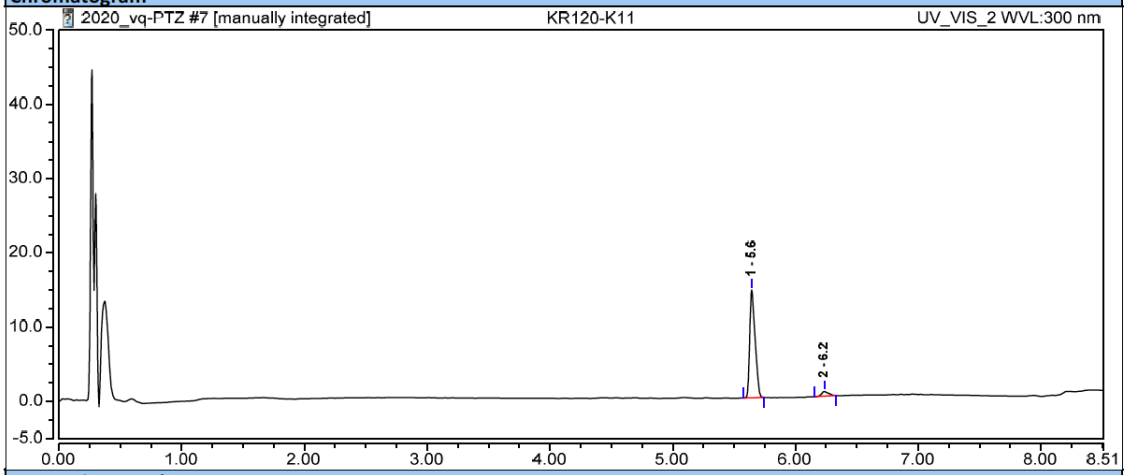

Integration Results

No.	Peak Name	Retention Time min	Area mAU*min	Height mAU	Relative Area %	Relative Height %	Amount n.a.
1		5.643	0.735	14.529	94.92	96.03	n.a.
2		6.237	0.039	0.600	5.08	3.97	n.a.
Total:			**0.774**	**15.130**	**100.00**	**100.00**	

Chromatogram

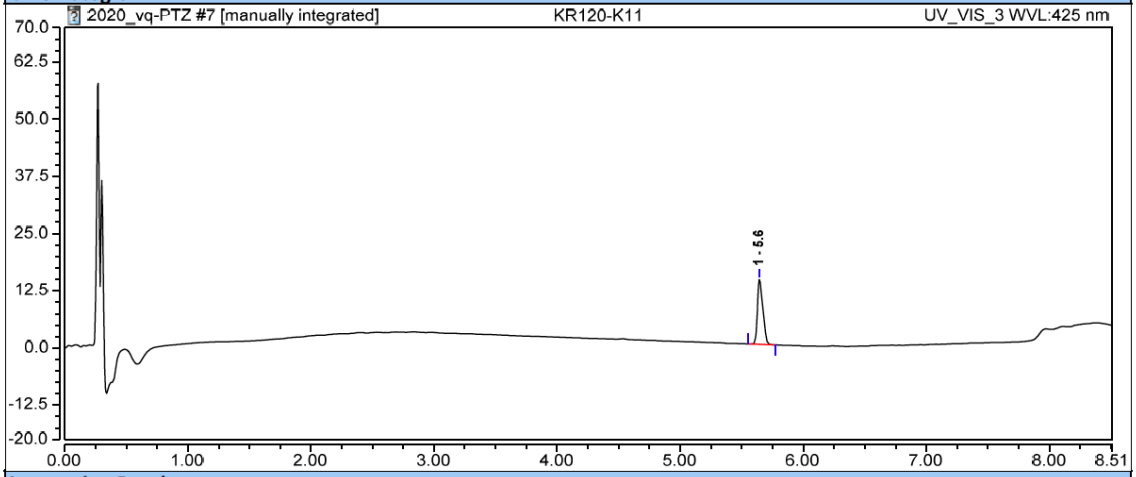

Integration Results

No.	Peak Name	Retention Time min	Area mAU*min	Height mAU	Relative Area %	Relative Height %	Amount n.a.
1		5.643	0.719	14.159	100.00	100.00	n.a.
Total:			**0.719**	**14.159**	**100.00**	**100.00**	

Chromatogram

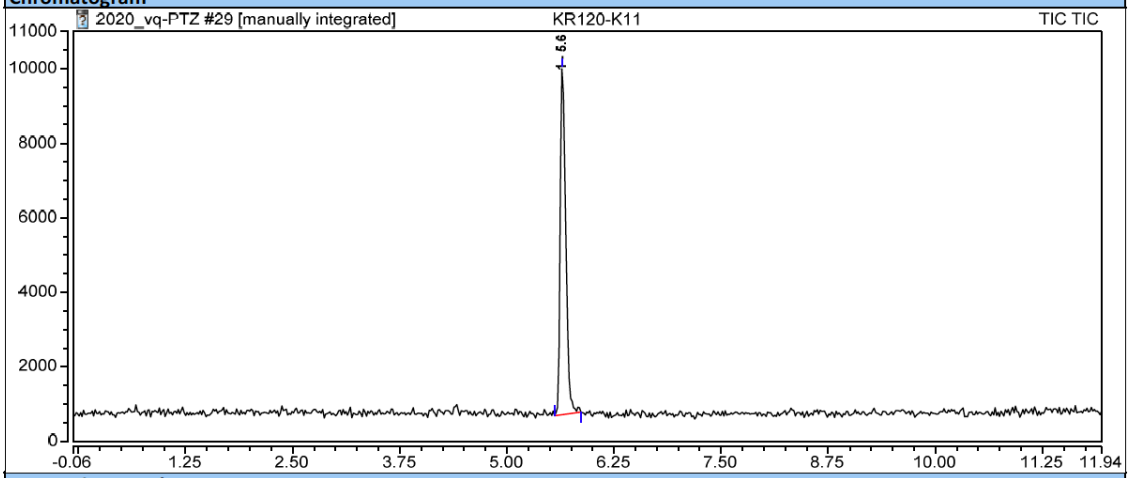

Integration Results

No.	Peak Name	Retention Time min	Area counts*min	Height counts	Relative Area %	Relative Height %	Amount n.a.
1		5.642	711.374	9283.821	100.00	100.00	n.a.
Total:			**711.374**	**9283.821**	**100.00**	**100.00**	

Chromatogram

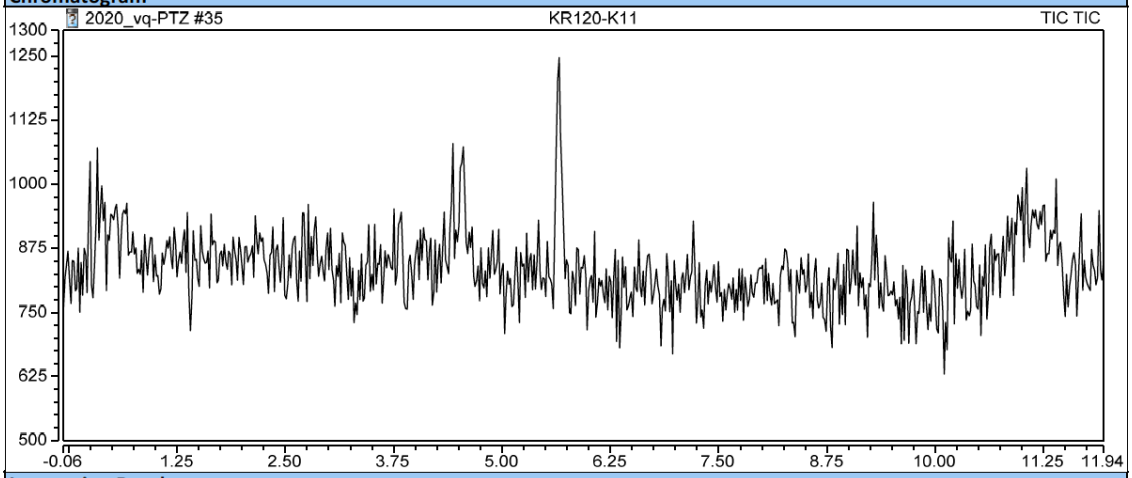

Integration Results

No.	Peak Name	Retention Time min	Area counts*min	Height counts	Relative Area %	Relative Height %	Amount n.a.
Total:			**0.000**	**0.000**	**0.00**	**0.00**	

Fig. S79. RP-HPLC elution profile (system E-MS) of PTZ-coumarin hybrid dye 10 after incubation with hypochlorite anion (1 equiv.) in PBS (pH 7.3). UV detection at 250 nm; UV detection at 300 nm; Visible detection at 425 nm; ESI+ mass detection (SIM1 mode at *m/z* 349.4 ± 0.5); ESI+ mass detection (SIM2 mode at *m/z* 365.4 ± 0.5) (top-down)

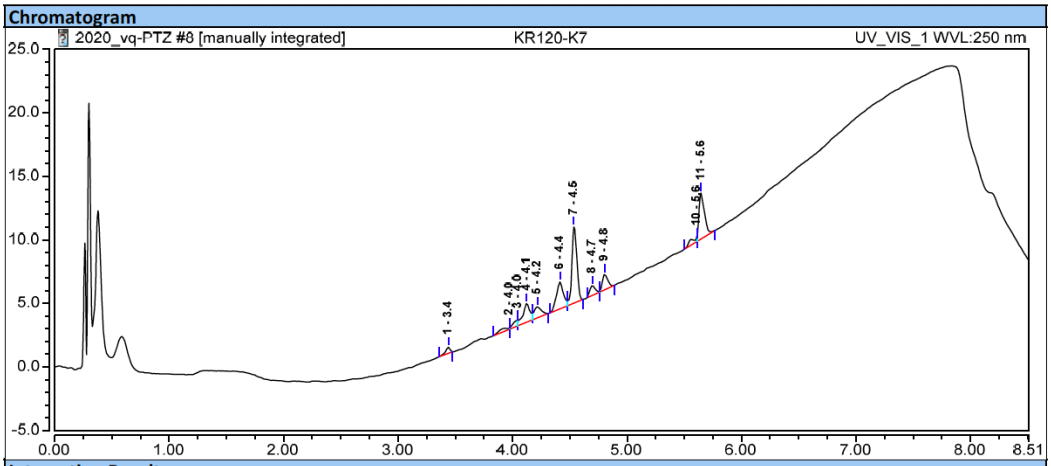

Integration Results

No.	Peak Name	Retention Time min	Area mAU*min	Height mAU	Relative Area %	Relative Height %	Amount n.a.
1		3.440	0.022	0.486	2.16	2.79	n.a.
2		3.973	0.021	0.096	2.09	0.55	n.a.
3		4.043	0.022	0.427	2.21	2.45	n.a.
4		4.123	0.105	1.494	10.26	8.58	n.a.
5		4.217	0.066	0.878	6.52	5.05	n.a.
6		4.413	0.147	2.121	14.48	12.19	n.a.
7		4.537	0.300	5.999	29.50	34.47	n.a.
8		4.697	0.042	0.762	4.12	4.38	n.a.
9		4.803	0.066	1.233	6.46	7.09	n.a.
10		5.610	0.026	0.292	2.56	1.68	n.a.
11		5.647	0.200	3.613	19.62	20.76	n.a.
Total:			**1.018**	**17.402**	**100.00**	**100.00**	

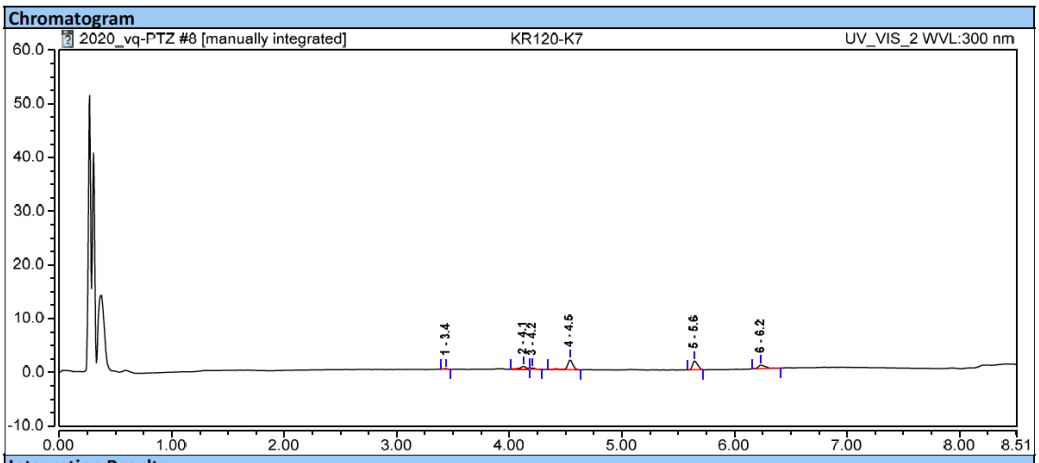

Integration Results

No.	Peak Name	Retention Time min	Area mAU*min	Height mAU	Relative Area %	Relative Height %	Amount n.a.
1		3.437	0.005	0.130	1.94	2.60	n.a.
2		4.123	0.032	0.489	11.32	9.75	n.a.
3		4.203	0.009	0.209	3.25	4.17	n.a.
4		4.537	0.101	1.847	35.79	36.81	n.a.
5		5.643	0.084	1.679	29.84	33.45	n.a.
6		6.233	0.050	0.663	17.86	13.22	n.a.
Total:			**0.281**	**5.018**	**100.00**	**100.00**	

Chromatogram

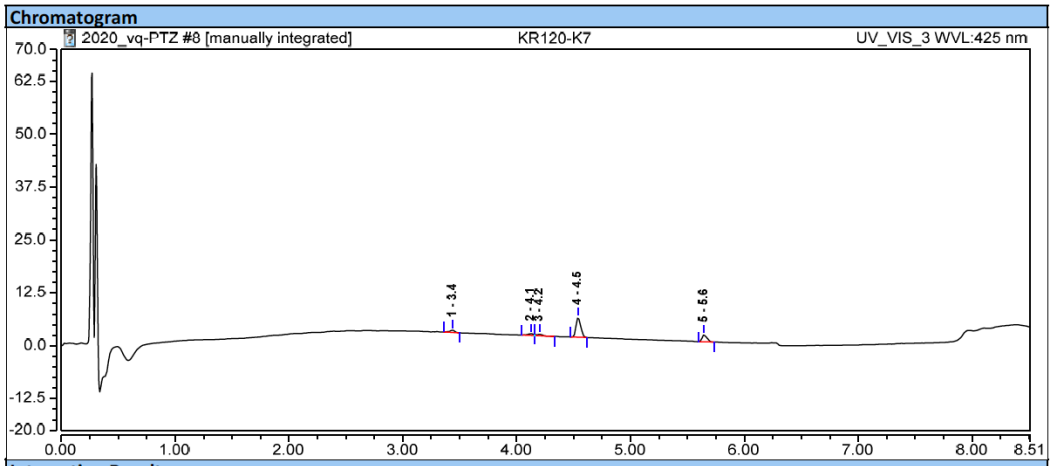

Integration Results

No.	Peak Name	Retention Time min	Area mAU*min	Height mAU	Relative Area %	Relative Height %	Amount n.a.
1		3.437	0.028	0.554	7.39	7.30	n.a.
2		4.123	0.023	0.398	6.15	5.24	n.a.
3		4.200	0.021	0.364	5.64	4.79	n.a.
4		4.537	0.221	4.645	59.03	61.18	n.a.
5		5.643	0.082	1.632	21.78	21.49	n.a.
Total:			**0.375**	**7.592**	**100.00**	**100.00**	

Chromatogram

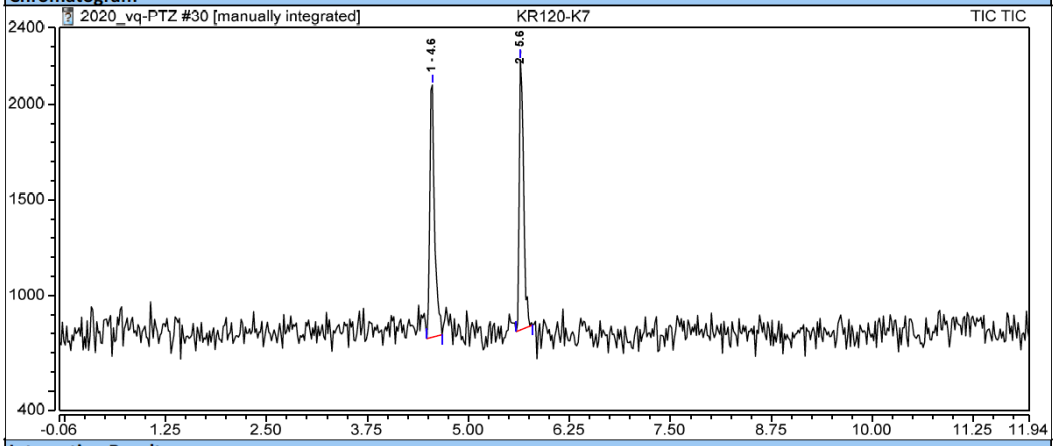

Integration Results

No.	Peak Name	Retention Time min	Area counts*min	Height counts	Relative Area %	Relative Height %	Amount n.a.
1		4.553	91.338	1318.987	51.08	48.26	n.a.
2		5.642	87.472	1414.138	48.92	51.74	n.a.
Total:			**178.810**	**2733.125**	**100.00**	**100.00**	

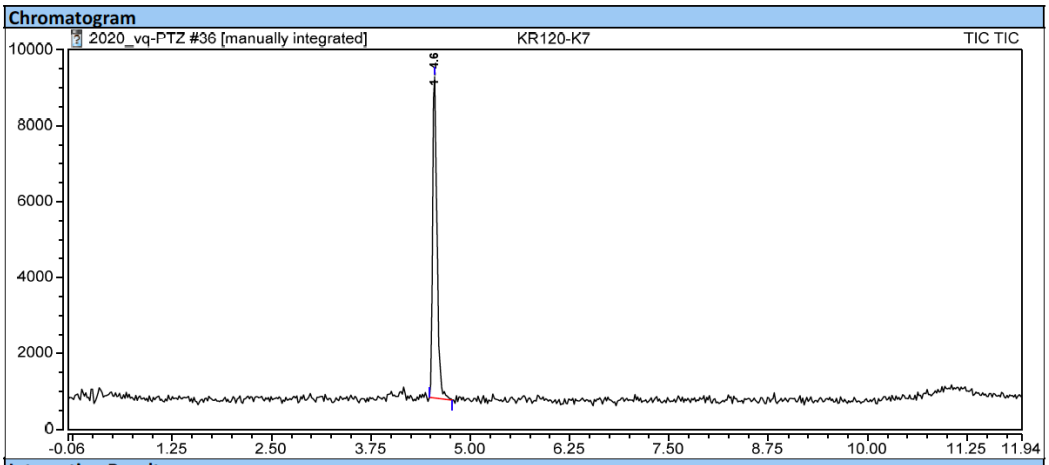

Integration Results

No.	Peak Name	Retention Time min	Area counts*min	Height counts	Relative Area %	Relative Height %	Amount n.a.
1		4.553	545.817	8465.731	100.00	100.00	n.a.
Total:			**545.817**	**8465.731**	**100.00**	**100.00**	

Please note: this SIM2 mode (m/z 365.4 ± 0.5) unambiguously confirms the identity of the newly formed peak at t_R= 4.6 min, assigned to sulfoxide derivative.

Fig. S80. RP-HPLC elution profile (system E-MS) of PTZ-coumarin hybrid dye 10 after incubation with hypochlorite anion (10 equiv.) in PBS (pH 7.3). UV detection at 250 nm; UV detection at 300 nm; Visible detection at 425 nm; ESI+ mass detection (SIM1 mode at *m/z* 349.4 ± 0.5); ESI+ mass detection (SIM2 mode at *m/z* 365.4 ± 0.5) (top-down)

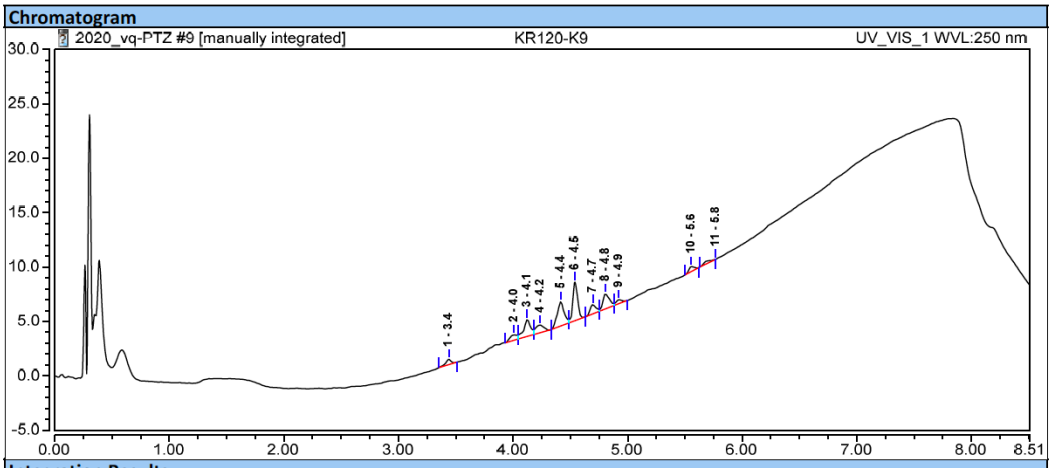

Integration Results

No.	Peak Name	Retention Time min	Area mAU*min	Height mAU	Relative Area %	Relative Height %	Amount n.a.
1		3.440	0.026	0.492	3.43	4.07	n.a.
2		4.010	0.036	0.481	4.76	3.98	n.a.
3		4.123	0.110	1.555	14.42	12.86	n.a.
4		4.237	0.060	0.703	7.90	5.81	n.a.
5		4.417	0.155	2.257	20.30	18.66	n.a.
6		4.540	0.172	3.557	22.53	29.41	n.a.
7		4.697	0.051	0.848	6.66	7.01	n.a.
8		4.807	0.091	1.379	11.87	11.40	n.a.
9		4.923	0.022	0.363	2.83	3.00	n.a.
10		5.557	0.024	0.460	3.17	3.80	n.a.
11		5.770	0.016	0.000	2.11	0.00	n.a.
Total:			**0.763**	**12.095**	**100.00**	**100.00**	

Chromatogram

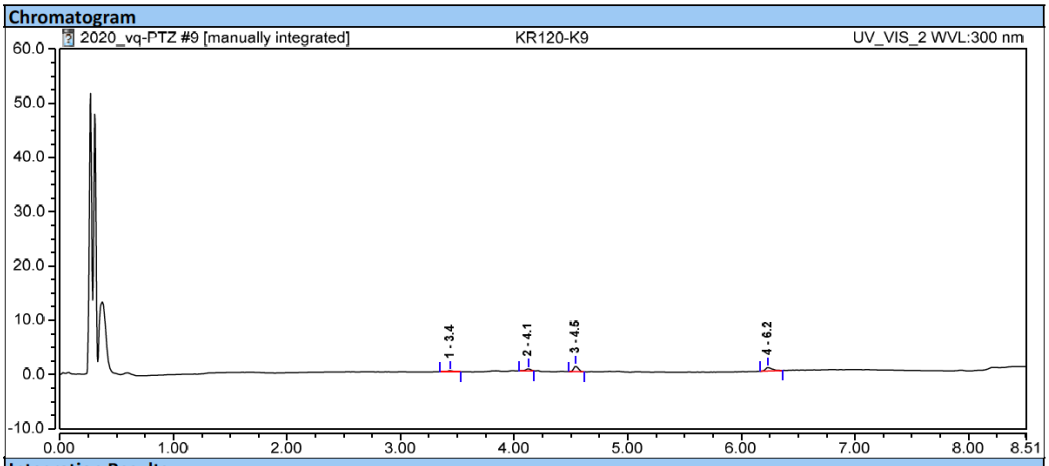

Integration Results

No.	Peak Name	Retention Time min	Area mAU*min	Height mAU	Relative Area %	Relative Height %	Amount n.a.
1		3.437	0.012	0.191	9.63	8.53	n.a.
2		4.123	0.019	0.384	16.01	17.18	n.a.
3		4.540	0.048	1.036	39.75	46.35	n.a.
4		6.233	0.042	0.624	34.61	27.93	n.a.
Total:			**0.121**	**2.235**	**100.00**	**100.00**	

Chromatogram

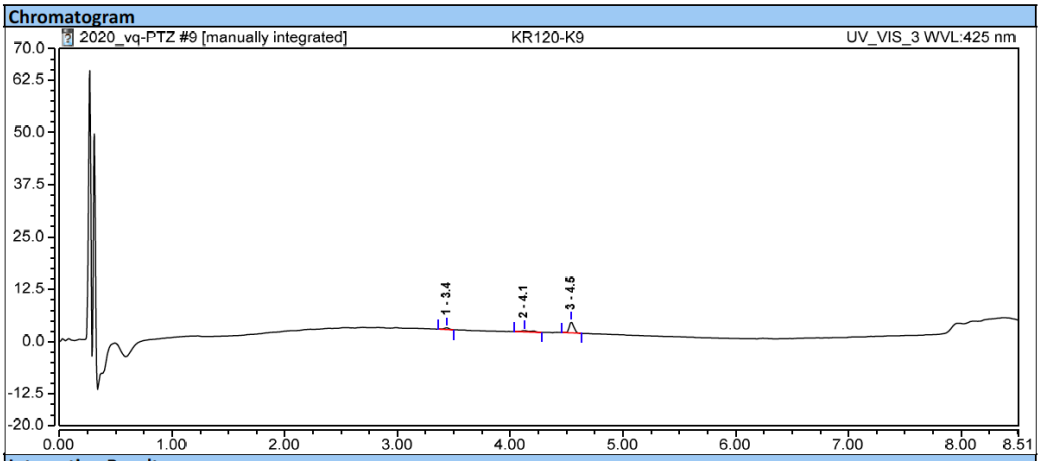

Integration Results

No.	Peak Name	Retention Time min	Area mAU*min	Height mAU	Relative Area %	Relative Height %	Amount n.a.
1		3.437	0.021	0.438	11.96	12.82	n.a.
2		4.123	0.034	0.332	19.37	9.73	n.a.
3		4.540	0.122	2.645	68.67	77.46	n.a.
Total:			**0.177**	**3.415**	**100.00**	**100.00**	

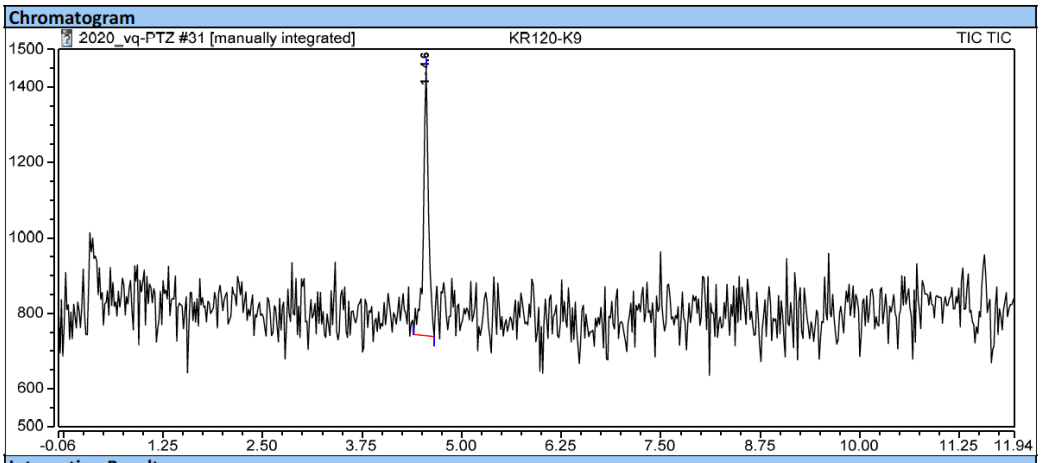

Integration Results

No.	Peak Name	Retention Time min	Area counts*min	Height counts	Relative Area %	Relative Height %	Amount n.a.
1		4.553	53.169	709.115	100.00	100.00	n.a.
Total:			**53.169**	**709.115**	**100.00**	**100.00**	

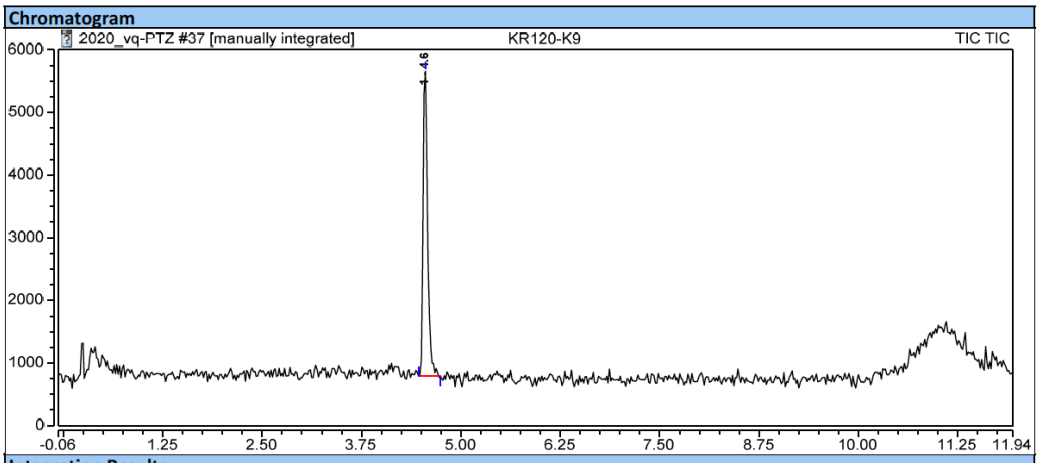

Integration Results

No.	Peak Name	Retention Time min	Area counts*min	Height counts	Relative Area %	Relative Height %	Amount n.a.
1		4.553	324.145	4868.246	100.00	100.00	n.a.
Total:			**324.145**	**4868.246**	**100.00**	**100.00**	

Please note: compared to the oxidation reaction conducted with 1 equiv. of NaOCl, the lower intensity of peak at t_R = 4.6 min confirms the partial conversion/degradation of sulfoxide derivative.

Fig. S81. RP-HPLC elution profile (system E-MS) of PTZ-coumarin hybrid dye 10 after incubation with hypochlorite anion (100 equiv.) in PBS (pH 7.3). UV detection at 250 nm; UV detection at 300 nm; Visible detection at 425 nm; ESI+ mass detection (SIM1 mode at *m/z* 349.4 ± 0.5); ESI+ mass detection (SIM2 mode at *m/z* 365.4 ± 0.5) (top-down)

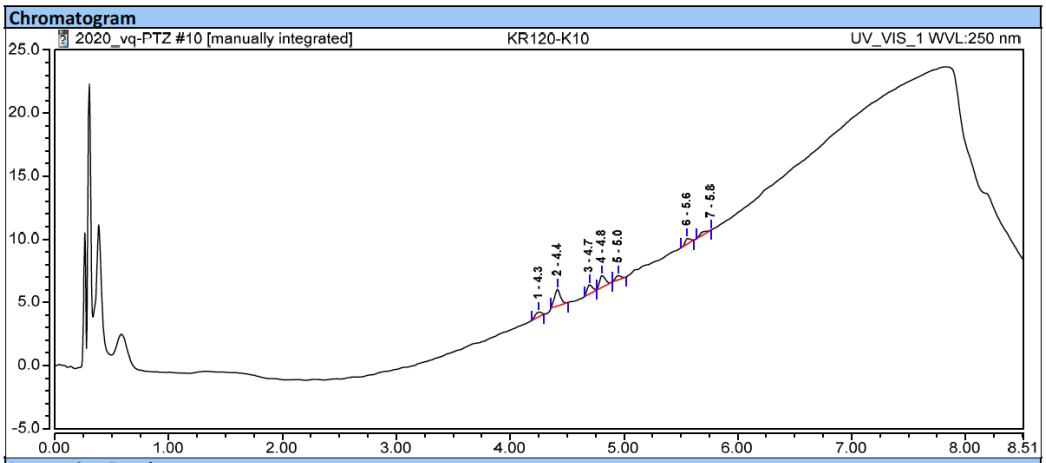

Integration Results

No.	Peak Name	Retention Time min	Area mAU*min	Height mAU	Relative Area %	Relative Height %	Amount n.a.
1		4.253	0.024	0.376	9.61	9.05	n.a.
2		4.417	0.079	1.334	31.39	32.09	n.a.
3		4.697	0.040	0.741	15.88	17.81	n.a.
4		4.807	0.053	0.943	21.20	22.67	n.a.
5		4.950	0.018	0.318	7.03	7.64	n.a.
6		5.557	0.022	0.446	8.80	10.73	n.a.
7		5.767	0.015	0.000	6.09	0.00	n.a.
Total:			**0.251**	**4.157**	**100.00**	**100.00**	

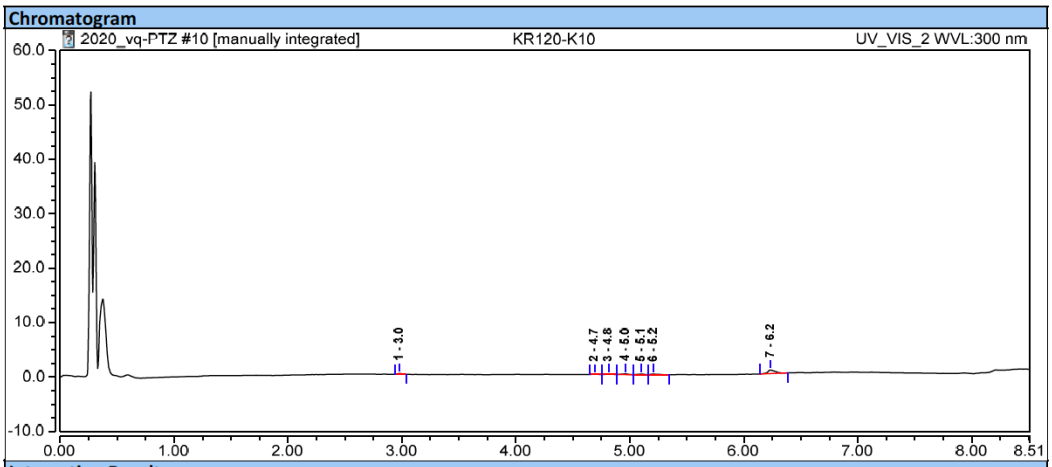

Integration Results

No.	Peak Name	Retention Time min	Area mAU*min	Height mAU	Relative Area %	Relative Height %	Amount n.a.
1		2.977	0.006	0.129	7.00	9.93	n.a.
2		4.690	0.003	0.047	3.52	3.66	n.a.
3		4.813	0.006	0.083	6.79	6.40	n.a.
4		4.960	0.010	0.133	10.33	10.27	n.a.
5		5.100	0.009	0.135	9.74	10.39	n.a.
6		5.207	0.010	0.122	10.63	9.39	n.a.
7		6.237	0.048	0.648	51.99	49.96	n.a.
Total:			**0.092**	**1.298**	**100.00**	**100.00**	

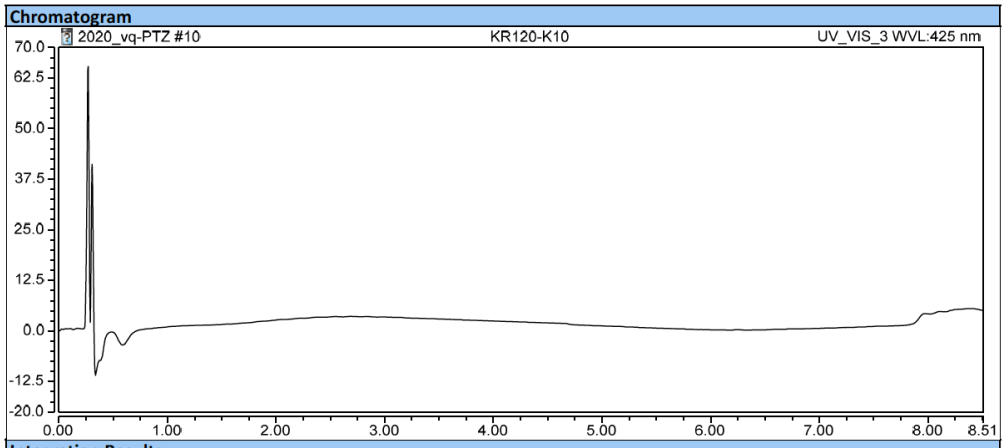

Integration Results

No.	Peak Name	Retention Time min	Area mAU*min	Height mAU	Relative Area %	Relative Height %	Amount n.a.
Total:			**0.000**	**0.000**	**0.00**	**0.00**	

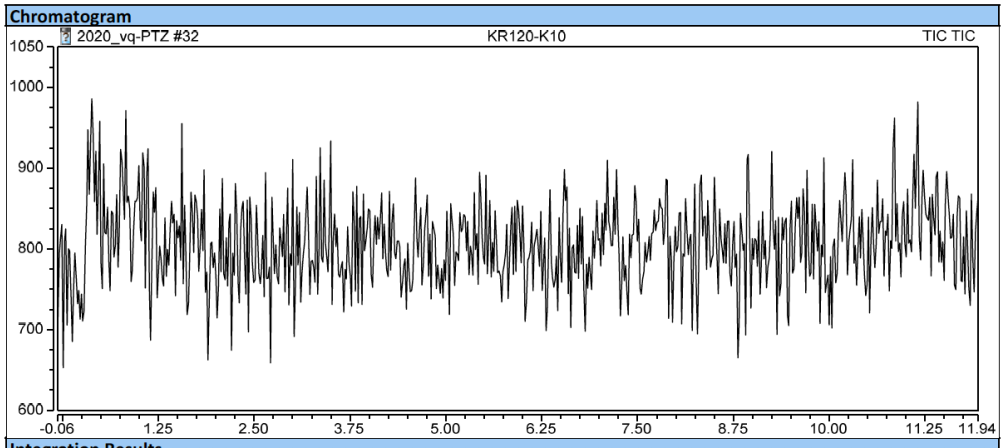

Integration Results

No.	Peak Name	Retention Time min	Area counts*min	Height counts	Relative Area %	Relative Height %	Amount n.a.
Total:			**0.000**	**0.000**	**0.00**	**0.00**	

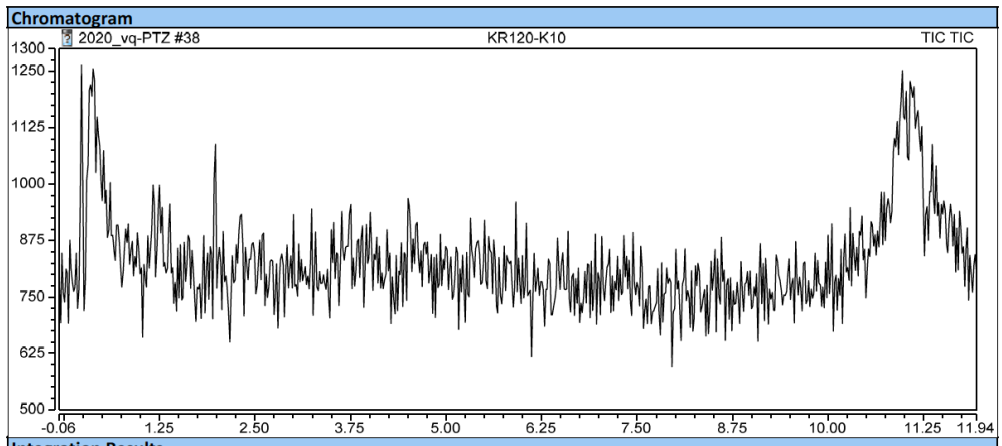

Integration Results

No.	Peak Name	Retention Time min	Area counts*min	Height counts	Relative Area %	Relative Height %	Amount n.a.
Total:			**0.000**	**0.000**	**0.00**	**0.00**	

Please note: the lack of peak at t_R = 4.6 min upon Ex. at 400 nm suggests that sulfoxide derivative may undergone over-oxidation (formation of sulfone derivative?) and subsequent degradation of PTZ heterocycle.

Fig. S82. RP-HPLC elution profile (system E-MS) of blank (injection of PBS alone). ESI+ mass detection (SIM1 mode at *m/z* 392.5 ± 0.5); ESI+ mass detection (SIM2 mode at *m/z* 408.5 ± 0.5) (top-down)

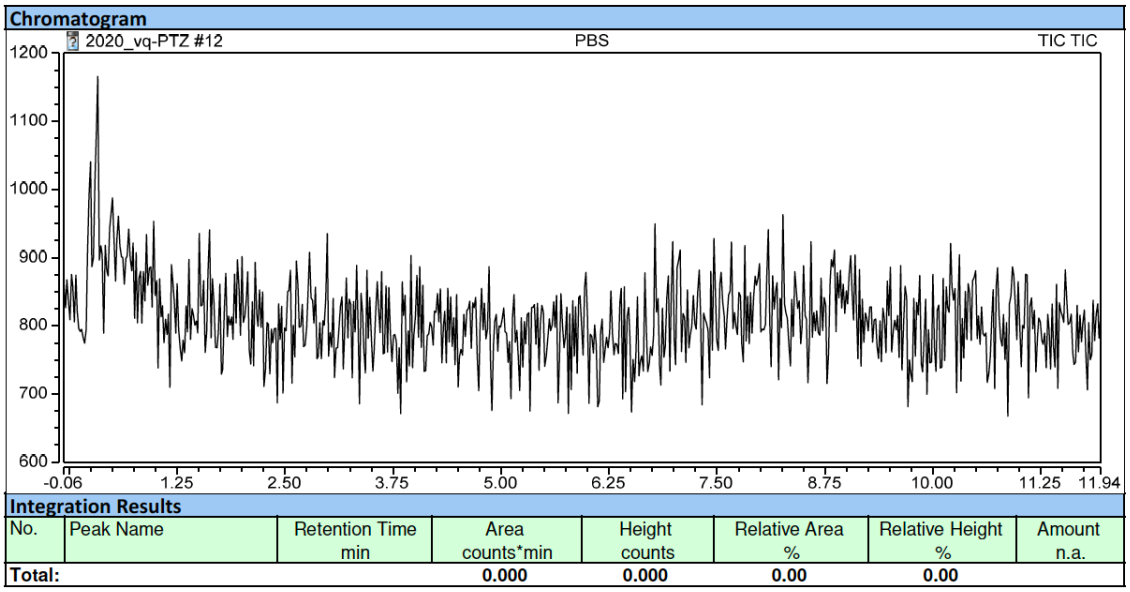

Integration Results

No.	Peak Name	Retention Time min	Area counts*min	Height counts	Relative Area %	Relative Height %	Amount n.a.
Total:			**0.000**	**0.000**	**0.00**	**0.00**	

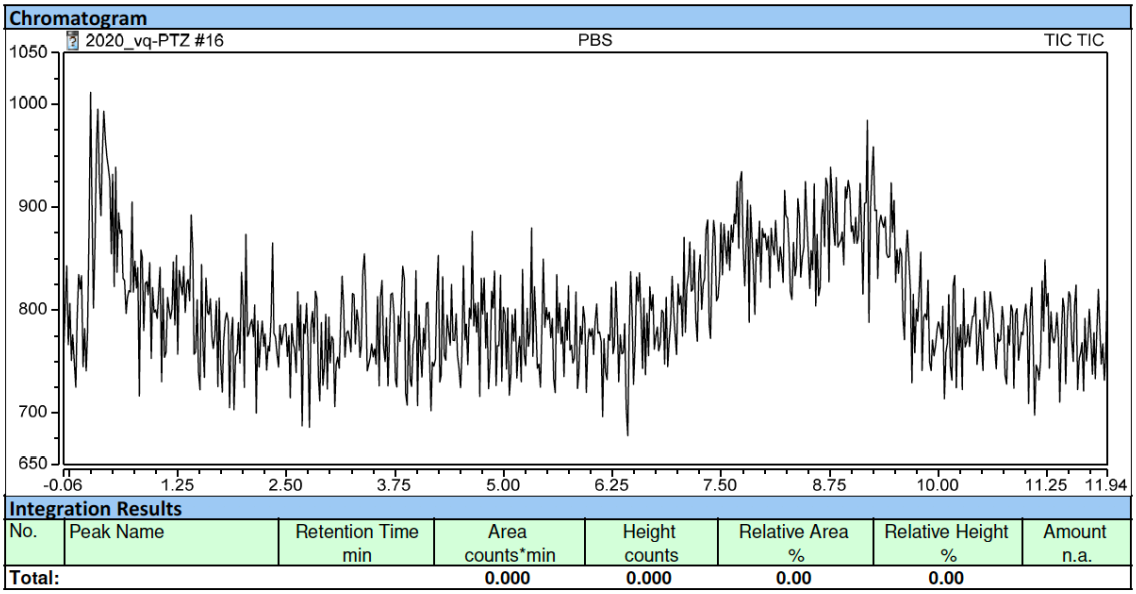

Integration Results

No.	Peak Name	Retention Time min	Area counts*min	Height counts	Relative Area %	Relative Height %	Amount n.a.
Total:			**0.000**	**0.000**	**0.00**	**0.00**	

Fig. S83. RP-HPLC elution profile (system E-MS) of PTZ-coumarin hybrid dye 15. ESI+ mass detection (SIM1 mode at *m/z* 392.5 ± 0.5)

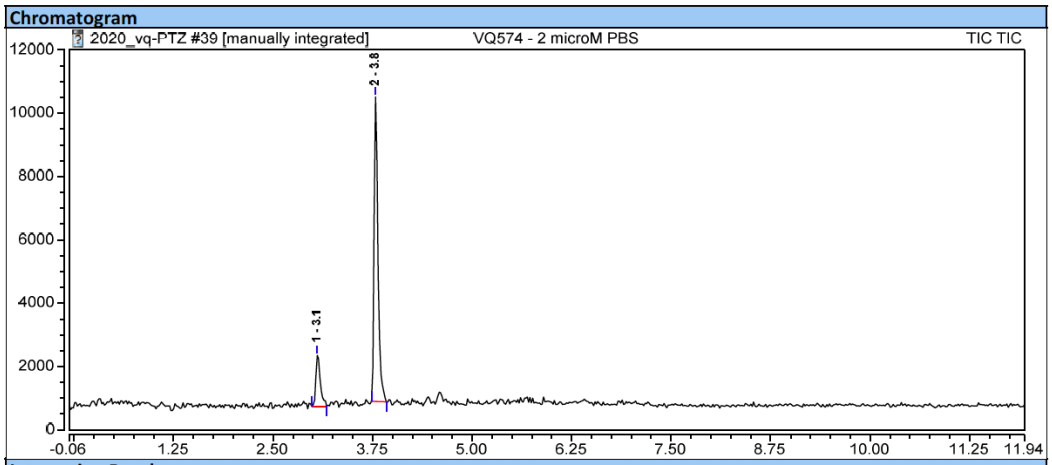

Integration Results

No.	Peak Name	Retention Time min	Area counts*min	Height counts	Relative Area %	Relative Height %	Amount n.a.
1		3.055	107.701	1613.035	16.57	14.36	n.a.
2		3.787	542.450	9619.197	83.43	85.64	n.a.
Total:			**650.151**	**11232.233**	**100.00**	**100.00**	

Fig. S84. RP-HPLC elution profile (system E-MS) of PTZ-coumarin hybrid dye 15 after incubation in PBS. UV detection at 250 nm; UV detection at 300 nm; Visible detection at 425 nm; ESI+ mass detection (SIM1 mode at *m/z* 392.5 ± 0.5); ESI+ mass detection (SIM2 mode at *m/z* 408.5 ± 0.5) (top-down)

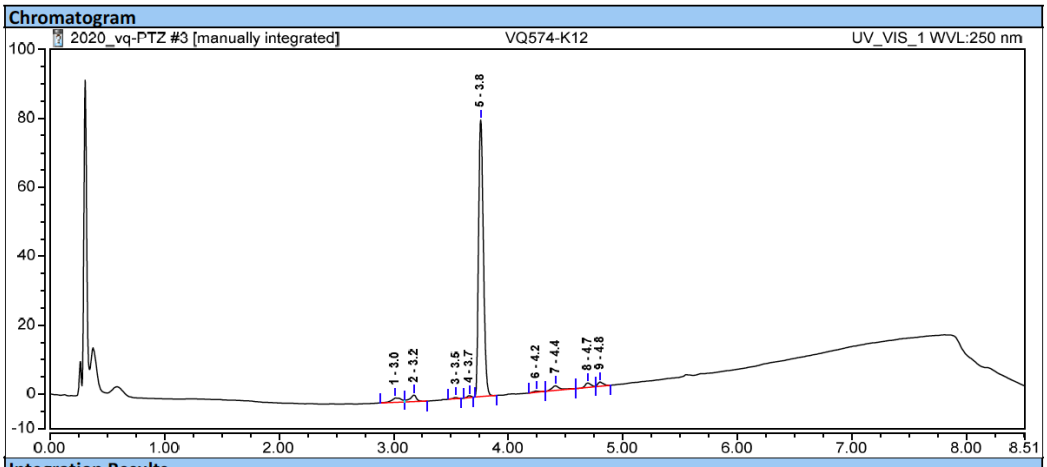

Integration Results

No.	Peak Name	Retention Time min	Area mAU*min	Height mAU	Relative Area %	Relative Height %	Amount n.a.
1		3.013	0.123	1.264	2.76	1.43	n.a.
2		3.177	0.128	1.974	2.87	2.23	n.a.
3		3.543	0.017	0.401	0.38	0.45	n.a.
4		3.660	0.020	0.547	0.45	0.62	n.a.
5		3.760	3.910	80.246	87.47	90.53	n.a.
6		4.243	0.022	0.344	0.49	0.39	n.a.
7		4.413	0.110	1.327	2.45	1.50	n.a.
8		4.693	0.072	1.285	1.60	1.45	n.a.
9		4.800	0.068	1.253	1.52	1.41	n.a.
Total:			**4.470**	**88.642**	**100.00**	**100.00**	

Chromatogram

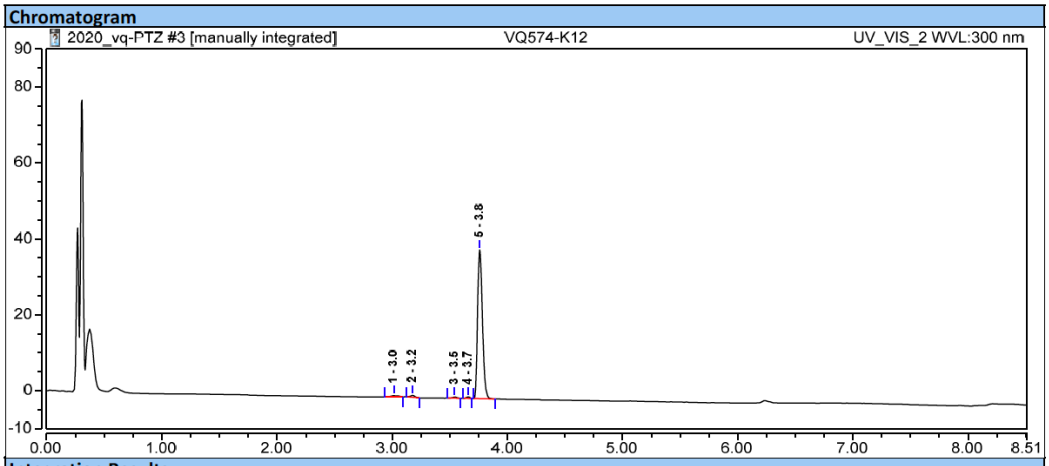

Integration Results

No.	Peak Name	Retention Time min	Area mAU*min	Height mAU	Relative Area %	Relative Height %	Amount n.a.
1		3.013	0.028	0.352	1.39	0.86	n.a.
2		3.177	0.023	0.522	1.15	1.28	n.a.
3		3.540	0.013	0.300	0.66	0.74	n.a.
4		3.660	0.013	0.393	0.65	0.96	n.a.
5		3.760	1.917	39.218	96.16	96.16	n.a.
Total:			**1.993**	**40.786**	**100.00**	**100.00**	

Chromatogram

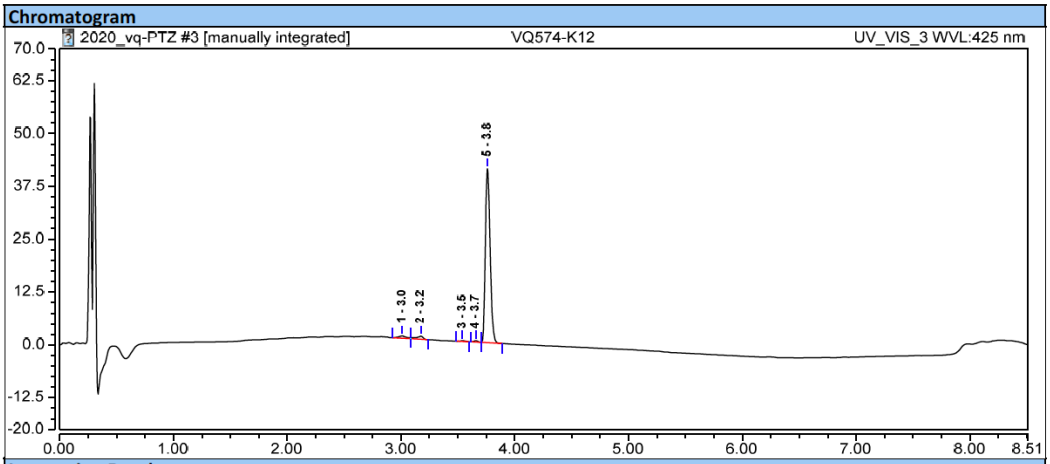

Integration Results

No.	Peak Name	Retention Time min	Area mAU*min	Height mAU	Relative Area %	Relative Height %	Amount n.a.
1		3.010	0.046	0.571	2.16	1.33	n.a.
2		3.173	0.051	0.747	2.40	1.74	n.a.
3		3.540	0.009	0.210	0.40	0.49	n.a.
4		3.657	0.012	0.347	0.57	0.81	n.a.
5		3.760	2.005	41.155	94.46	95.64	n.a.
Total:			**2.123**	**43.031**	**100.00**	**100.00**	

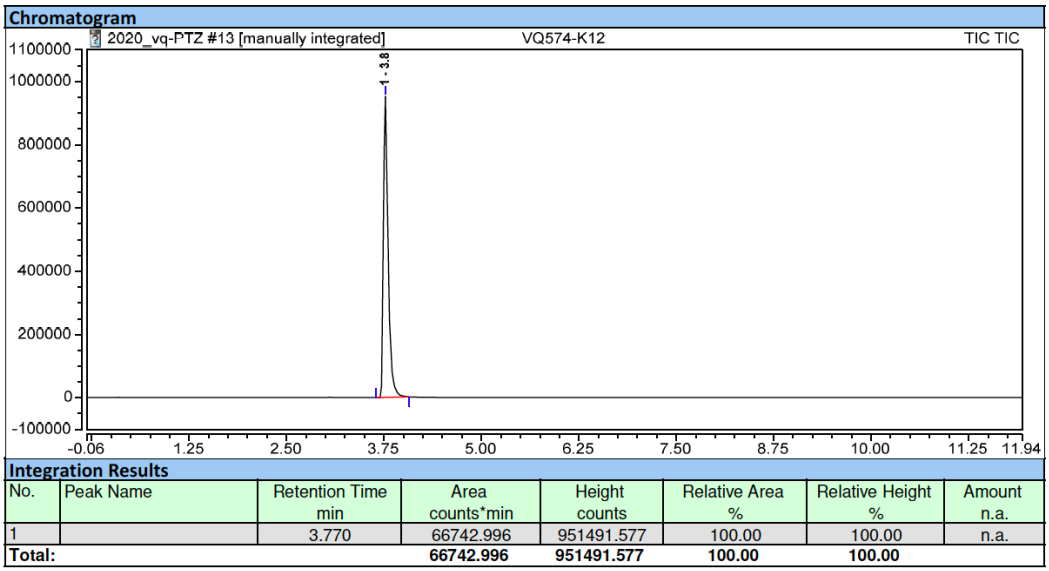

Integration Results

No.	Peak Name	Retention Time min	Area counts*min	Height counts	Relative Area %	Relative Height %	Amount n.a.
1		3.770	66742.996	951491.577	100.00	100.00	n.a.
Total:			**66742.996**	**951491.577**	**100.00**	**100.00**	

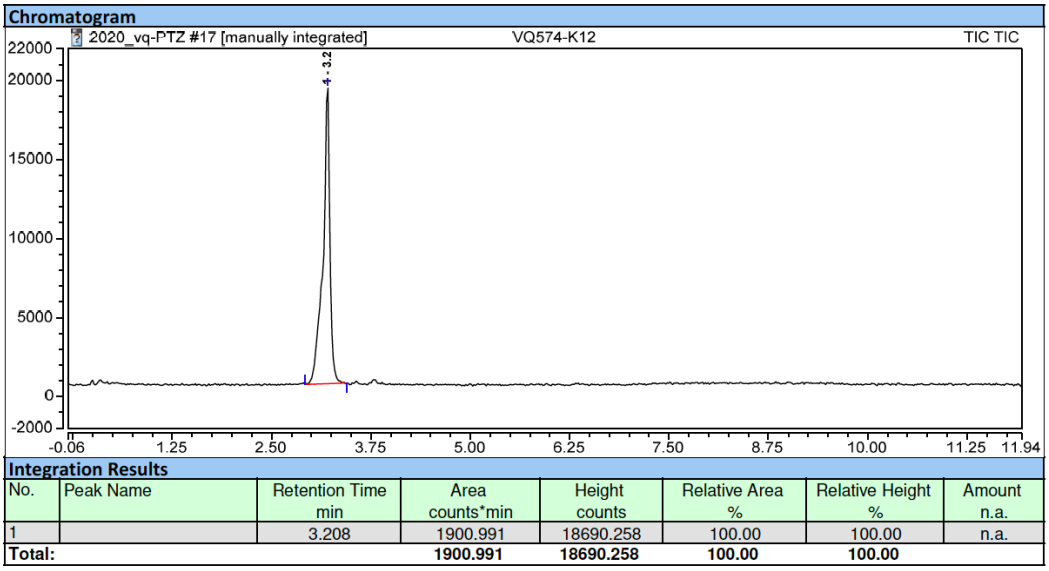

Integration Results

No.	Peak Name	Retention Time min	Area counts*min	Height counts	Relative Area %	Relative Height %	Amount n.a.
1		3.208	1900.991	18690.258	100.00	100.00	n.a.
Total:			**1900.991**	**18690.258**	**100.00**	**100.00**	

Please note: this SIM2 mode (m/z 408.5 ± 0.5) unambiguously confirms the formation of sulfoxide derivative (peak at t_R= 3.2 min) without NaOCl, probably through a singlet oxygen-mediated oxidation reaction. This latter ROS being produced by photosensitization process.

Fig. S85. RP-HPLC elution profile (system E-MS) of PTZ-coumarin hybrid dye 15 after incubation with hypochlorite anion (1 equiv.) in PBS (pH 7.3). UV detection at 250 nm; UV detection at 300 nm; Visible detection at 425 nm; ESI+ mass detection (SIM1 mode at *m/z* 392.5 ± 0.5); ESI+ mass detection (SIM2 mode at *m/z* 408.5 ± 0.5) (top-down)

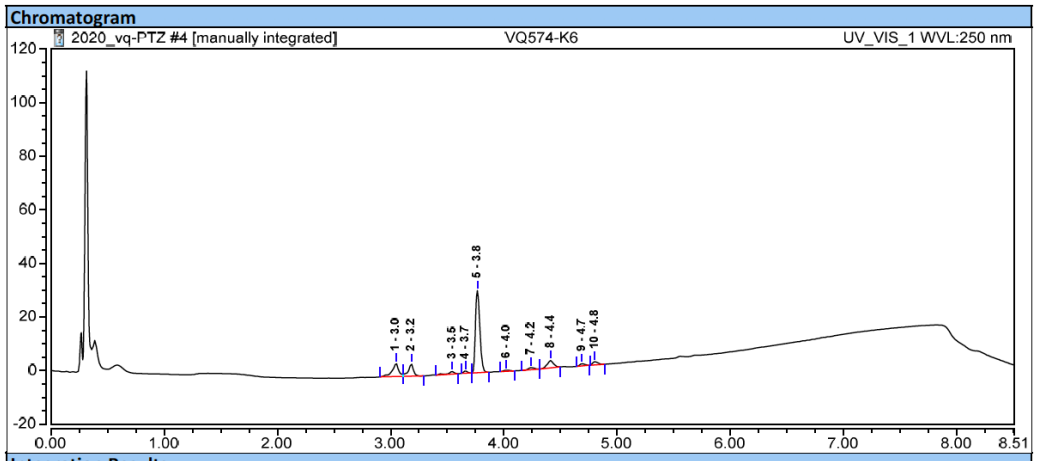

Integration Results

No.	Peak Name	Retention Time min	Area mAU*min	Height mAU	Relative Area %	Relative Height %	Amount n.a.
1		3.047	0.332	4.948	13.80	10.29	n.a.
2		3.183	0.239	4.576	9.91	9.52	n.a.
3		3.543	0.064	0.934	2.66	1.94	n.a.
4		3.660	0.032	0.840	1.33	1.75	n.a.
5		3.767	1.381	30.718	57.42	63.89	n.a.
6		4.023	0.024	0.414	1.01	0.86	n.a.
7		4.240	0.048	0.817	1.99	1.70	n.a.
8		4.413	0.178	2.771	7.39	5.76	n.a.
9		4.690	0.042	0.802	1.76	1.67	n.a.
10		4.803	0.065	1.259	2.72	2.62	n.a.
Total:			**2.406**	**48.078**	**100.00**	**100.00**	

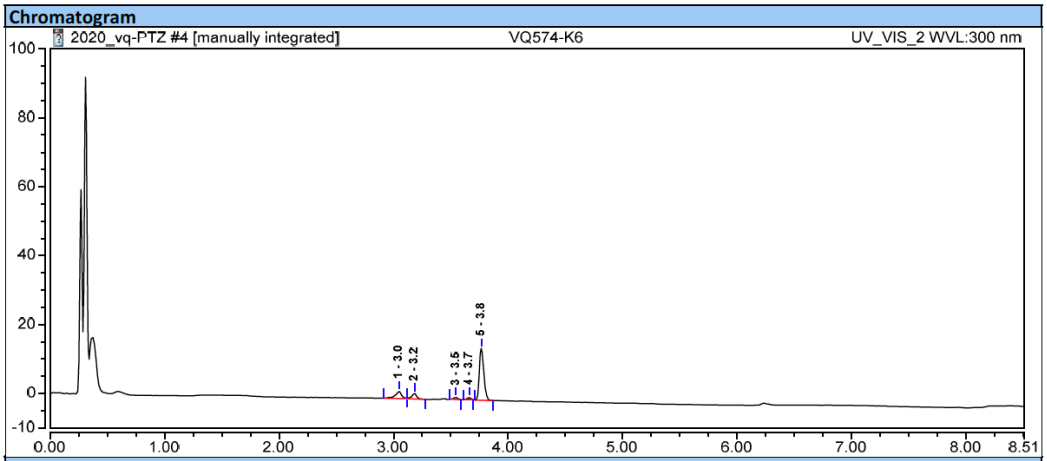

Integration Results

No.	Peak Name	Retention Time min	Area mAU*min	Height mAU	Relative Area %	Relative Height %	Amount n.a.
1		3.047	0.138	2.143	14.58	10.69	n.a.
2		3.183	0.082	1.668	8.67	8.32	n.a.
3		3.543	0.024	0.576	2.58	2.87	n.a.
4		3.660	0.023	0.628	2.45	3.13	n.a.
5		3.767	0.678	15.044	71.72	75.00	n.a.
Total:			**0.945**	**20.059**	**100.00**	**100.00**	

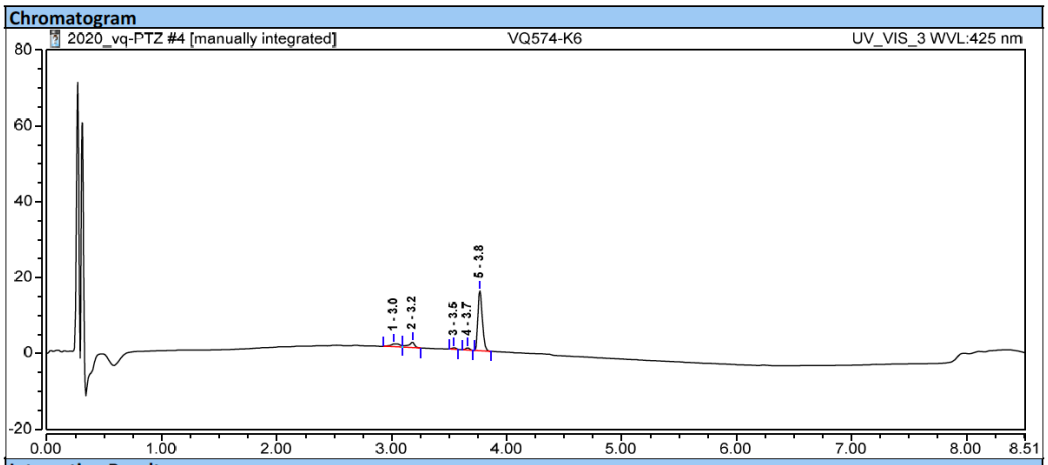

Integration Results

No.	Peak Name	Retention Time min	Area mAU*min	Height mAU	Relative Area %	Relative Height %	Amount n.a.
1		3.017	0.074	0.750	8.20	3.96	n.a.
2		3.180	0.088	1.440	9.70	7.61	n.a.
3		3.540	0.014	0.394	1.59	2.08	n.a.
4		3.660	0.023	0.591	2.54	3.12	n.a.
5		3.767	0.708	15.757	77.97	83.23	n.a.
Total:			**0.908**	**18.931**	**100.00**	**100.00**	

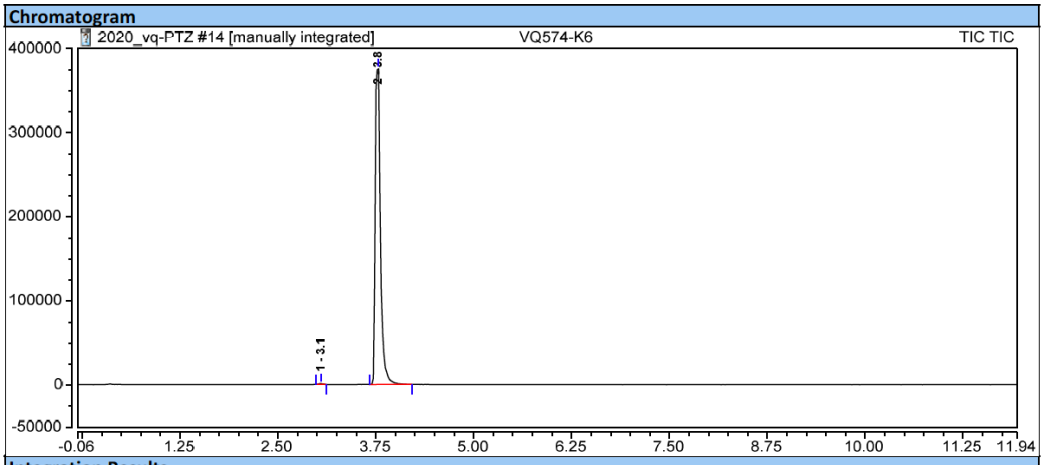

Integration Results

No.	Peak Name	Retention Time min	Area counts*min	Height counts	Relative Area %	Relative Height %	Amount n.a.
1		3.055	59.671	984.778	0.20	0.26	n.a.
2		3.787	29238.080	375096.459	99.80	99.74	n.a.
Total:			**29297.751**	**376081.237**	**100.00**	**100.00**	

*Please note: compared to the NaOCl-mediated oxidation of PTZ-coumarin hybrid dye **10**, the remaining amount of starting probe **15** is dramatically higher.*

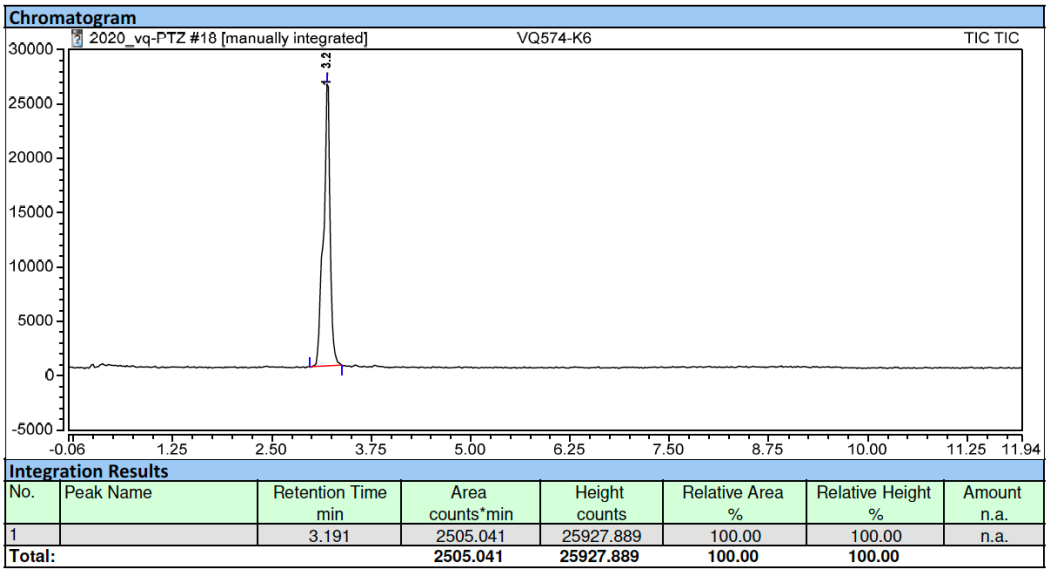

Integration Results

No.	Peak Name	Retention Time min	Area counts*min	Height counts	Relative Area %	Relative Height %	Amount n.a.
1		3.191	2505.041	25927.889	100.00	100.00	n.a.
Total:			**2505.041**	**25927.889**	**100.00**	**100.00**	

Fig. S86. RP-HPLC elution profile (system E-MS) of blank (injection of PBS alone). ESI+ mass detection (SIM1 mode at *m/z* 500.6 ± 0.5); ESI+ mass detection (SIM2 mode at *m/z* 516.6 ± 0.5) (top-down)

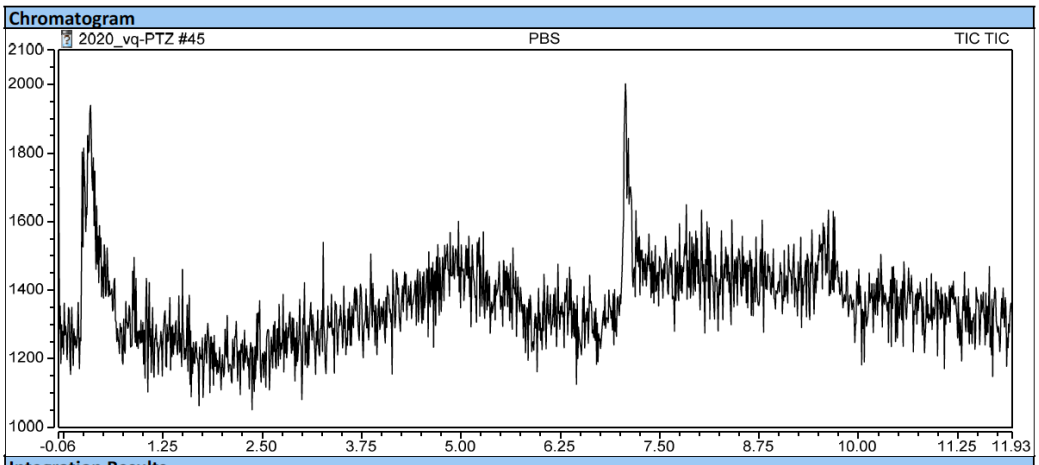

Integration Results

No.	Peak Name	Retention Time min	Area counts*min	Height counts	Relative Area %	Relative Height %	Amount n.a.
Total:			**0.000**	**0.000**	**0.00**	**0.00**	

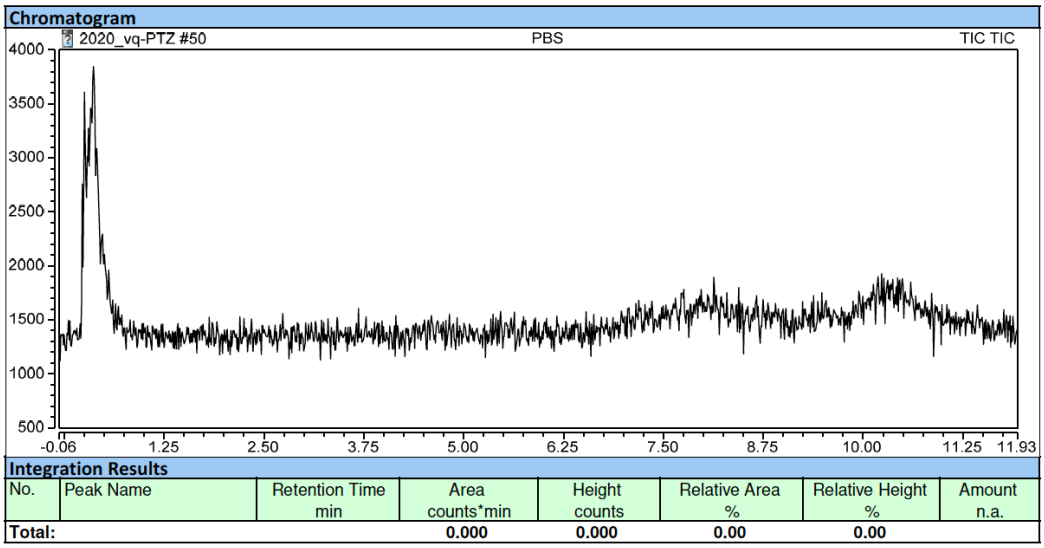

Integration Results

No.	Peak Name	Retention Time min	Area counts*min	Height counts	Relative Area %	Relative Height %	Amount n.a.
Total:			**0.000**	**0.000**	**0.00**	**0.00**	

Fig. S87. RP-HPLC elution profile (system E-MS) of PTZ-coumarin hybrid dye 16. ESI+ mass detection (SIM1 mode at *m/z* 500.6 ± 0.5)

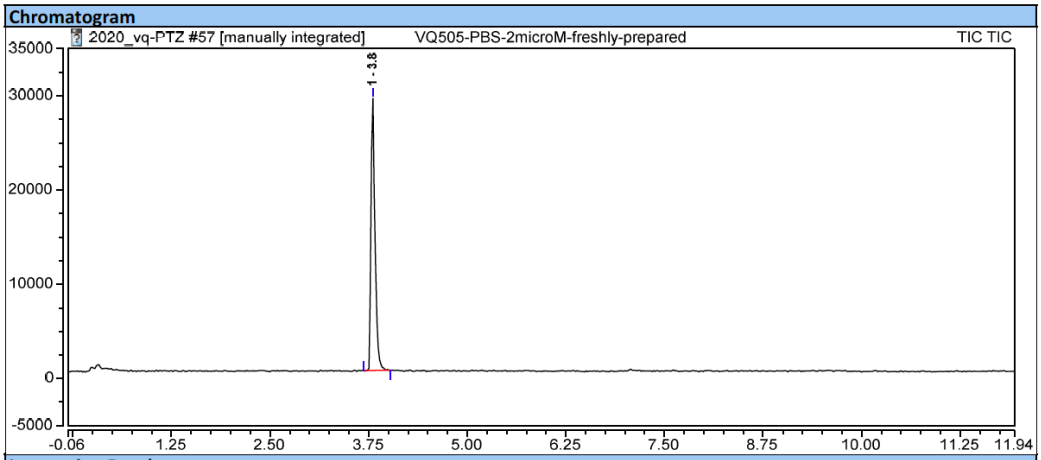

Integration Results

No.	Peak Name	Retention Time min	Area counts*min	Height counts	Relative Area %	Relative Height %	Amount n.a.
1		3.804	1701.865	28871.805	100.00	100.00	n.a.
Total:			**1701.865**	**28871.805**	**100.00**	**100.00**	

Fig. S88. RP-HPLC elution profile (system E-MS) of PTZ-coumarin hybrid dye 16 after incubation in PBS. UV detection at 250 nm; UV detection at 300 nm; Visible detection at 425 nm; ESI+ mass detection (SIM1 mode at *m/z* 500.6 ± 0.5); ESI+ mass detection (SIM2 mode at *m/z* 516.6 ± 0.5); ESI+ mass detection (SIM3 mode at *m/z* 532.6 ± 0.5) (top-down)

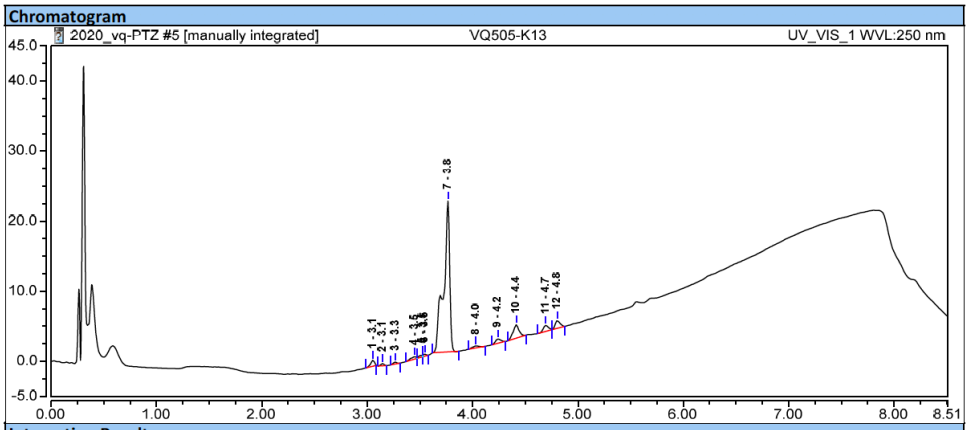

Integration Results

No.	Peak Name	Retention Time min	Area mAU*min	Height mAU	Relative Area %	Relative Height %	Amount n.a.
1		3.053	0.036	0.853	1.99	2.99	n.a.
2		3.143	0.011	0.309	0.59	1.08	n.a.
3		3.267	0.010	0.258	0.55	0.90	n.a.
4		3.450	0.022	0.337	1.21	1.18	n.a.
5		3.527	0.011	0.211	0.62	0.74	n.a.
6		3.547	0.009	0.294	0.51	1.03	n.a.
7		3.767	1.444	21.518	78.86	75.38	n.a.
8		4.033	0.021	0.286	1.14	1.00	n.a.
9		4.240	0.035	0.610	1.93	2.14	n.a.
10		4.413	0.124	1.919	6.79	6.72	n.a.
11		4.693	0.048	0.854	2.63	2.99	n.a.
12		4.803	0.059	1.095	3.20	3.83	n.a.
Total:			**1.831**	**28.545**	**100.00**	**100.00**	

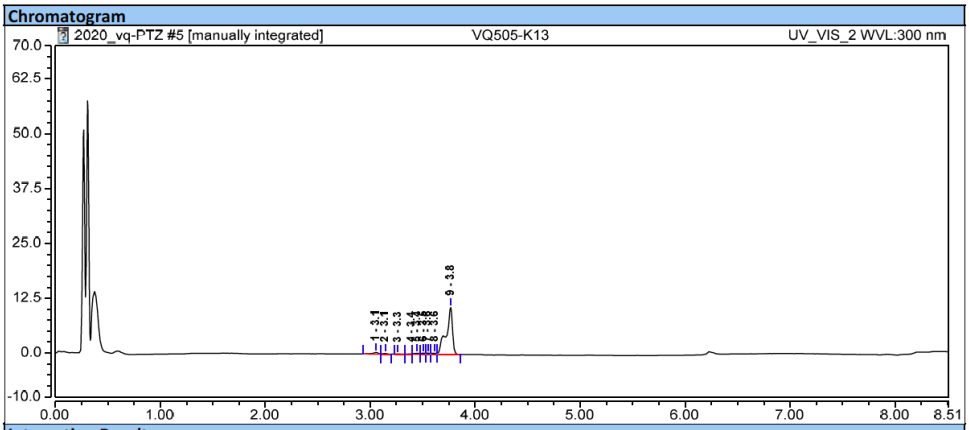

Integration Results

No.	Peak Name	Retention Time min	Area mAU*min	Height mAU	Relative Area %	Relative Height %	Amount n.a.
1		3.053	0.026	0.392	3.06	3.15	n.a.
2		3.143	0.008	0.169	0.95	1.36	n.a.
3		3.263	0.004	0.088	0.44	0.70	n.a.
4		3.397	0.003	0.093	0.41	0.75	n.a.
5		3.443	0.014	0.211	1.68	1.69	n.a.
6		3.507	0.011	0.274	1.36	2.20	n.a.
7		3.550	0.012	0.275	1.49	2.21	n.a.
8		3.617	0.014	0.257	1.69	2.06	n.a.
9		3.767	0.742	10.714	88.92	85.89	n.a.
Total:			**0.835**	**12.474**	**100.00**	**100.00**	

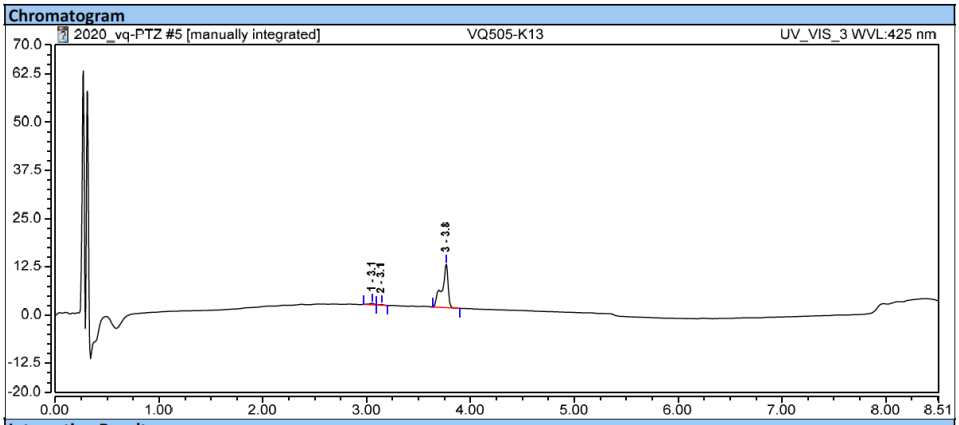

Integration Results

No.	Peak Name	Retention Time min	Area mAU*min	Height mAU	Relative Area %	Relative Height %	Amount n.a.
1		3.053	0.020	0.407	2.50	3.41	n.a.
2		3.143	0.009	0.200	1.10	1.68	n.a.
3		3.767	0.768	11.303	96.40	94.90	n.a.
Total:			**0.796**	**11.910**	**100.00**	**100.00**	

Please note: peak broadening/splitting is caused by the counter-ion effect for sulfobetain pendant arm.

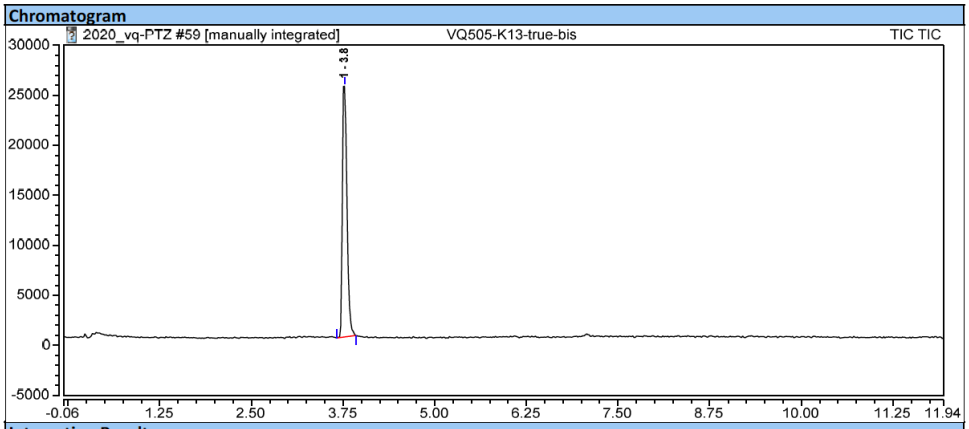

Integration Results

No.	Peak Name	Retention Time min	Area counts*min	Height counts	Relative Area %	Relative Height %	Amount n.a.
1		3.770	1833.263	25064.394	100.00	100.00	n.a.
Total:			**1833.263**	**25064.394**	**100.00**	**100.00**	

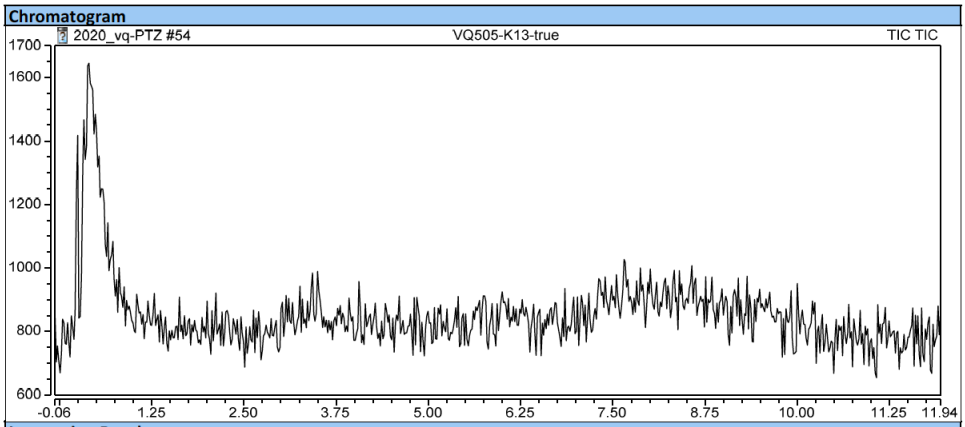

Integration Results

No.	Peak Name	Retention Time min	Area counts*min	Height counts	Relative Area %	Relative Height %	Amount n.a.
Total:			**0.000**	**0.000**	**0.00**	**0.00**	

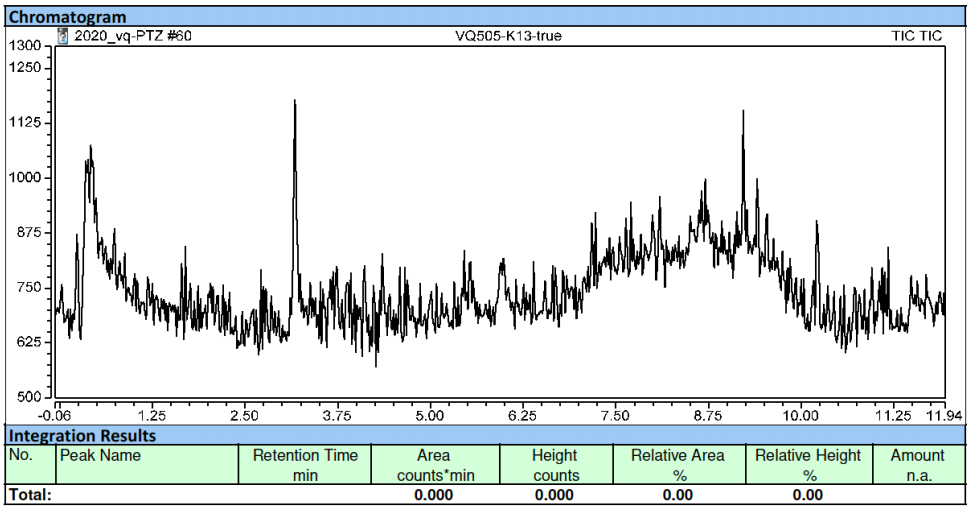

Integration Results							
No.	Peak Name	Retention Time min	Area counts*min	Height counts	Relative Area %	Relative Height %	Amount n.a.
Total:			**0.000**	**0.000**	**0.00**	**0.00**	

Fig. S89. RP-HPLC elution profile (system E-MS) of PTZ-coumarin hybrid dye 16 after incubation with hypochlorite anion (1 equiv.) in PBS (pH 7.3). UV detection at 250 nm; UV detection at 300 nm; Visible detection at 425 nm; ESI+ mass detection (SIM1 mode at *m/z* 500.6 ± 0.5); ESI+ mass detection (SIM2 mode at *m/z* 516.6 ± 0.5); ESI+ mass detection (SIM3 mode at *m/z* 532.6 ± 0.5) (top-down)

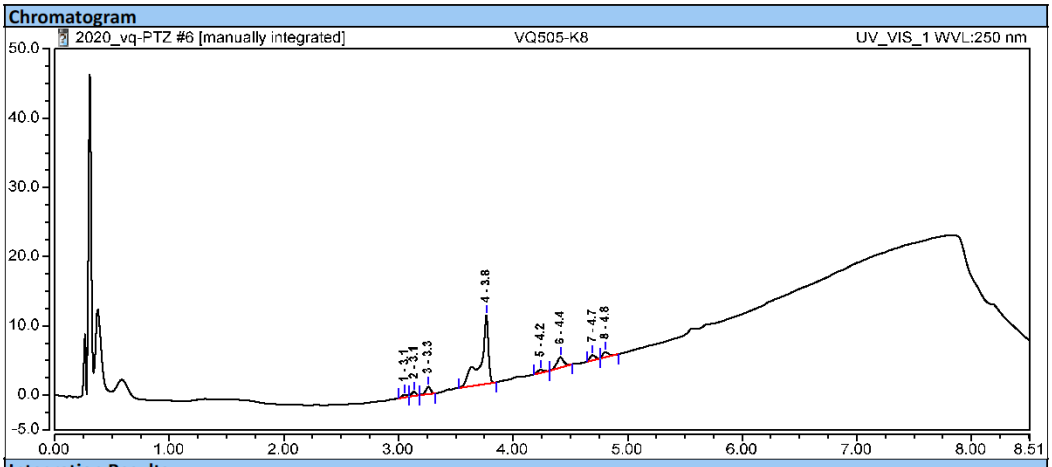

Integration Results							
No.	Peak Name	Retention Time min	Area mAU*min	Height mAU	Relative Area %	Relative Height %	Amount n.a.
1		3.057	0.022	0.361	1.95	2.33	n.a.
2		3.137	0.029	0.606	2.58	3.91	n.a.
3		3.260	0.051	1.102	4.57	7.11	n.a.
4		3.767	0.798	9.898	71.78	63.82	n.a.
5		4.240	0.027	0.442	2.43	2.85	n.a.
6		4.413	0.102	1.552	9.20	10.00	n.a.
7		4.693	0.041	0.764	3.70	4.93	n.a.
8		4.803	0.042	0.784	3.79	5.06	n.a.
Total:			**1.111**	**15.510**	**100.00**	**100.00**	

Chromatogram

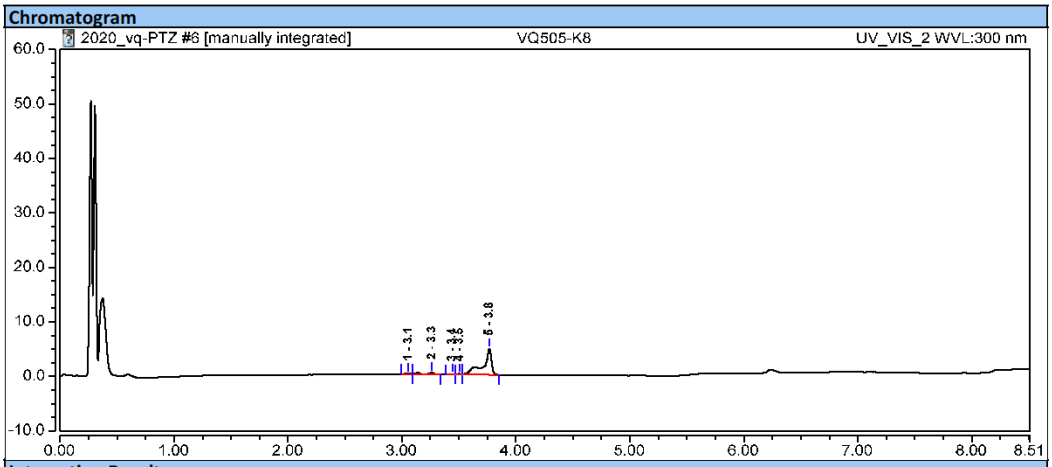

Integration Results

No.	Peak Name	Retention Time min	Area mAU*min	Height mAU	Relative Area %	Relative Height %	Amount n.a.
1		3.057	0.009	0.149	1.97	2.66	n.a.
2		3.263	0.031	0.371	6.71	6.62	n.a.
3		3.440	0.004	0.074	0.87	1.32	n.a.
4		3.503	0.005	0.112	1.15	1.99	n.a.
5		3.767	0.406	4.895	89.30	87.41	n.a.
Total:			**0.455**	**5.600**	**100.00**	**100.00**	

Chromatogram

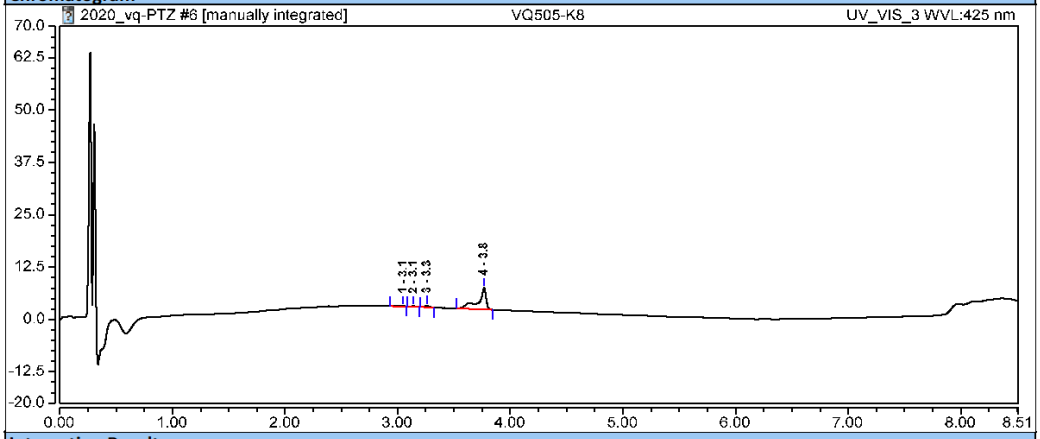

Integration Results

No.	Peak Name	Retention Time min	Area mAU*min	Height mAU	Relative Area %	Relative Height %	Amount n.a.
1		3.050	0.011	0.138	2.43	2.37	n.a.
2		3.140	0.007	0.150	1.48	2.58	n.a.
3		3.260	0.016	0.369	3.55	6.34	n.a.
4		3.767	0.421	5.164	92.54	88.71	n.a.
Total:			**0.455**	**5.821**	**100.00**	**100.00**	

Chromatogram

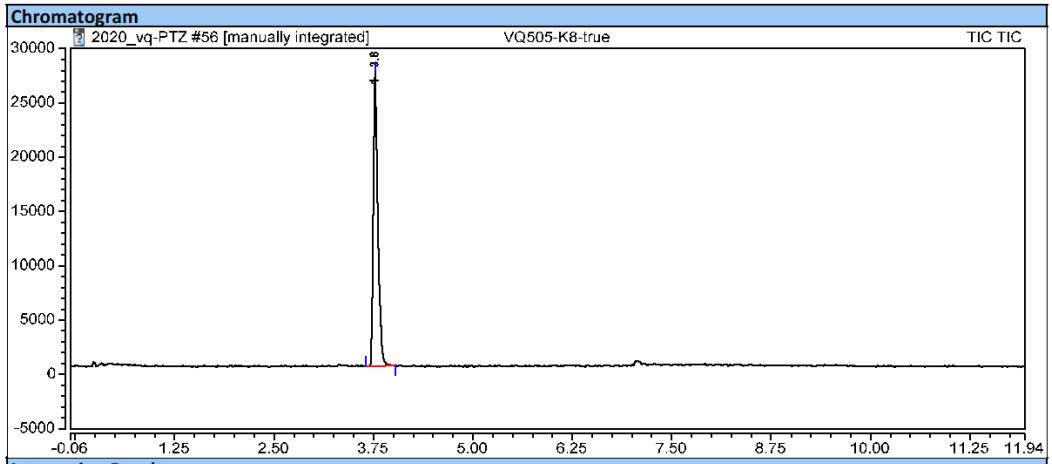

Integration Results

No.	Peak Name	Retention Time min	Area counts*min	Height counts	Relative Area %	Relative Height %	Amount n.a.
1		3.770	1770.989	27019.009	100.00	100.00	n.a.
Total:			**1770.989**	**27019.009**	**100.00**	**100.00**	

Chromatogram

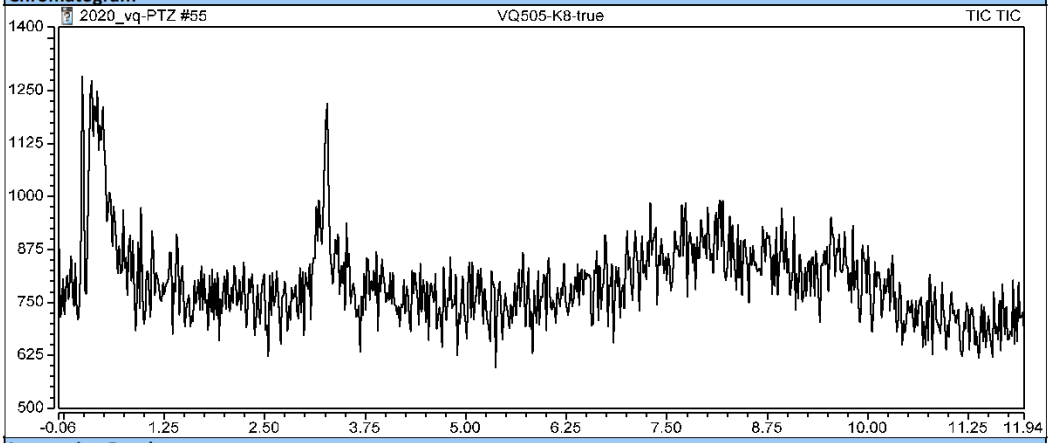

Integration Results

No.	Peak Name	Retention Time min	Area counts*min	Height counts	Relative Area %	Relative Height %	Amount n.a.
Total:			**0.000**	**0.000**	**0.00**	**0.00**	

Chromatogram

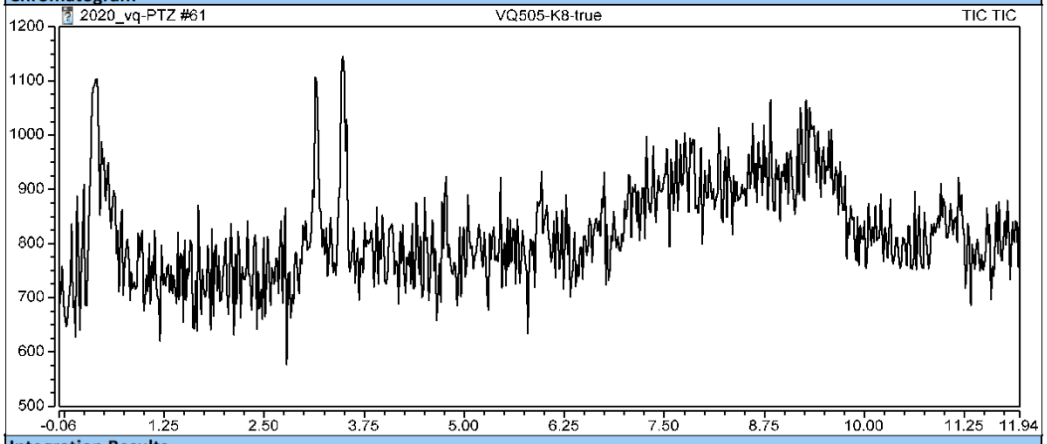

Integration Results

No.	Peak Name	Retention Time min	Area counts*min	Height counts	Relative Area %	Relative Height %	Amount n.a.
Total:			**0.000**	**0.000**	**0.00**	**0.00**	

Fig. S90. ESI+ mass spectra (low resolution, recorded during the RP-HPLC-MS analysis, system E-MS) of two main products stemming from NaOCl-mediated oxidation of PTZ-coumarin hybrid dye 10 (after incubation with 1 equiv. of NaOCl in PBS (pH 7.3), see Fig. S79).

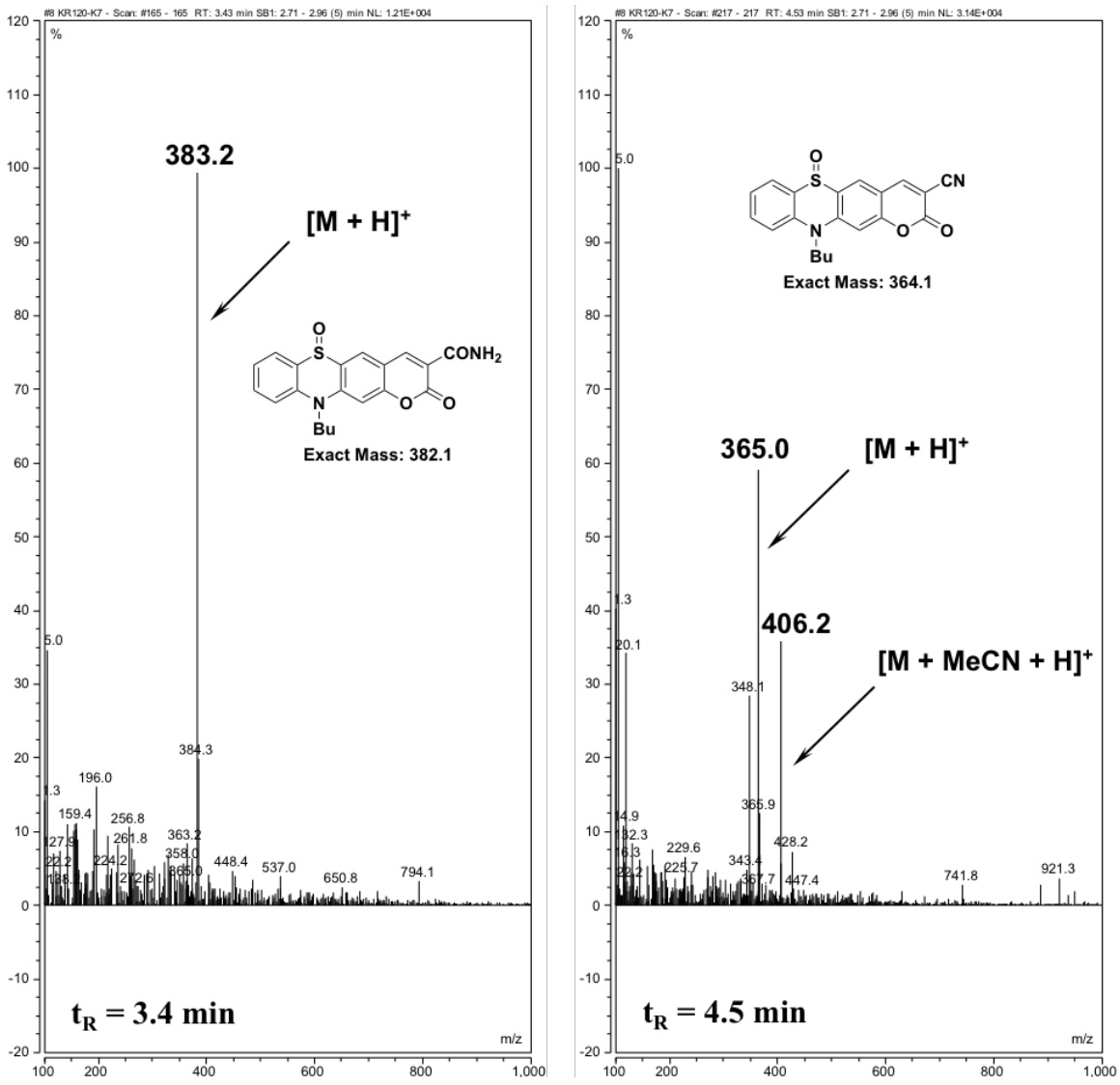

Fig. S91. ESI+ mass spectra (low resolution, recorded during the RP-HPLC-MS analysis, system E-MS) of two main products stemming from NaOCl-mediated oxidation of PTZ-coumarin hybrid dye 15 (after incubation with 1 equiv. of NaOCl in PBS (pH 7.3), see Fig. S85).